Chair of Physical Metallurgy

Master's Thesis

Computational analysis of chemical vapor deposition for nitride-based hard coatings

Michael Martin Wurmitzer, BSc

February 2023

Table of content

MONTANUNIVERSITÄT LEOBEN
www.unileoben.ac.at

EIDESSTATTLICHE ERKLÄRUNG

Ich erkläre an Eides statt, dass ich diese Arbeit selbständig verfasst, andere als die angegebenen Quellen und Hilfsmittel nicht benutzt, und mich auch sonst keiner unerlaubten Hilfsmittel bedient habe.

Ich erkläre, dass ich die Richtlinien des Senats der Montanuniversität Leoben zu "Gute wissenschaftliche Praxis" gelesen, verstanden und befolgt habe.

Weiters erkläre ich, dass die elektronische und gedruckte Version der eingereichten wissenschaftlichen Abschlussarbeit formal und inhaltlich identisch sind.

Datum 21.02.2023

Wurmitzer

Unterschrift Verfasser/in
Michael Martin Wurmitzer

Abstract English

The kinetics of gas phase and surface chemistry from three nitride based hard coating chemical vapor deposition systems were analyzed using a simulation-based approach. These three systems include the titanium nitride, the aluminum nitride and the titanium-aluminum nitride CVD systems which used $TiCl_4$, $AlCl_3$ and NH_3 as the precursor gas. As a first step surface site densities of the substrates were theoretically determined by the use of a crystalline model surface. Ab-initio calculations were performed in an effort to obtain thermodynamic data of the molecules in the gas phase. A reaction model for titanium-aluminum nitride was created using the proposed co-deposition of AlN and TiN respectively. All of the aforementioned analyses were necessary in order to perform a reacting flow simulation at the reactor scale. As a final step the growth behavior of the different systems with respect to different deposition parameters were examined. The results of all reacting flow simulations were within good agreement to experimental data.

Kurzfassung

Die Kinetik der Gasphasen- und die Oberflächenchemie von drei Systemen zur chemischen Gasphasenabscheidung von Hartstoffschichten auf Nitridbasis wurden mithilfe eines simulationsbasierten Ansatzes analysiert. Bei diesen drei Systemen handelt es sich um das Titannitrid-, das Aluminiumnitrid- und das Titan-Aluminiumnitrid-CVD-System, bei denen $TiCl_4$, $AlCl_3$ und NH_3 als Vorläufergas verwendet wurden. In einem ersten Schritt wurden die Oberflächenplatzdichten der Substrate theoretisch mit Hilfe von kristallinen Modelloberfläche bestimmt. Ab-initio-Berechnungen wurden durchgeführt, um thermodynamische Daten der Moleküle in der Gasphase zu erhalten. Ein Reaktionsmodell für Titan-Aluminium-Nitrid wurde unter Verwendung der vorgeschlagenen gemeinsamen Abscheidung von AlN bzw. TiN erstellt. Alle vorgenannten Analysen waren notwendig, um eine reaktive Strömungssimulation im Reaktormaßstab durchführen zu können. In einem letzten Schritt wurde das Wachstumsverhalten der verschiedenen Systeme in Bezug auf unterschiedliche Abscheidungsparameter untersucht. Die Ergebnisse aller Simulationen stimmten gut mit den experimentellen Daten überein.

Acknowledgements

I would like to acknowledge and give a thank you to my supervisor Univ. Prof. Dipl. Ing. Dr. Lorenz Romaner for the support and guidance through this thesis. I would also like to give a special thank you to my partner Sophie Kaltenecker B.A. for supporting me in many different aspects during this thesis.

1 Introduction

1.1 Basic concepts of Chemical Vapor Deposition (CVD)

Chemical vapor deposition (CVD) involves the formation
of a deposit on a substrate caused by the reaction of the substrate with chemicals in the vapor phase. (1) CVD systems used in technical applications are of high complexity, this is mostly a consequence of the synthesis from a gaseous phase. This directly applies to both the understanding of the chemistry of a given system and the nucleation process. Nowadays CVD is an important technique for the synthesis of high purity bulk materials (e.g. silicon CVD) as well as thin film coatings (e.g. hard coatings). (2) CVD can be classified in many ways for example in low and high pressure, cold or hot and the energy source. There are both gas phase and surface reactions taking place during the CVD process.

1.1.1 Mechanistic steps during a CVD process

There are seven steps in the mechanistic model of the CVD process. (2) These steps are:

1. Transport of the reaction gas
2. Intermediate reactants form from reactant gases
3. Diffusion of reactant gases through the boundary layer to the substrate
4. Adsorption of the gases onto the surface of the substrate
5. Surface reactions are taking place
6. Desorption of the product gases
7. The gases are being pushed out of the system

Simulation of the CVD process in principle must take into account all of these steps. In this thesis, the main focus is laid on understanding the impact of gas phase chemistry for the growth rate of titanium nitride, the aluminum nitride and the titanium-aluminum nitride CVD system.

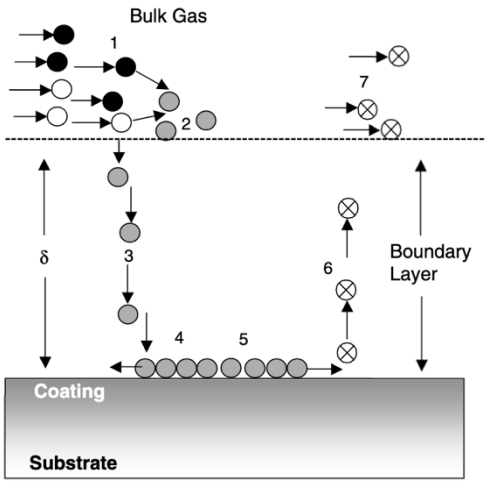

Figure 1 Schematic diagram of the mechanistic steps, [Source: (2)]

1.1.2 Thermodynamics of CVD processes

For any CVD system the first step is to consider the thermodynamics of the reaction in terms of viability for a process. (3) To determine this the Gibbs free energy approach is used. The Gibbs free energy G_r is calculated and based on the result one can assume the reaction is likely going to happen (negative G_r) or is not going to happen (positive G_r). If there are several possible reactions in a system, the one with the most negative G_r should be selected because it leads to the thermodynamically most stable products. For the determination of the Gibbs free energy of a reaction one has to know or calculate the Gibbs free energy of formation (ΔG_f) for all products and reactants. When all the Gibbs free energies of formation are known then the Gibbs free energy of a reaction can be obtained by summing up all ΔG_f.

$$\Delta G_r = \sum \Delta G_f(products) - \sum \Delta G_f(educts) \quad [1]$$

ΔG_f can also be determined by the following equation:

$$\Delta G_f = \Delta H_f^0(298K) + \left(\int_{298K}^{T} C_p dT\right) - T * \left(S^0 + \left(\int_{298K}^{T} \frac{C_p}{T} dT\right)\right) \quad [2]$$

The thermodynamic data of most species can be found in databases. The equilibrium constant for a reaction can be written as:

$$k_{equ} = exp\left(-\frac{\Delta G_r}{R * T}\right) \quad [3]$$

With the equilibrium constant and the law of mass action (described in the chapter “Basics of chemical kinetics”) one can relate the equilibrium constant to the partial pressures of a given species. This can be expressed as:

$$k_{equ} = \frac{\prod_{i=0}^{N}(p_i)^{\nu_i}\,(products)}{\prod_{i=0}^{N}(p_i)^{\nu_i}\,(educts)} \quad [4]$$

Where p_i is the partial pressure of the species and ν_i is the stoichiometric coefficient of the species.

In order to obtain realistic results for the simulation of a CVD process, the gas phase chemistry needs to be considered. (4) Gas phase transport and parasitic reaction losses have a heavy influence on the final deposition rates and should therefore be considered in the simulations. (3) Also the modeling of the gas phase reaction system might exhibit information about possible gas phase phenomena’s that could be very influential for some special CVD system.

Ever since CVD requires a reaction to take place on the surface of the substrate, the surface chemistry is an important aspect. The surface chemistry includes the adsorption and desorption of the gas phase molecules as well as the consideration of active sites and the heterogenous reaction itself. The heterogenous reactions can be further divided into adsorption/desorption reactions, reactions occurring between the gaseous species with the solid surface and solid deposition reaction. It is very difficult to extract features for a single phenomenon, so the most

common approach to quantify the adsorption and the subsequent heterogenous reaction based on the isotherm adsorption theory (Langmuir isotherm).

Adsorption and desorption

In the Langmuir isotherm it is assumed that the substrate surface can be treated as a finite number of surface sites (N) on which a gaseous species can be adsorbed. (3) The surface coverage is defined as the ratio of the sites with gaseous species attached to the number of total sites. The enthalpy of adsorption is the same for every site and it is independent of the surface coverage (Θ). Also the adsorbed species do not interact with each other. Adsorption rates for a gaseous species (r_{ads}) are dependent on the partial pressure of the gaseous species and the number of vacant sites. Meanwhile the desorption rates (r_{des}) are proportional to the occupied surface sites. The adsorption and desorption can be described with the following equations:

$$r_{ads} = k_{ads} * (1 - \Theta) * N * P \quad [5]$$

$$r_{des} = k_{des} * \Theta * N \quad [6]$$

In this formula k_{ads} and k_{des} are the constants for adsorption and desorption respectively and P is the pressure. For equilibrium conditions the number of adsorbed atoms is equal to the number of desorbed atoms. Therefore r_{ads} is equal to r_{des}. So, the following equation can be established.

$$k_{ads} * (1 - \Theta) * N * P = k_{des} * \Theta * N \quad [7]$$

For a fixed temperature the equation relating the fraction of occupied sites to the partial pressure in the vapor (p_i) at, can be expressed using the mathematical term:

$$\Theta_i = k_{ads} * p_i \frac{1}{(k_{des} + k_{ads} * p_i)} \quad [8]$$

Or as:

$$\Theta_i = k * p_i \frac{1}{(1 + k * p_i)} \quad [9]$$

Where k is the surface equilibrium constant (the ratio of k_{ads} to k_{des}).

Due to the exothermic nature of the adsorption process, the surface coverage decreases with an increase in temperature. For heterogeneous reaction the rate is correlated to the coverage. While for weakly adsorbed species the reaction can be treated as a first-order reactions, the reaction of a strongly adsorbed species is described by zeroth order. The reaction rate in this context is independent of the partial pressure. For species within the intermediate case the rate may become a fraction. The behavior of a heterogeneous reaction with respect to temperature is more complex than that of a homogeneous reaction. In the case of

homogeneous reaction its activation energy can be directly predicted by log(-1/T) curves. However for heterogenous reactions the activation energy (E*) is expressed by:

$$E^* = E^*_s - \Delta H_{ads} \quad [10]$$

where E^*_s is the activation energy of the surface reaction and ΔH_{ads} is the heat of adsorption. (3)

If two species compete for one surface site, then both can still be treated by the Langmuir isotherm and the one with the higher value for surface coverage gets adsorbed. (3)

$$\Theta_a = k_a * p_a * \frac{1}{(1 + k_a * p_a + k_b * p_b)}$$
$$and\ \Theta_b = k_b * p_b * \frac{1}{(1 + k_a * p_a + k_b * p_b)} \quad [11]$$

The reaction rate is proportional to the surface coverage.

$$r_g = k_{ab} * \Theta_a * \Theta_b \quad [12]$$

Calculation of site densities

The site density (or the total number of sites) is an important feature for the calculation/simulation of surface reactions. (5) Since a site is the crystallographic plane at which a molecule can stick to the surface, one can just use crystallography and geometry (periodicity of a crystal) to calculate the sites per cm^2. During the surface reactions, the number of sites is conserved.

Langmuir-Hinshelwood and Eley-Rideal reactions

Ever since surface reactions are often described by an overall reaction instead of a series of elementary reaction one needs specific models for the description of these overall reactions. The most used global rate expression models in surface chemistry are the Langmuir-Hinshelwood model and the Eley-Rideal model. In the Langmuir-Hinshelwood model adsorption and desorption are assumed to be in equilibrium. For this case it is assumed that reactions take place at the surface as adsorbed species. In the case of Langmuir Hinshelwood models all reaction sites are independent of each other and the surface coverage only influences the number of available adsorption sites and not the energetics of the adsorption/desorption process. An example of the Langmuir Hinshelwood model is given by the following system which was taken from (6). In this form (s) is a surface species.

$$a + O(s) <=> a(s) \quad [13]$$

$$b + O(s) <=> b(s) \quad [14]$$

$$a(s) + b(s) => c(s) + d(s) \quad [15]$$

$$c(s) <=> c + O(s) \quad [16]$$

$$d(s) <=> d + O(s) \quad [17]$$

$$A + B => C + D \quad [18]$$

Where the rate limiting step is the reaction between the adsorbed species. The elementary reaction is replaced by the single overall reaction. Site blocking by adsorbed species is in terms of the adsorption/desorption equilibria. The effect of this lumping of elementary reactions is that the expression of rate changes significantly from the simple mass action rate expression. The rate equation is given by the following expression:

$$q = \frac{k * K_A * [X_A] * K_B * [X_B]}{(1 + K_A * [X_A] + K_B * [X_B] + K_C * [X_C] + K_D * [X_D])^2} \quad [19]$$

With the Ki's as the equilibrium constants for adsorption and desorption and the [Xi] as the concentrations of a given surface species. The products are not in numerator but ever since they block surface sites causes them to appear in the denominator. Often even the equilibrium constants from the numerator are lumped together. Which can be stated in a generalized form by the following equation:

$$q = k' * \frac{\prod_i {X_i}^{l_i}}{(1 + \sum_i K_i * {X_i}^{n_i})^m} \quad [20]$$

Where l_i might different than the stoichiometric coefficient (reaction order) and m might be different from two. Also n_i is sometimes different from the stoichiometric coefficients.

The Eley-Rideal model describes the reaction between a gas phase species and adsorbed species where this reaction(s) is (are) the rate limiting steps. This type of reaction is way less common. The following example is again taken from (6) and might illustrate the Eley-Rideal model.

$$a + O(s) <=> a(s) \quad [21]$$

$$a(s) + b => c(s) \quad [22]$$

$$c(s) <=> c + O(s) \quad [23]$$

$$A + B => C \quad [24]$$

In this system the reaction of the adsorbed species a(s) and the gas species b is assumed to be irreversible and the rate limiting step, whereas the adsorption/desorption is assumed to be in equilibrium. (6) In the Eley-Rideal model, the elementary reactions are yet again replaced by the single overall reaction which does not contain any surface species at all. For this system the rate expression can be given as:

$$q = \frac{k * K_A * [X_A] * [X_B]}{1 + K_A * [X_A] + K_C * [X_C]} \quad [25]$$

In the generalized form, the equation is the same as the Langmuir-Hinshelwood but without an exponent in the denominator. This equation is as followed:

$$q = k' * \frac{\prod_i X_i^{\nu_i}}{1 + \sum_i K_i * X_i} \quad [26]$$

Growth kinetics, nucleation and film formation of a CVD process

As stated above, there are a number of consecutive steps with different influencing factors mainly mass transport and reaction kinetics. (7) In high temperature CVD systems the thermodynamics of the precursor reaction system is also a key factor. This correlation in the growth kinetics is usually represented by plotting the growth rate versus the deposition temperature in an Arrhenius chart. In the Arrhenius plot it becomes obvious that there are three main regimes for the rate determining mechanism/factor.

The film growth is controlled by a combination of thermodynamics and kinetics. A general way to describe trends for the thin film growth is with a thermodynamic model considering the surface and interfacial energies. Three general growth modes can be distinguished. The first one is the layer-by-layer growth (Frank van der Merve model), where the film atoms are bound more strongly to the surface than to each other. As a result of this, every layer is fully completed before the next layer starts to grow. That means that there is only a two-dimensional growth happening. The second growth mode is the island growth (Vollmer-Weber model) which happens when the film atoms are more strongly bound to each other than to the film. In this case the film forms three-dimensional islands which nucleate and grow directly on the substrate. The third growth mode is a combination of the layer-by-layer and the island model. In this growth mode the island growth follows after the completion of the two-dimensional layers.

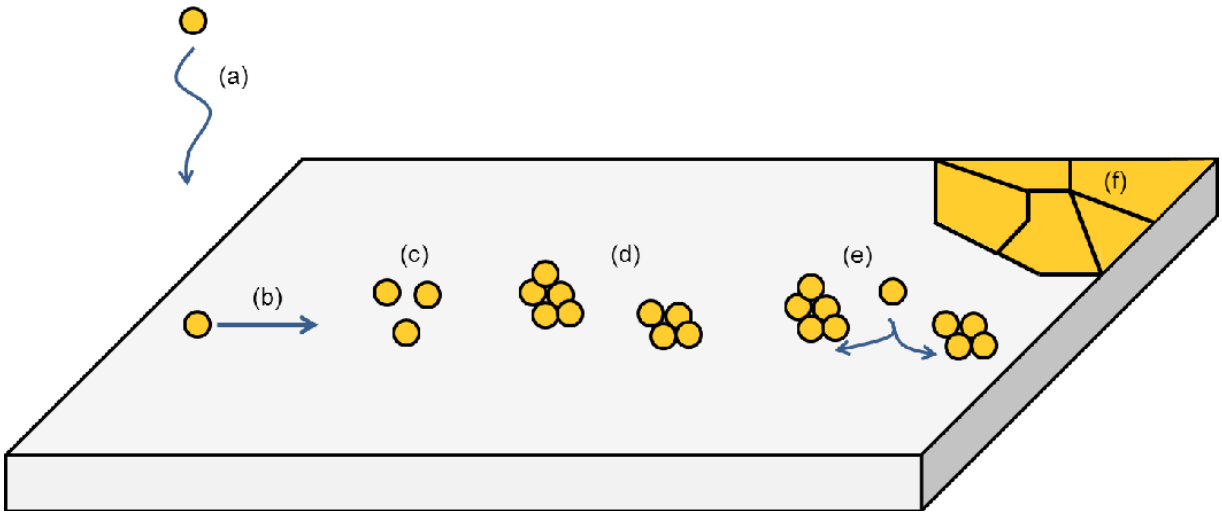

Figure 2 Typical steps during the growth of a thin film, [Source: (8)] The material is transported towards the substrate (a), where it deposits. The adatoms diffuse (b) over the surface, moving towards low energ energy sites.

As more adatoms arrive, agglomerates begin to form (c) and the first islands nucleate (d). The new arrived adatoms are incorporated into the islands (e), which grow until they reach each other and coalesce, forming the grain boundaries (f).

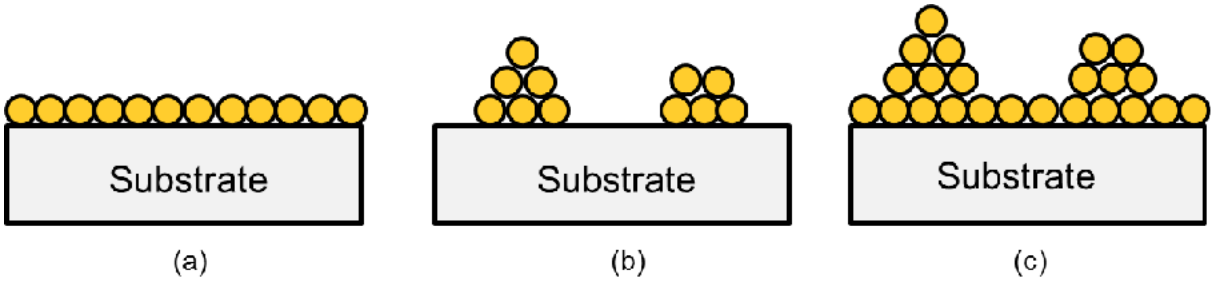

Figure 3 The three modes of film growth: Frank-van der Merwe (a), Volmer-Weber (b), and Stransky-Karastanov (c), [Source: (9)]

1.2 Theoretic concepts of modelling chemical reactors

1.2.1 Basics of chemical kinetics

The knowledge of chemical kinetics is crucial for the development and modelling of any CVD process. (2) It describes the rates at which a reaction takes place in a certain system. The complexity of the kinetics in a CVD system arises not only from the fact that there are numerous steps taking place during the CVD process but that there are several important factors like temperature and concentration gradient, geometric effects, and gas flow patterns in the reaction zones.

Stoichiometry and reaction mechanisms

The overall reaction (better known as stoichiometric reaction) describes the molar ratios between a reactant and its products. (10) These stoichiometric reactions however are very rare in real chemistry. In most reaction systems an intermediary species is formed. These intermediate species can react with each other or the reactants in order to produce further intermediates or the final products. All of these individual intermediary reactions are the so-called elementary reactions (which refers to reaction where no macroscopic intermediate species is observed between reactants and products.) The reaction systems with intermediary reactions are called the reaction mechanism. (10) For a given reaction mechanism the number of elementary reaction steps mechanism can typically range from ten to several ten thousands. This depends on many factors like the chemical process itself, the reaction conditions and the needed accuracy of the chemical kinetic model. A kinetic reaction mechanism includes the stoichiometric equations and the corresponding rate coefficient for each of the steps.

Activation energy

The activation energy E_a of an arbitrary reaction is the energy needed to move from the starting configuration to the product. (11) It comes from the fact that the bonds of an initial molecule need to be split before a reaction can take place. It can be defined as a function of the reaction coordinate. The same principle also applies to the reverse reaction E_r. The peak of the energy profile is the so-called transition state (activated complex).

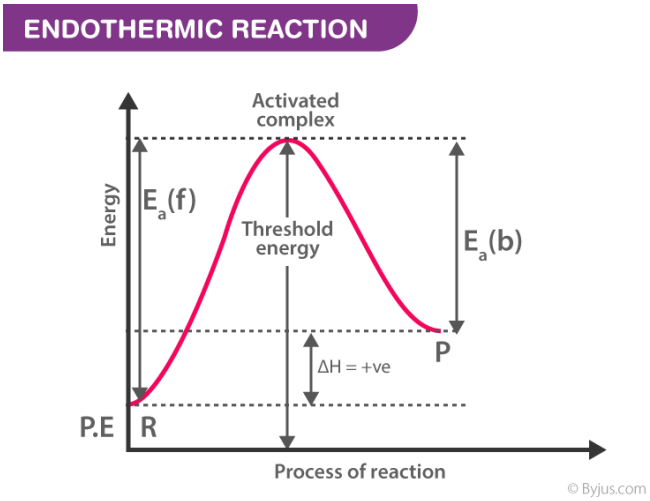

Figure 4 Example of an energy profile for an arbitrary reaction, [Source: (11)]

Reaction rates, Arrhenius equation and reaction order

The reaction rate of a reaction is the change in product (yield) with respect to a given time. (10) The reaction rate for a given reaction with the species A, B, C, D and their according stoichiometric coefficient (a, b, c, d) can be expressed as:

$$aA + bB \rightarrow cC + dD \quad [27]$$

$$r = \frac{-1}{a} * \frac{d[A]}{dt} = \frac{-1}{b} * \frac{d[B]}{dt} = \frac{1}{c} * \frac{d[C]}{dt} = \frac{1}{d} * \frac{d[D]}{dt} \quad [28]$$

The reaction rate can also be given as a function of the rate coefficient k where the terms in square brackets stand for the concentration of the species.

$$r = k_f * [A]^m * [B]^n - k_r * [C]^p * [D]^q \quad [29]$$

k_f and k_r are the forward and reverse reaction coefficients. In the case of an irreversible reaction this can be written as:

$$r = k * [A]^m * [B]^n \quad [30]$$

The exponents for a given species are called the reaction orders. The sum of all reaction orders determines the overall reaction order. For elementary reaction the reaction order is always the stoichiometric coefficient (called the mass action principle), whereas the reaction order for the overall reaction is usually not equal to the stoichiometric coefficients and has to be found empirically. This is due to the fact that intermediate species are formed. The rate coefficient is independent in terms of concentrations but may be dependent on temperature and pressure. For both cases special equations have been found with the most common one being the Arrhenius equation for the temperature dependent rate equation.

$$k = A * exp\left(-\frac{E_a}{R * T}\right) \quad [31]$$

Where A is the so-called pre-exponential factor, E_a is the activation energy for the reaction, R is the gas constant and T is the temperature. In high temperature gas phase systems the rate constant is usually described with the modified Arrhenius equation.

$$k = A * T^{\beta} * exp\left(-\frac{E}{R * T}\right) \quad [32]$$

β is called the temperature exponent but E is no longer the activation energy and A is not the same as in the original Arrhenius equation.

As stated above the elementary reactions follow the mass action principle which means the kinetic system can be expressed as a set of ordinary differential equation.

$$\frac{d[Y_j]}{dt} = \sum_{i=1}^{Nr} \nu_{ij} * r_i \quad j = 1,2,\dots,Ns \qquad [33]$$

With υ_i being the stoichiometric coefficient of a given species and r_i being the reaction rate of a given reaction and Ns being the number of species. For every species in the reaction system there is an equation of ODE to solve. With these all being coupled they can be solved simultaneously.

Surprisingly for large chemical reaction systems the production rate of a reactant or final product of the overall chemical reaction may depend to a large extend on the rate coefficient of a single reaction step. (10) This is the so-called rate-determining step. There are several rate determining steps in CVD but the most important are the mass transport and the surface kinetics. (2) If it's the case that the mass transport through the boundary layer is sufficiently high the surface reactions mainly control the overall rate of the system.

For the construction a chemical reaction mechanism, it is necessary to provide data on the thermodynamics and reaction kinetics parameters for the different species and reaction steps. (10) The biggest part of chemical kinetics is the determination of such parameters via a variety of methods such as functional fitting to experiments, theoretical calculations based on quantum chemistry, transition state theory, approximations using thermochemical rules and the use of the structure reactivity approach. In quantum chemistry, the chemical kinetics can be obtained by the means of transition state theory. (12) (13) Simpler models of TST adopt the idea that the formation of a transition state is the limiting step for the reaction rate. If experimental data is available one can simulate the system and fit the reaction rates of the given system. Even though this approach appears to be simple it can be quite difficult and tedious especially for large systems or if the experimental data does not describe the whole process. E.g. for some simulations, it might be enough to simply fit data to a growth rate, however for more advanced simulations full knowledge should be available regarding inflow of gas and measuring the chemistry of the outflowing gas. In some cases even microstructural data must be present.

1.2.2 Basic concepts used in Ansys Chemkin

To foreshadow the methodology, all computational fluid dynamics/ reacting flow analysis were performed with the chemical kinetics (Chemkin) software package from Ansys. (14) Ansys Chemkin enables to simulating complex chemical (flow) reaction systems. It includes a framework for a lot of reacting flow systems (this also includes CVD systems) which makes it a good option for the simulation at a reactor scale and maybe to obtain some new information about the chemical kinetics and thermodynamics of the systems of interest. Please take notice that all information below in the remaining chapter was drawn from the two manuals given by ref. (6) and (15). There are several reactor models which can be simulated just to name a few important once for our use case: the perfectly stirred reactor (PSR), Stagnation flow and spinning disk reactors, Equilibrium simulation and mechanism analyzer. Besides chemically reacting flow models, Chemkin can be used to model chemical equilibria. The model determines the chemical state of the mixture under equilibrium conditions where any gas phase and bulk species may be considered. Surface species on the other hand are not considered. The Chemkin code uses an elemental potential method which is embodied in the

Stanjan software package. The model determines the phase/composition equilibrium. The output is only influenced by the starting compositions and conditions as well as the thermodynamic properties of a given species in the input file. The starting composition gives the relative ratios of the elements in the system. It is assumed that all gases mixtures are ideal and the bulk phases are ideal solutions. There are different ways to specify the important state parameters such as temperature, pressure, volume, enthalpy and entropy. Species may also be set as fixed points. Continuations may be used to link results from a previous calculation and use them as starting points for the new one. The approach for the elemental potential method of thermodynamic equilibria is to minimize the Gibbs free energy. The Gibbs function for a given system can be written as:

$$G = \sum_{k=1}^{K} \overline{g}_k N_k \qquad [34]$$

Where $\overline{g}_k$ is the partial molal Gibbs function and N_k is the number of moles for a given species. In ideal systems the partial molar Gibbs function is given by the following equation:

$$\overline{g}_k = g_k(T,p) + RT * X_k \ln(X_k) \qquad [35]$$

The equilibrium solution is given by the distribution of N_K that minimizes the systems Gibbs function at the given pressure and temperature. The atomic population constraint is given by the equation:

$$\sum_{k=1}^{K} n_{jk} N_k = p_j \; j = 1 \ldots M \qquad [36]$$

n_{jk} is the number of the atom j in the molecule k, p_j is the total population of j in the system and M is the total number of different elements.

The perfectly stirred reactor (PSR) is a zero-dimensional reactor system. This in turn means contents are assumed to be nearly spatially uniform due to strong turbulent mixing and/or high diffusion rates. Therefore the conversion of educts to products is only controlled by chemical kinetics and not by mass transport/mixing. A good use case for this approximation low pressure systems, in which the diffusion is dominant. This holds true for low pressure CVD systems and plasma etching reactors. The benefit of this reactor type is its low computational demands, which in turn allows for larger (more complex) systems to be analyzed. For a well-mixed reactor, all the conservation equations need to be fulfilled, this includes conservation of mass, energy and species (elements). The actual equations solved can be found in (6 S. 91-105).

Thermodynamic databases

There are four main input files which are called “the thermodynamic input file”, “the gas-phase kinetic input file”, “the surface kinetic input file” and “the gas transport input file”. Regarding the thermodynamic input file, every chemical species that appears in simulation needs associated thermodynamical data. The thermodynamic data includes the standard enthalpy of formation, the standard entropies at 298 Kelvin and the specific heat capacity. Thermodynamic

data may be extracted from a thermodynamical data base (e.g. therm.dat or therm_nasa.dat which are included in the Chemkin-Pro package), or they might be stated in the gas-phase kinetic file or in the surface kinetic file. The thermodynamic data is at default written in a slightly modified format of the Nasa-7 format proposed by Gordon and McBride for the Thermodynamic Database in the NASA Chemical Equilibrium code. With that said the Ansys Chemkin software accepts the Nasa-9 format which allows for bigger molecules, more than two different temperature ranges and different midpoint fits.

Standard state thermodynamic properties

The Chemkin software assumes that the standard state thermodynamic properties only rely on the temperature and can therefore as stated above represented by polynomials.

Specific heat capacity at constant pressure:

$$\frac{c_{pk}^{o}}{R} = \sum_{m=1}^{M} a_{mk} * {T_k}^{m-1} \quad [37]$$

With a_{mk} being the coefficients of polynomial fitting.

Molar enthalpy in the standard state is given as:

$$H_k^o = \int_0^{Tk} c_{pk}^o * dT + H_k^o(0) \quad [38]$$

And therefore the polynomial fit can be expressed as:

$$\frac{H_k^o}{R * T_k} = \sum_{m=1}^{M} \frac{a_{mk} * {T_k}^{m-1}}{m} + \frac{a_{M+1,k}}{T_k} \quad [39]$$

Where $a_{M+1,k}$*R is the standard heat of formation at 0K but it is usually evaluated from the standard heat of formation at 298K.

Molar entropy at its standard state can be by the following expression:

$$S_k^o = \int_{298}^{T_k} \frac{c_p^o * k}{T} * dT + S_k^o(0) \quad [40]$$

Which can be written in polynomial form as:

$$\frac{S_k^o}{R} = a_{1k} * \ln(T_k) + \sum_{m=2}^{M} \frac{a_{mk} * {T_k}^{m-1}}{(m-1)} + a_{M+2,k} \quad [41]$$

Where the integration constant $a_{M+2,k}$ can be calculated from the standard state entropy at 298K.

All of the above equations can be used for any order of polynomial but the default for Chemkin is as stated above in the form of the Nasa chemical equilibrium code, i.e. that the polynomial is evaluated at M=5 (or Nasa 7).

The gas-phase kinetics input file contains information on the elements, species, thermodynamic data, real gas data, transport data for gaseous species and the reaction mechanism with the related kinetic data. Each species in a reaction mechanism must only be composed of elements or isotopes of elements that need to be specified. All chemical species used in the simulation have to be identified in the species line. The reaction mechanism section may consist of any number of chemical reactions involving the species from the species data. These reactions can either be reversible or irreversible and they may involve a wide variety of effects. These effects include a third body reaction, pressure dependent reactions or photon absorption and emission. Every reaction entry line is divided into two fields, with one being the symbolic description of the reaction itself and the second one being the Arrhenius coefficients for the description of the chemical kinetics.

Many chemical processes (including CVD) contain reaction at the interface between the solid and gas. For the symbolic description of the surface chemistry reaction mechanism one needs to provide a surface kinetics input file. This input file encompasses all information about surface sites, surface species, bulk phases, bulk species, thermodynamic data, and the reaction mechanism. The default formulation for the reaction mechanism is the assumption of elementary reactions that follow the mass action principle but also global reactions can be specified with an arbitrary reaction order. It is also possible to use Langmuir-Hinshelwood or Eley-Rideal rate expressions. It is possible to include completely different surface mechanisms in one surface chemistry input file with the utilization different materials. All surface species exist on sites and therefore a site has to be specified. The site data starts with the keyword SIDE followed by the optional name, the surface density starting with the keyword SDEN and with the value the site density in moles per cm^2. The species that reside on these sites are specified by the species names which can be written in the same line or in additional ones. Every species is followed by the site occupancy number for the given species. The bulk data set may consist of one or more condensed phase species. For a species k the net production rates can be represented as the sum of all production rates for all reactions where k is involved. This is illustrated by the following equation:

$$\dot{s}_k = \sum_{i=1}^{I} \upsilon_{ki} * q_i \qquad [42]$$

As already discussed above, the stoichiometric coefficients can be non-integers for gas-phase species. The reaction rates for surface reactions are given in Arrhenius form. However as stated above the reverse reaction rates can be related to the forward reaction rates via the equilibrium constant. For surface reaction, both the surface states and the gas-phase state must be considered for the calculation of the equilibrium constant. Therefore the following expression can be derived:

$$K_{ci} = \left(\frac{P_{atm}}{RT}\right)^{\sum_{k=1}^{Kg} \upsilon_{ki}} \prod_{n=N_s^f}^{N_s^l} \Gamma_n^{0} \sum_{k=K_s^f}^{K_s^l \upsilon_{ki}} \prod_{k=K_s^f(n)}^{K_s^l(n)} \sigma^{-\nu_{ki}} * K_{pi} \quad [43]$$

With n being the site type, P_{atm} being the atmospheric pressure and Γ_n^0 being the standard state site density for the species n. When solving chemically reacting-flow problems, chemical processes are often balanced by mass transport due to convection, diffusion and/or conduction. In many important cases, transport of species and energy can become the rate limiting factor. Determining the molecular transport properties in a multicomponent gaseous mixture requires the measurement or calculation of diffusion coefficients, viscosities, thermal conductivities. Although evaluation of pure species properties follows standard kinetic theory expressions, one can choose from a range of possibilities for evaluating mixture properties. Gas mixture properties can be obtained from pure species properties via certain approximate mixture averaging rules. The input parameters for the mixture averaging calculations in Chemkin are:

- An index which describes if a molecule is monatomic, linear or nonlinear. If the index is 0, the molecule is a single atom. If the index is 1 the molecule is linear, and if it is 2, the molecule is nonlinear.
- The Lennard-Jones potential well depth in Kelvins.
- The Lennard-Jones collision diameter in angstroms.
- The dipole moment in Debye.
- The polarizability in cubic angstroms.
- The rotational relaxation collision number at 298 K.

1.3 Theory of atomistic (ab-initio) modelling

1.3.1 The Hartree Fock method (HF)

The Hartree-Fock method is describing a wave function in terms of the product of one electron spin orbitals. (16) (17)

$$\psi(r_1 \dots r_N) = \chi(r_1) * \chi(r_2) \dots * \chi(r_N), \qquad E = \sum E_{j,i} \tag{44}$$

The one electron wave functions are called spin orbitals. In order calculate these spin orbitals with a computer, they need to be defined using a finite number of functions that will be added together to approximate exact spin orbitals. This can be written as:

$$\chi_j(r) = \sum_{i=1}^{K} \alpha_{i,j} * \phi_i(r), \qquad i \in 1..K, \qquad j \in 1 \dots N \tag{45}$$

This set of functions $\phi_i(r)$ is called the basis set (more to this later on). $\alpha_{i,j}$ is called the expansion coefficient. The wave function in this method is constructed by Slater determinant for a many body system with N electrons which can be expressed as:

$$\psi(r_1, r_2 \dots . r_n) = \frac{1}{\sqrt{N!}} * \begin{vmatrix} \chi_1(r_1) & \chi_2(r_1) & \dots & \chi_N(r_1) \\ \chi_1(r_2) & \chi_2(r_2) & \dots & \chi_N(r_2) \\ \vdots & \vdots & \ddots & \vdots \\ \chi_1(r_N) & \chi_2(r_N) & \dots & \chi_N(r_N) \end{vmatrix} \tag{46}$$

A Hartree-Fock calculation is set up in the following manner where equ. 47 is the Hartree-Fock equation:

$$F\chi_i(x_1) = \epsilon_i \chi_i(x_1) \tag{47}$$

With F the Fock operator:

$$F = h(x_1) + \sum_i [J_i(x_1) - K_i(x_1)] \tag{48}$$

P in this case refers to a specific electron in the system. $F(p)$ are the so called Fock-operators. When it comes to the HF equation $h(p)$ is the one electron operator with respect to the kinetic and nucleus-electron attraction. $J(x_k)$ is the so-called Coulomb operator and $K(x_k)$ is the exchange operator. In order to obtain the HF-Energy one needs to calculate the eigenvalues ϵ_i of the expression 46. This leads to the following equation in Dirac notation:

$$E_{HF} = \sum_i^{occ} \epsilon_i - \frac{1}{2} \sum_i^{occ} < ij||ji > \tag{49}$$

In this case $< ij||ji >$ denotes a special scalar product which is e.g. explained in ref. (18).

Extensions to HF (post Hartree-Fock)

Post Hartree-Fock methods rely on a single reference determinant (Slater determinant). (19) There are a lot of those methods with the most prominent being the coupled cluster (CC) and the Moller Plesset perturbation theory MP (more on those two later).

1.3.2 Density functional theory (DFT)

Density functional theory is useful tool for modern day quantum chemistry analysis. (20) (21) With DFT it is possible to evaluate stable molecule and solid-state geometries and it is possible calculate thermodynamic, electronic and material properties and interatomic/intermolecular potential. It is also possible to predict the feasibility of a reaction and its reaction rate using transition states (Saddle points in the potential energy surface). The main concept of DFT is to calculate the electron density of a many body system. The idea was built around two theorems of Kohn and Hohenberg. (22) With an energy minimization approach in the exchange correlation functional in mind the Kohn-Sham (KS) equations were derived. (20) (21)

$$\left[\frac{h}{2m}\nabla^2 + V(r) + V_H(r) + V_{xc}(r)\right]\psi_i(r) = \varepsilon_i\psi_i(r) \qquad [50]$$

This equation only depends on one three-dimensional spatial variable. The first potential on the left side V(r) describes the interaction between the electrons and the atomic nuclei. The second one is the Hartree potential and it is used to describe the Coulomb repulsion of an electron (in one Kohn Sham equation) and the electron density caused by all electrons in the system. This however leads to the problem self-interaction which. The self-interaction comes from the fact that the electron that is described in the equation is also contributing to the electron density. The Hartree potential can be written as:

$$V_H(r) = e^2 * \int \frac{n(r')}{|r - r'|} d^3r' \qquad [51]$$

The correctional term for this problem is lumped together with descriptions of other effects to define the exchange-correlation potential (V_{xc}) which can written in a derivative form:

$$V_{xc} = \frac{\partial E_{xc}(r)}{\partial n(r)} \qquad [52]$$

The formulation of appropriate exchange-correlation functionals has been a large theoretical effort. (23) There are several approach for different functionals. One is local density approximation (LDA) where it is assumed that there is a uniform electron gas. In this case the electron density is constant so the functional can be exactly derived. There are also other functionals like the generalized gradient approximations (GGA), which uses information on the local electron density). More details on hybrid functionals can be found in the “Hybrid functionals”.
In order to solve the Kohn Sham equations an iterative procedure is chosen. This includes four basic steps:

1. Define an initial “guess” for the electron density n(r)
2. For this initial guess solve the KS equation and solve for the single particle wave functions
3. From this single particle wave function calculate the electron density $n_{KS}(r)$
4. If this electron density is equal to the initially guessed the ground state electron density is reached (The KS equation is self-consistent) and it can be used to calculate. If that is not the case then the “initial guess” must be updated and the procedure starts again.

1.3.3 Basis sets

The basis sets in DFT and HF calculations are used to describe the el. wave function. (24) (25) This is needed in order to solve the partial differential equations using computational methods. When using basis sets the orbitals are converted to a linear combination of basis functions. There are many types of orbitals which are usually split into plane wave-based sets and atomic orbital. The first one is mostly used in modelling solids. The atomic orbitals can be further divided into Slater-Type orbitals (STO), Gaussian-Type orbitals, on which we will mainly focus, and other mostly numerical based methods. The Pople basis sets are among the most used Gaussian basis sets today. These were developed with the thought in mind that mostly valence electrons contribute to the formation of bonds. As a consequence, basis sets with multiple functions corresponding to each valence atomic orbital were created. These basis sets are named after the number of functions for each orbital, i.e. double, triple and quadruple zeta. Each Pople basis set is named by a number to describe the count of primitive Gaussian functions for each core atomic orbital. This is followed by a few variables where each corresponds to the basis functions used to describe the valence atomic orbital (with the quantity of variables describing doubles, triples, quadruples etc.). One or more pluses specify the addition of one or more diffuse functions and the same goes for asterisks but with polarization functions. For more detailed information see (24) and (25). The correlational consistent basis sets are the most used besides the ones created by Pople. The reason for this is that these basis sets were designed to converge post HF methods. These methods, however, are too elaborate to profoundly cover in this thesis. Thus, it is recommended to examine the information given in references (26) (27) (28) (29) (30) (31) (32) (33) .

1.3.4 Hybrid functionals

Hybrid functionals are constructed as a combination of exact Hartree Fock exchange functionals and exchange and correlation density functionals. (34) (35) (36) One of this functionals is B3LYP, which stands for Becke, three parameter, Lee-Yang-Paar. In this case the Becke is a reference to the Becke88 exchange functional. Lee Yang and Paar on the other hand developed the correlation functional. The exchange functional follows the form:

$$E_{cx}^{B3LYP} = (1-a)E_x^{LSDA} + aE_x^{HF} + b\Delta E_x^B + (1-c)E_C^{LSDA} + cE_c^{LYP} \quad [53]$$

Where a and b are constants, c includes a generalized gradient approximation (GGA), E_x^{LSDA} and E_C^{LSDA} are exchange/correlational functionals using a local spin density approximation, E_x^{HF} is the Hartree Fock exchange functional, E_x^B is the Becke88 exchange functional and E_c^{LYP} is the Lee-Yang-Paar correlational functional.

1.3.5 Moller Plesset Perturbation Theory (MPPT)

The MPPT is an extensively used method for the calculating approximation for the correlational energy. (37) Each MPPT approach has a number assigned to it determining the order of perturbation theory. The second order (level 2) Moller Plesset perturbation theory (MP2) is one of the most easily manageable and useful methods. Also the fourth order MPPT (MP4) is used a lot in thermochemical composite methods like G3 and G4. In MPPT a small perturbation is added to the unperturbed Hamiltonian operator, this approach is known in a general sense as a Rayleigh-Schrödinger perturbation theory. This can be written as:

$$H = H_0 + \lambda * V \qquad [54]$$

With:

$$H^0 = \sum_p F(p) = \sum_p h(p) + \sum_{p,i} [J_i(p) - K_i(p)] \qquad [55]$$

In this case, λ is a real number parameter, H_0 is the unperturbed Hamiltonian operator obtained by summing over all Fock-operators and V is the perturbation operator. What distinguishes the MPPT from other perturbation theories is that it starts the perturbation expansion using an HF calculation. Therefore, the zeroth order wave function is given by the sum of Fock operators. This is expressed by the two equations 46 and 47. When using the perturbation operator V, the first correctional energy results as:

$$E_{MP}^1 = < \phi^0 | V | \phi^0 > = -\frac{1}{2} * \sum_{i,j} < ij||ji > \qquad [56]$$

Therefore, the first order correlational energy correction (MP1 energy) is equal to the HF energy which is expressed by:

$$E_{MP}^1 = E_{HF} = \sum_i^{occ} \epsilon_i - \frac{1}{2} \sum_i^{occ} < ij||ji > \qquad [57]$$

In this case i and j are the occupied orbitals. The second order correlational energy correction (MP2 energy) is described by the expression below:

$$E_{MP}^2 = \sum_{s>0} \frac{V_{0s} * V_{so}}{E_0 - E_s} \qquad [58]$$

If the Slater-Condon rule is used, the second order correction equates to the mathematical statement beneath:

$$E_{MP}^2 = \frac{1}{4} \sum_{i,j}^{occ} \sum_{a,b}^{vir} < ij||ab > a_{ij}^{ab} \quad with \quad a_{ij}^{ab} = \left(\epsilon_i + \epsilon_j - \epsilon_a - \epsilon_b\right)^{-1} < ab||ij > \qquad [59]$$

Where i and j are once again the the occupied orbitals and a and b are the "virtual" orbitals. a_{ij}^{ab} is the D excitation amplitude and ϵ_i, ϵ_j, ϵ_a and ϵ_b are the orbital energies. For the description of higher versions of MPn theory look at ref. (37).

1.3.6 Coupled cluster methods (CC)

The coupled cluster method develops a multi-electron wave function from basic HF molecular orbitals. (38) (39) (40) This is done by creating an exponential cluster operator to consider the electron correlation. The wave function in CC is expressed by an exponential ansatz which is written as:

$$|\Psi> = e^T|\Phi_0> \quad [60]$$

In this case, T stands for the cluster operator which takes the form below, $|\Phi_0>$ is the reference wave function which is typically determent using a Slater-determinant from HF-MO.

$$T = T_1 + T_2 + T_3 \ldots \quad [61]$$

With:

$$T_n = \frac{1}{(n!)^2} * \sum_{i1\ldots in} \sum_{a1\ldots an} t_{a1\ldots an}^{i1\ldots in} a^{a1} a^{a2} \ldots a^n a_{in} \ldots a_{i2} a_{i1} \quad [62]$$

The number stands for the excitation states, therefore the number one is used to express single excitations (which means T1, it is therefore the operator of all single excitations), the number two stands for double excitations, etc. In the expression a^a and a_i are creation and annihilation operators, the index i stands for the occupied orbitals while the index a stands for unoccupied orbitals. t are the unknown coefficients which need to be solved for. The Schrödinger equation for the CC method is formulated in the following manner:

$$H|\Psi_0> = He^T|\Phi_0> = Ee^T|\Phi_0> \quad [63]$$

The name for different types of CC methods is given by the letter CC as well as S, D, T and Q which respectively stands for singles, doubles, triples and quadruples. For perturbation theory-based calculations terms in round brackets are being used, e.g. the CCSD(T) stands for singles and doubles using the CC method and triples utilizing many-body perturbation theory.

1.3.7 Calculation of frequencies

Vibrational frequencies (modes) are acquired by analysis of the Hessian matrix being the matrix form of the second derivative of the energy with respect to geometry. (41) (42)
Each element of the Hessian matrix can be written as:

$$H_{i,j} = \frac{\delta^2 E}{\delta x_i \delta x_j} \quad [64]$$

For the analysis with regards to the vibrational frequencies, mass needs to be added to the system which is done by:

$$H_{i,j}^{m} = \frac{H_{i,j}}{\sqrt{M_i * M_j}} \quad [65]$$

M_i and $M_j$are the atomic weights in amu. Matrix diagonalization gives back the eigenvalues ϵ_i which can be used to calculate the vibrational frequencies υ. The modes are then computed by means of:

$$\upsilon = \frac{f}{c} = \frac{1}{2\pi c} * \sqrt{\epsilon_i} \quad [66]$$

In this formula c is the speed of light. The vibrational frequencies are given in inverse centimeters because of spectroscopy conventions.

1.3.8 Calculation of thermodynamic properties in ab initio (Rigid rotor harmonic oscillator)

As a mean to calculate thermodynamic properties using ab initio quantum chemistry calculations, statistical thermodynamics are needed to convert the molecular energy levels into useful thermodynamic data. (12) These molecular energy levels originate from a molecule's translation, rotation, vibration and electronic excitation. This represents the molecule's spectroscopy. The results always need to be corrected based on temperature and molecular spectroscopy. This is achieved using the molecular partition function Q, which is calculated from the molecular energy levels ϵ_i.

$$Q(T) = \sum \exp\left(-\frac{\epsilon_i}{kT}\right) \quad [67]$$

Usually the lowest energy level in the system represents the energy level zero. This means there are no negative energy levels. There are four important equations linking the thermodynamic properties with the partition function.

$$S(T) = N_A * k * \left[\frac{\partial}{\partial T}(T * \ln(Q) - \ln(N_A) + 1\right] \quad [68]$$

$$c_v(T) = N_A * k * T * \frac{\partial^2}{\partial T^2}(T * \ln(Q)) \quad [69]$$

$$c_p(T) = c_v + R \quad [70]$$

$$[H(T) - H_0] = \int_0^T c_p dT = \frac{R * T^2}{Q} * \frac{\partial Q}{\partial T} + RT \quad [71]$$

In this case S is entropy, c_v is the heat capacity at constant volume, c_p is the heat capacity at constant pressure, N_A is the Avogadro constant and k is the Boltzmann constant. However most times the complete set of energy levels is not available therefore it is approximated that translation, rotation vibration and excitation are all unaffected by each other. This in turn means the partition function can be separated into the four parts.

$$Q \approx Q_{vib} Q_{rot} Q_{trans} Q_{el} \quad [72]$$

Translational partition function and thermodynamic function

The translational partition function is approximated using an integral over all translational energy levels. (12) This results in the following equations:

$$Q_{trans} = (2 * \pi * m * k * T)^{2/3} * h^{-3} * V \; where \; V = \frac{R * T}{p} \quad [73]$$

$$S_{trans} = R\left[\frac{3}{2} * \ln(2 * \pi * m * h^{-2}) + \frac{5}{2} * \ln(k * T) - \ln(p) + \frac{5}{2}\right] \quad [74]$$

$$c_{p,trans} = \frac{5}{2}R \quad [75]$$

$$[H(T) - H_0]_{trans} = \frac{5}{2}R \quad [76]$$

In this case m is the weight of the molecule in amu, h is the Planck constant and p is the pressure.

Rotational partition function and thermodynamic function

The rotation of a rigid molecule is a quantized property. (12) The rotational spectra are characterized by three constant which are given with the formulas:

$$A = \frac{h}{8 * \pi^2 I_A}, \qquad B = \frac{h}{8 * \pi^2 I_B}, \qquad C = \frac{h}{8 * \pi^2 I_C}, \quad [77]$$

$$with \; the \; convention \; that \; I_A < I_B < I_c$$

Where the I's are the (principal) moments of inertia. With that we obtain the following equations for linear and nonlinear molecules:

$$Q_{rot} = \frac{8 * \pi^2}{\sigma * h^3} * (2 * \pi * k * T)^{\frac{3}{2}} * (I_A I_B I_C)^{\frac{1}{2}} \quad [78]$$

$$S_{rot} = R * \left[\frac{3}{2} * \ln\left(\frac{k * T}{h}\right) - \frac{1}{2} * \ln\left(\frac{A * B * C}{\pi}\right) - \ln(\sigma) + \frac{3}{2}\right] \quad [79]$$

$$c_{p,rot} = \frac{3}{2} * R \quad [80]$$

$$[H(T) - H_0]_{rot} = \frac{3}{2} * R * T \quad [81]$$

$$Q_{rot}^{linear} = \frac{8 * \pi^2 * I * k * T}{\sigma * h^2} \quad [82]$$

$$S_{rot}^{linear} = R * \left[ln\left(\frac{k * T}{\sigma * h * B}\right) + 1 \right] \quad [83]$$

$$c_{p,rot}^{linear} = R \quad [84]$$

$$[H(T) - H_0]_{rot}^{linear} = R * T \quad [85]$$

In this case σ is the so-called external symmetry number which depends on the symmetry (point group) of the molecule.

Vibrational partition function and thermodynamic function

For a molecule with N atoms there are N-6 molecular frequencies (modes) that need to be considered. (12) If the molecule is linear then there are N-5 frequencies that need to be considered. The according thermodynamic functions are:

$$Q_{vib} = \prod_i \frac{1}{1 - exp\left(-\frac{\nu_i * h}{k * T}\right)} \quad [86]$$

$$S_{vib} = -R * \sum_i ln\left(1 - exp\left(-\frac{\nu_i * h}{k * T}\right)\right) + R * \sum_i \frac{\nu_i * h}{k * T} * \frac{exp\left(-\frac{\nu_i * h}{k * T}\right)}{\left(1 - exp\left(-\frac{\nu_i * h}{k * T}\right)\right)} \quad [87]$$

$$c_{p,vib} = R * \sum_i \left(\frac{\nu_i * h}{k * T}\right)^2 * \frac{exp\left(-\frac{\nu_i * h}{k * T}\right)}{\left(1 - exp\left(-\frac{\nu_i * h}{k * T}\right)\right)^2} \quad [88]$$

$$[H(T) - H_0]_{vib} = R * T * \sum_i \frac{\nu_i * h}{k * T} * \frac{exp\left(-\frac{\nu_i * h}{k * T}\right)}{\left(1 - exp\left(-\frac{\nu_i * h}{k * T}\right)\right)} \quad [89]$$

Electronic partition function and thermodynamic function

Most molecules don't have low-lying electronic excitation states. (12) Some however have degenerate ground state. The degeneracy or multiplicity (g) is therefore the most important quantity in the determination of el. partition and thermodynamic functions. The el. partition and thermodynamic functions are therefore given by the following equations:

$$Q_{el} = \sum g_i * \exp\left(-\frac{\epsilon_i}{k * T}\right) \quad [90]$$

$$S_{el} = R * ln\left(\sum g_i * \exp\left(-\frac{\epsilon_i}{k * T}\right)\right) + R * \frac{\sum g_i * \exp\left(-\frac{\epsilon_i}{k * T}\right) * \left(\frac{\epsilon_i}{k * T}\right)}{\sum g_i * \exp\left(-\frac{\epsilon_i}{k * T}\right)} \quad [91]$$

$$c_{p,el} = R * \left(\frac{\sum g_i * \exp\left(-\frac{\epsilon_i}{k * T}\right)^2 * \left(\frac{\epsilon_i}{k * T}\right)}{\sum g_i * \exp\left(-\frac{\epsilon_i}{k * T}\right)}\right) - R * \left(\frac{\sum g_i * \exp\left(-\frac{\epsilon_i}{k * T}\right) * \left(\frac{\epsilon_i}{k * T}\right)}{\sum g_i * \exp\left(-\frac{\epsilon_i}{k * T}\right)}\right)^2 \quad [92]$$

$$[H(T) - H_0]_{el} = R * T * \frac{\sum g_i * \exp\left(-\frac{\epsilon_i}{k * T}\right) * \left(\frac{\epsilon_i}{k * T}\right)}{\sum g_i * \exp\left(-\frac{\epsilon_i}{k * T}\right)} \quad [93]$$

1.3.9 Obtaining enthalpies of formation using ab initio

It is not a trivial task to calculate enthalpies of formation using ab initio methods but there are several standard approaches. One of those is the method described by (43) which we will refer to as the energy approach. For this method every enthalpy of formation of every other species besides the species of interest must be known. First, the total energy for each species is calculated using the same ab initio method and basis set. Then, the reaction energy is calculated by multiplying each of the total energies with their according stoichiometric coefficients and then adding them up for the product species as well as subtracting the ones from the reactants. The next method is the so-called quantum chemistry composite method. (44) (45) In this approach, several different calculations using a higher-level of theory with smaller basis sets as well as lower-level theories with larger basis sets are being combined. This approach aims for a high chemical accuracy. The two most common methods are the G3/G3MP2 and the G4/G4x6. Other used methods are the ccCA-S4 method and the ccCA-CC(2,3) method. The G3 procedure includes the following steps:

- An MP2/6-31G(d) geometry optimization
- Quadratic configuration interaction (QCISD(T)/6-31G(d)), MP2 and MP4 calculations
- An MP4/6-31G(2df,p) calculation for the evaluation of the effects of polarization functions
- An MP4/6-31+G(d,p) calculation for the evaluation of the effect of the diffuse functions

- MP2 calculation using large basis set called G3large
- An HF/6-31G(d) geometry optimization
- An HF/6-31G(d) calculation for the determination of the ZPVE (zero-point vibrational energy)

In the end, the various energy changes are added together to the combined energy.

1.4 Aluminum (III)-Nitride (AlN) from $AlCl_3$, H_2 and NH_3

Aluminum nitride coating are used in many electronic applications such as high energy electronics. (46) (47) This is because of their thermal conductivity and low thermal expansion coefficient. Aluminum nitride crystallizes in a wurtzite crystal structure (P 63 m c). The CVD process of AlN in the $AlCl_3$-H_2-NH_3 system is performed using temperatures between 700 and 1500K with working pressures between 10 to 50 Torr.

Description of the reaction mechanism

The reaction mechanism consisting of 11 gas phase and 4 surface reaction were developed previously. (47) The surface reactions were originally proposed in ref. (48). Most of the gas phase reactions were developed for combustion systems and can be reused for CVD. The table below gives a representation of the reactions taking place and the according Arrhenius parameters.

Reaction mechanism for the AlN-CVD system

Surface Reaction				
Reaction nr.	Reaction	α	β	E_a/R
S1	$AlCl_3 + N(S) \rightarrow N(B) + Al(S) + Cl_2 + Cl$	1,59E+08	0,5	8654
S2	$Al(S) + NH_3 \rightarrow Al(B) + N(S) + H + H_2$	4,45E+08	0,5	7700
S3	$AlCl_2NH_2 + Al(S) \rightarrow Al(B) + N(S) + 2\ HCl$	1,72E+08	0,5	5100
S4	$AlCl_2NH_2 + N(S) \rightarrow N(B) + Al(S) + 2\ HCl$	1,72E+08	0,5	5100

Gas phase reactions				
Reaction nr.	Reaction	α	β	E_a/R
G1	$AlCl_3 + NH_3 \rightarrow AlCl_2NH_2 + HCl$	4,21E+13	0	4198
G2	$H + Cl + M \rightarrow HCl + M$	7.20E+21	-2	0
G3	$Cl + Cl + M \rightarrow Cl_2 + M$	2.00E+14	0	-901
G4	$H + HCl \rightarrow Cl + H_2$	1.69E+13	0	2082
G5	$Cl_2 + H \rightarrow Cl + HCl$	8.60E+13	0	590
G6	$H + H + H_2 \rightarrow H_2 + H_2$	9,70E+16	-0,6	0
G7	$H_2 + M \rightarrow 2\ H + M$	2,20E+14	0	48365
G8	$HCl + M \rightarrow H + Cl + M$	7,90E+25	-3	53589
G9	$Cl + H_2 \rightarrow H + HCl$	2,95E+13	0	2567
G10	$H_2 + H_2 \rightarrow H + H + H_2$	8,80E+14	0	48364
G11	$2\ H + M \rightarrow H_2 + M$	6,53E+17	-1	0

Table 1 Reaction mechanism of the AlN CVD system ©

Thermodynamics of the $AlCl_3$-H_2-NH_3 system

The thermodynamics of the AlN-CVD system were analyzed in the ref. (47) and the resulting graph is:

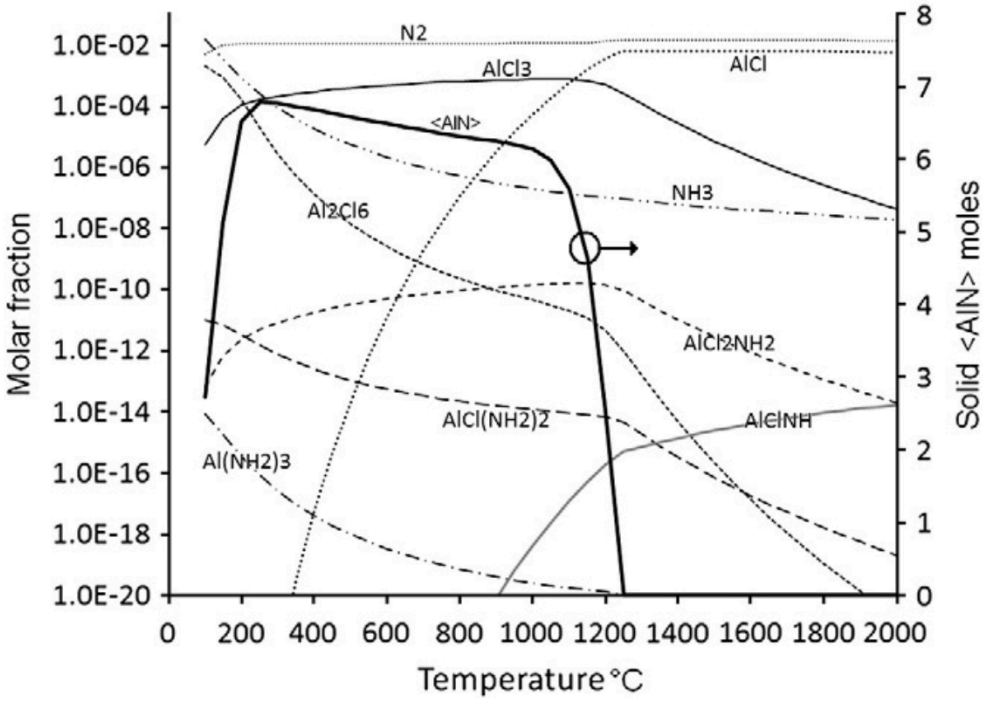

Figure 5 Equilibrium molar fraction of the TiN CVD system

The graph shows that aluminum-trichloride is the most stable form of aluminum-chloride in the for CVD reasonable temperature ranges (Therefore has the highest equilibrium molar fractions). Furthermore, the most stable compound formed with ammonia is $AlCl_2NH_2$. However, keep in mind that these graphs only consider equilibrium conditions. For most CVD processes the conditions are far from equilibrium and are mostly determined by reaction kinetics but the equilibrium calculations can still be seen as a first indicator toward a working CVD process especially for high temperature CVD (thermodynamical regime).

1.5 Titanium (III)-Nitride (TiN) from TiCl4, H2 and NH3

Because of their high hardness, good chemical/thermal stability and excellent thermal and electrical conductivity TiN thin films (coatings) are widely used in machining and forming tools as well as diffusion barriers in microelectronics. (49) (50) (51) They are produced either by PVD or CVD. When it comes to the production via CVD usually a system is used, that consists of the gases $TiCl_4$, H_2 and NH_3 or $TiCl_4$, H_2 and N_2. The CVD with NH_3 in the system is usually carried out between 323K and 1900K and a pressure between 1-50 Torr. The CVD system with the N_2 on the other hand needs a more specific temperatures ranging from 900 to 1200°C.

Description of the reaction mechanism

The reaction mechanism used for simulations was first proposed by (52) and was later reduced by (50). For a more realistic deposition rate, we considered additionally an unreactive complex formation proposed by (49). The upcoming table gives an overview of the considered reactions in the $TiCl_4$-H_2-NH_3 system and the corresponding Arrhenius parameters. Also a feature of this system worth mentioning is the transition of the oxidation state from (IV) in $TiCl_4$ to (III) in TiN.

Reaction mechanism for the TiN-CVD system				
Surface Reaction				
Reaction nr.	Reaction	α	β	E_a/R
S1	$TiCl_3 + NH_2(S) \rightarrow N(B) + TiCl_2(S) + HCl$	1,00E+14	0,5	4900
S2	$TiCl_4 + NH_2(S) \rightarrow N(B) + TiCl_3(S) + HCl$	1,00E+14	0,5	4900
S3	$TiCl_3(S) + NH_3 \rightarrow Ti(B) + NH_2(S) + HCl + Cl_2$	2,40E+11	0,5	4900
S4	$TiCl_2(S) + NH_3 \rightarrow Ti(B) + NH_2(S) + HCl + 0{,}5\ Cl_2$	2,40E+11	0,5	4900
Gas phase reactions				
Reaction nr.	Reaction	α	β	E_a
G1	$TiCl_4 \rightarrow TiCl_3 + Cl$	2,32E+20	-1,17	387,9
G2	$TiCl_3 \rightarrow TiCl_2 + Cl$	1,02E+18	-0,742	422,6
G3	$TiCl_2 \rightarrow TiCl + Cl$	3,65E+20	-1,06	509,6
G4	$TiCl_4 + H \rightarrow TiCl_3 + HCl$	5,11E+06	2,5	12,6
G5	$TiCl_3 + H \rightarrow TiCl_2 + HCl$	1,11E+06	2,5	33,5
G6	$TiCl_2 + H \rightarrow TiCl + HCl$	3,05E+06	2,5	145,2
G7	$TiCl + H \rightarrow Ti + HCl$	4,09E+05	2,5	24,7
G8	$H + Cl + M \rightarrow HCl + M$	7,20E+21	-2	0
G9	$HCl + M \rightarrow H + Cl + M$	7,90E+25	-3	445,6
G10	$Cl + Cl + M \rightarrow Cl_2 + M$	2,00E+14	0	7,5
G11	$H + HCl \rightarrow Cl + H_2$	1,69E+13	0	17,2
G12	$Cl + H_2 \rightarrow H + HCl$	2,95E+13	0	21,3
G13	$Cl_2 + H \rightarrow Cl + HCl$	8,60E+13	0	5
G14	$H + H + H_2 \rightarrow H_2 + H_2$	9,70E+16	-0,6	0
G15	$H_2 + M \rightarrow 2\ H + M$	2,20E+14	0	402,1
G16	$TiCl_4 + 2\ NH_3 \rightarrow TiCl_4{:}(NH3)_2$	1,75E+18	0	38,2
G17	$H + H + M \rightarrow H_2 + M$	6,53E+17	-1	0

Table 2 Reaction mechanism of the TiN CVD system ©

Thermodynamics of the $TiCl_4$-H_2-NH_3 system

The thermodynamic simulations which are seen below are taken from (53).

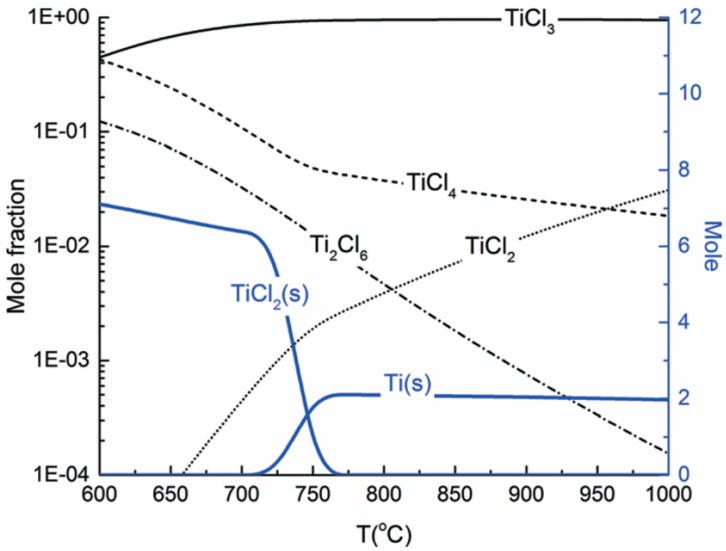

Figure 6 Equilibrium molar fraction of the TiN CVD system

The graph indicates that in reasonable temperature range for TiN deposition $TiCl_3$ is the dominant species in equilibrium. Unfortunately however in this graph no complex/compound formation with ammonia was considered.

1.6 Titanium-Aluminum-Nitride ($Ti_xAl_{1-x}N$) from $TiCl_4$, $AlCl_3$, H_2 and NH_3

Although titanium-aluminum-nitride is the main focus of this thesis, very little is known about the reactions taking place in the system, i.e. there is no agreed upon reaction mechanism. (54) (55) (56) (57) (58) (59) The interest in this topic, however, yields from the properties of the thin films created by CVD. Mainly the phase stability and the microstructure have been analyzed. In the microstructural studies, chemically periodic gradients have been discovered. The same studies also suggest that there are self-organized micro-lamellar structures. It is shown that the lamella periodicity predominantly depends on the pressure during the deposition process. Firstly, it was suggested that spinodal decomposition was the cause for the formation of these characteristics but this has been disproven by the same group. Both of these features can be seen in the images below.

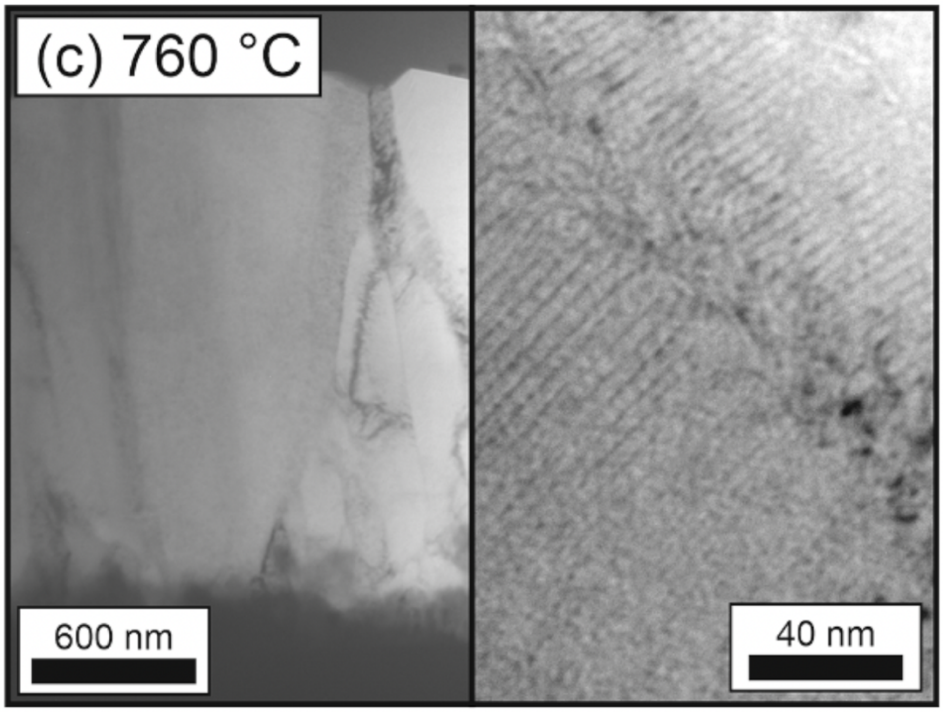

Figure 7 TiALN microstructure with lamella periodicity [Source: (60)]

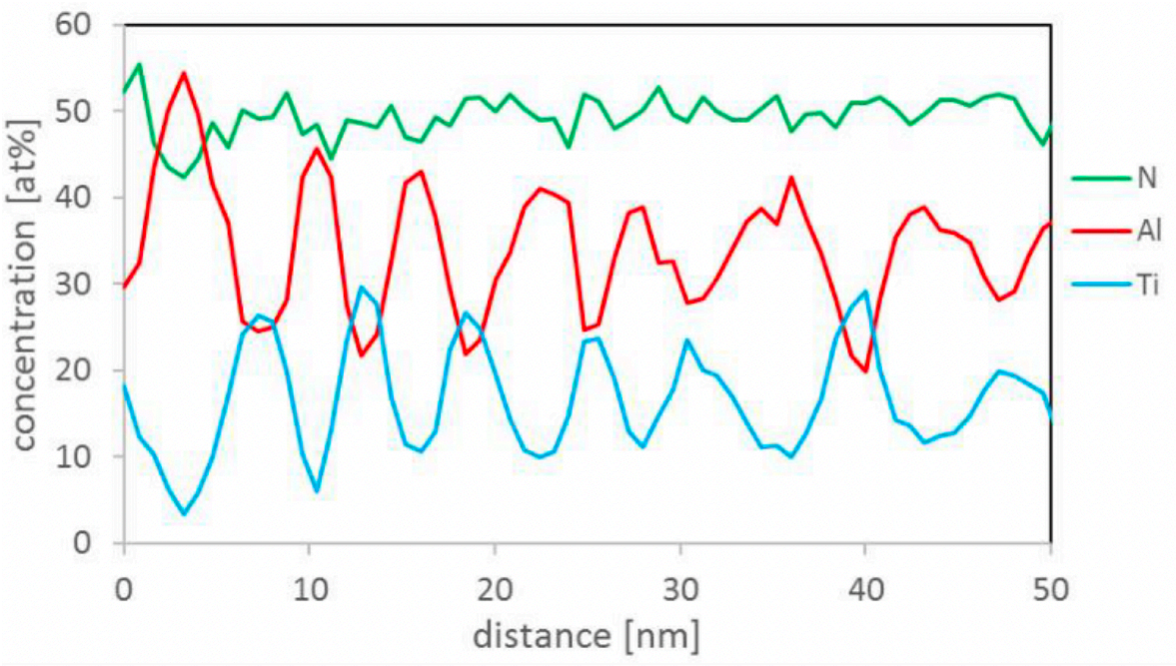

Figure 8 Chemical composition of a TiAlN system using atom probe tomography [Source: (61)]

2 Methodology

2.1 Ab Initio calculations

Ab initio calculations were performed in order to find thermodynamic, thermochemical and transport properties of different molecules. All ab initio calculations were performed using the GAMESS software package (62), which is an open-source software. (63) GAMESS offers many different ab initio models, which includes DFT, MP, CC, molecular dynamics and even some Monte Carlo methods. All molecule designs and all the input files for GAMESS were created using Avogadro software, which is also open source.

2.1.1 Geometry optimization

The geometry of each of the molecules is optimized with different basis-sets (3-21G, 6-31G, 6-31G* with both the B3LYP (DFT) Methods as well as Moller Plesset perturbation theory (MP2)) and if available compared to the CCCBDB Database. The SCF type used for all calculations is open shell restricted Hartree Fock (ROHF).

2.1.2 Vibrational analysis and thermochemistry

The analysis of the vibrational frequencies is performed using the same basis sets as for the geometry optimization. The vibrational frequencies were used in order to calculate the thermochemical properties including the standard state entropy (S(T)), the heat capacity (Cp(T)), the integrated heat (H(T)-H0) and the Gibbs free energy (G(T)). This is done utilizing the rigid rotator harmonic oscillator approximation derived from the different partition functions (translational, rotational, vibrational and electronic) as described in the introduction. In the simulations no symmetry is used which means the rotational entropy must be corrected by hand using the equation 79. Also the vibrational components of the integrated heat capacity need to be recalculated (equation 89) because GAMESS uses wrong frequencies.

2.1.3 Calculating enthalpies of formation (Composite thermochemistry methods)

In order to obtain the enthalpies of formation, various approaches are tried including the G3MP2 method for the aluminum compounds as well as the “energy approach” utilizing a MP2/6-31* level of theory for the titanium compounds. This is done because the G3MP2 method does not support the transition metals.

2.1.4 Dipole moments and polarizability

Both the dipole moments and polarizability were calculated using the B3LYP/6-31G* method. Using GAMESS, the dipole moments were analyzed during a run with the run type “energy” and including the group/input $ELMOM IEMOM=1 WHERE=COMASS $END. This method determines the directional dipole moments in the center of mass and for each Cartesian coordinate although as a transport property, only the radial dipole moments are needed. This, in turn, means that the directional dipole moments need to be averaged. For the polarizability, “FFIELD” calculation was performed. While using this sort of calculation, the most common method is the finite field which allows the study of linear polarizabilities and the second order

hyperpolarizabilities. Large basis sets and high accuracy of the wavefunctions are needed for accurate finite field calculations which is the reason why the accuracy recommendations from (64) are implemented.

2.1.5 Fitting the data to Nasa-Polynomials

The fitting procedure for the thermodynamic ab initio data is performed using the FitDat utility from Ansys. This requires the input of the species information as well as the thermodynamic data for different temperature ranges. The fits are done by a using a least square fit method with given constraints which are explained by ref. (65).

2.2 Ansys Chemkin

The different CVD systems, i.e. TiN, TiAlN and AlN, were simulated at the reactor scale using the Chemkin software package. Perfectly stirred reactors simulations were set up and the systems were analyzed with regards to the deposition rate at different gas temperatures, substrate temperatures and pressures. Both the TiN and the AlN simulations were performed at a fixed substrate temperature and fixed gas composition. When it comes to the TiAlN PSR simulations, the gas composition is varied with respect to the inlet gas. This is realized by setting the molar fractions of NH_3: $TiCl_4$: $AlCl_3$ to 2:0,5:1,5 to 2:1:1 and respectively to 2:1,5:1. Also gas phase temperature is varied in the TiAlN system. All input files and set up parameters can be found in the appendix.

3 Results

3.1 Theoretical calculation of surface site densities

As stated in the introduction it is possible to calculate surface site densities in most crystalline systems. For most technical applications there are three common crystal structures with well-defined sites. These two are the hexagonal structures and the face centered cubic (FCC) and the body centered cubic (BCC). The surface site density is defined as the number of surface sites per area. The chosen approach was to calculate the surface site density in terms of a pre-factor (depends on the number of sites in the area of interest and the geometry) which is given by the crystal structure and one characteristic length for the crystal structure.

$$s_{den} = \frac{N_{sites}}{A} = f * \frac{1}{l^2} \quad [94]$$

Hexagonal structures and FCC (111)

The possible adsorption sites in hexagonal systems are the bridges between two neighboring atoms, in the gap between three atoms and on top of every atom. (66) This is shown in the following illustration.

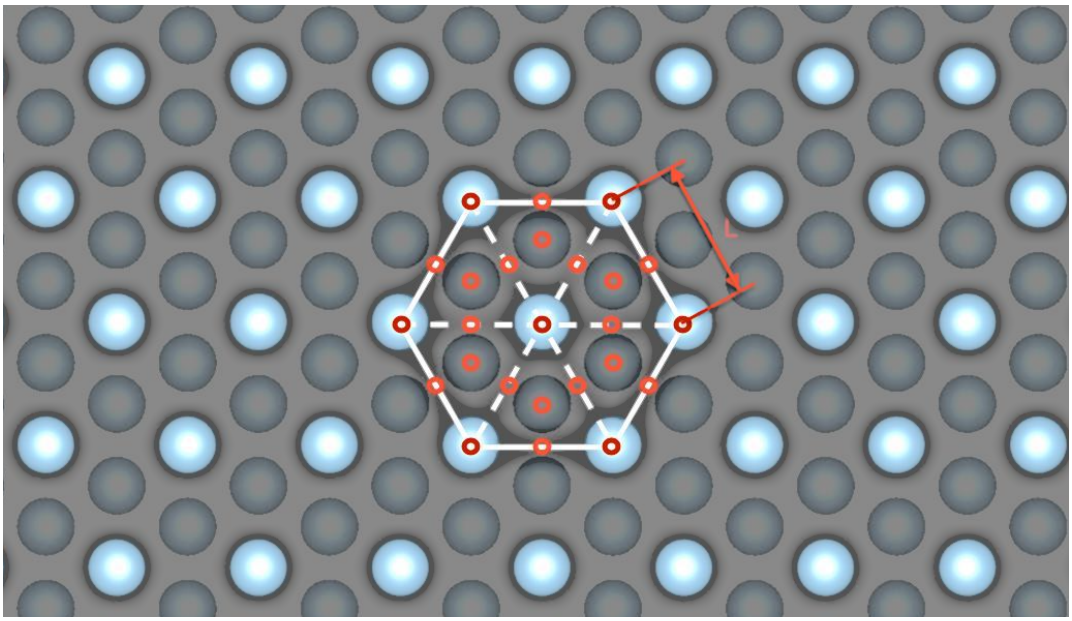

Figure 9 Illustration of the possible adsorption sites (red dots) in a FCC (111) system. The light grey atoms are the surface atoms and the dark atoms are the atoms in the layer below.©

The pre-factor for the hexagonal (0001) crystal and the FCC (111) structure is:

$$N_{sites,hex} = N_{top} + N_{bridge,2} + N_{gap,3} = \left(6 * \frac{1}{6} + 1\right) + \left(6 * \frac{1}{2} + 6\right) + 6 = 17 \quad [95]$$

$$A_{HEX} = \frac{3 * \sqrt{3}}{2} * l^2 \quad [96]$$

$$f_{Hex} = \frac{17 * 2}{3 * \sqrt{3}} \approx 6{,}53 \quad [97]$$

The characteristic length the case of a hexagonal system is the side length. The number 17 comes from the possible adsorption sites in the hexagonal structure the rest is just to obtain the area of the hexagonal shape with the characteristic length.

FCC (001)

The possible sites in the FCC (001) system include the gaps between four atoms, the bridges between two atoms and the tops of each atom. (66)

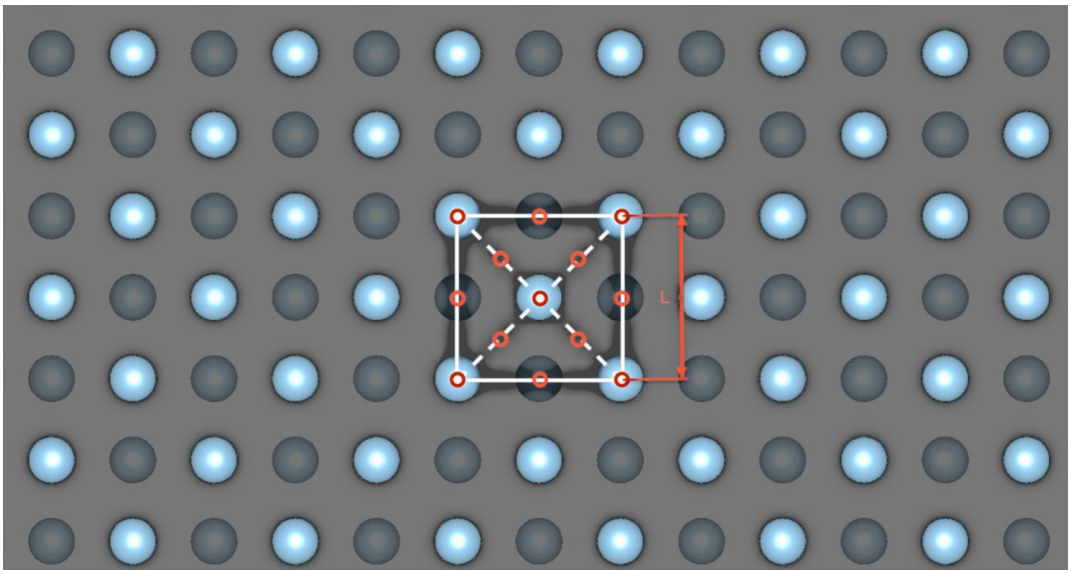

Figure 10 Illustration of the possible adsorption sites (red dots) in a FCC (001) system where the light grey atoms are the surface atoms and the dark grey atoms are the atoms in the layer below. ©

The pre-factor for the FCC (001) crystal structure is:

$$N_{sites,hex} = N_{top} + N_{bridge,2} + N_{gap,4} = \left(4 * \frac{1}{4} + 1\right) + 4 + \left(4 * \frac{1}{2}\right) = 8 \quad [98]$$

$$A_{FCC} = l^2 \quad [99]$$

$$f_{FCC} = 8 \quad [100]$$

This factor arises from the fact that there are eight adsorption sites in the FCC (001). The area is just the square of the side length of one unit cell (i.e. the lattice parameter), which mean there is no influence on the pre-factor. This calculation should also be valid for systems like the NaCl (001) structure (the Fm-3m space group). All structures in this chapter are created with the Vesta software package and crystallographic data from the crystallography open database.

Titanium nitride (TiN)

The structure of TiN is a Fm-3m space group which corresponds to the NaCl structure. The lattice constant is 4,244 Angstroms. The surface was modeled in the (001) and (111) directions.

The titanium-nitride (001) surface:

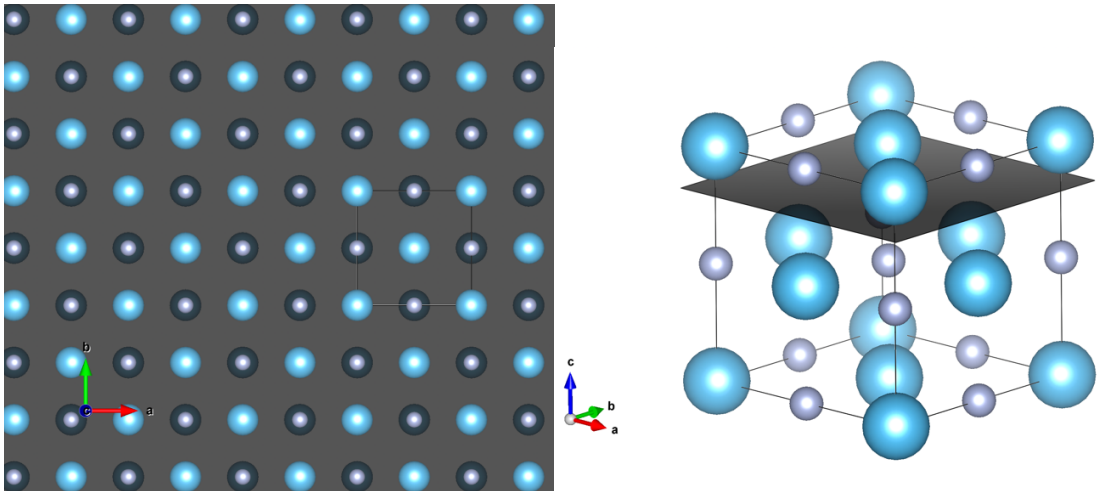

Figure 11a Surface of TiN on the (001) plane and 3-dimensional Illustration of TiN and the (001) plane ©

The calculated surface site density for the TiN (001) surface is 7,376E-09 mole/cm^2.

The titanium-nitride (111) surface:

The TiN (111) surface is as stated above a system with "hexagonal" symmetry with a characteristic length of l=3,00096 Angstroms.

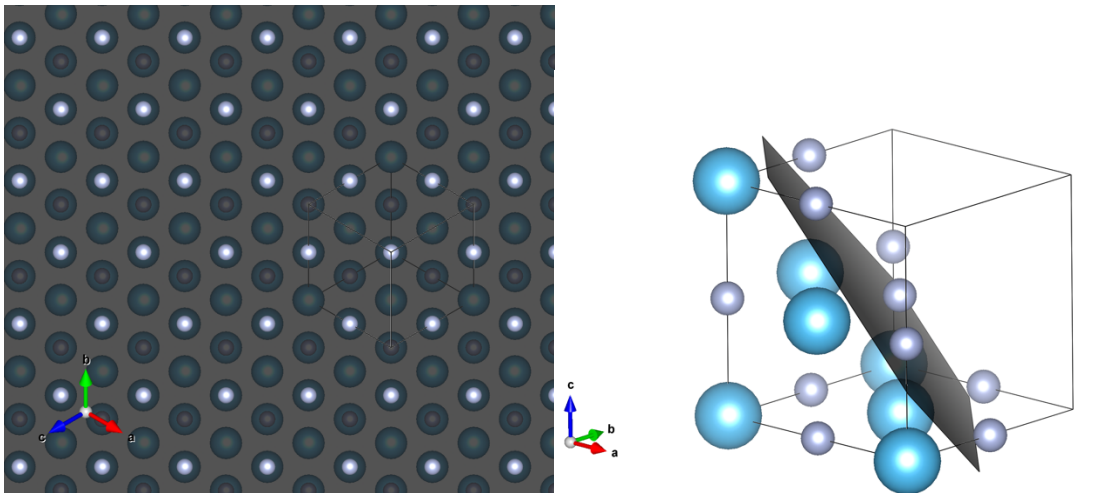

Figure 12a Surface of TiN on the (111) plane and 3-dimensional Illustration of TiN and the (111) plane ©

For the titanium-nitride (111), a surface density of 1,207E-08 mole/cm^2 was calculated.

Titanium

Both crystal structures for titanium were considered. The alpha structure is a hexagonal structure of the P 63/m m c space group with lattice parameters of 2.9064, 2.9064, 4.6667

90°, 90° and 120°. The beta structure is a FCC structure in the Fm-3m space group with a lattice parameter of 2.9064 Angstroms.

The α -Ti (0001) surface:

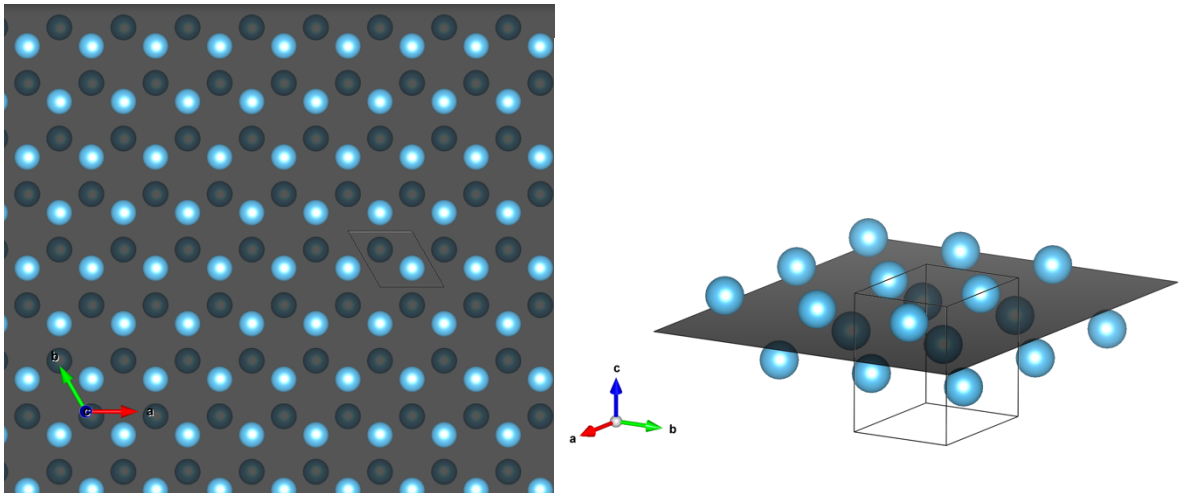

Figure 13a Surface of Ti on the (0001) plane and 3-dimensional Illustration of Ti and the (0001) plane ©

The critical length of the alpha titanium (0001) surface is l=2,9064 Angstroms and the evaluated surface site density is 1,286E-08 mole/cm^2.

The β-Titanium (001) surface:

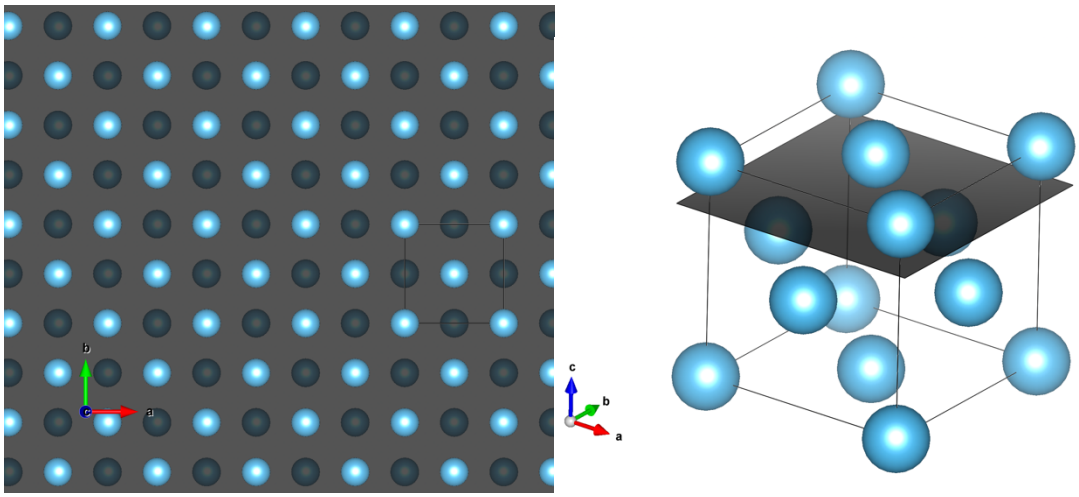

Figure 14a Surface of Ti on the (001) plane and 3-dimensional Illustration of Ti and the (001) plane ©

The surface site density for this surface is 8,059E-09 mole/cm^2.

The β -Titanium (111) surface:

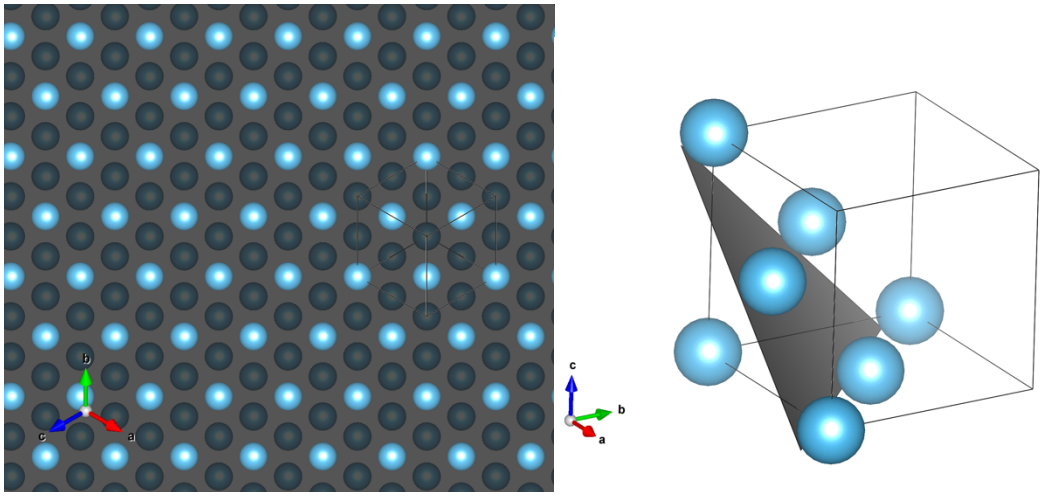

Figure 15a Surface of Ti on the (111) plane and 3-dimensional Illustration of Ti and the (111) plane ©

The surface site density on the beta titanium (111) surface is 1,318E-08 mole/cm^2.

Aluminum oxide (α-Al_2O_3)

The alpha structure of aluminum oxide is a rhombohedral crystal structure with a R -3 c:H space group. The lattice parameters are 4.7606, 4.7606, 12.994, 90°, 90° and 120°. Ever since the adsorption is mostly happening on the oxygen sites, a simplified representation of the sites is used. In our model the oxygens are in a nearly hexagonal on the (0001) surface. For this system the count of adsorption sites per hexagon is 2 (1 for the central atom and 6/6 for the oxygen atoms on the outside). Therefore f will be 0,769800359 and the critical length will be l=2,8663 Angstroms. This system leads to a surface density of 1,556E-09, which is comparable to the typical value for technical oxides.

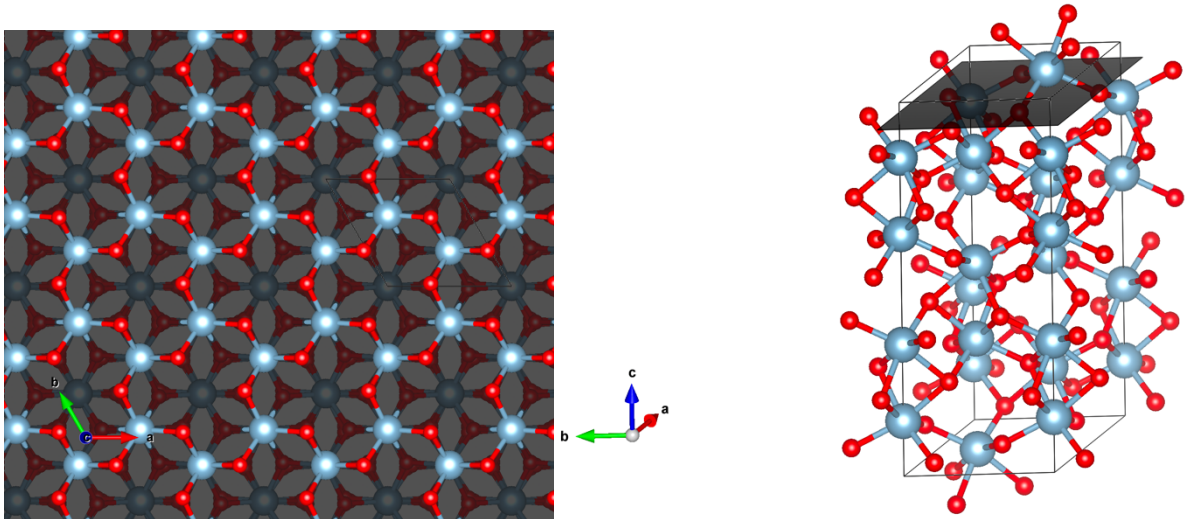

Figure 16a Surface of Al2O3 on the (0001) plane and b 3-dimensional Illustration of Al2O3 and the (0001) plane ©

Note: The systems for the calculation of the surface site densities are heavily simplified. However they are accurate enough for our use case. For more exact results adsorption experiments need to be conducted on the systems and later on evaluated by either adsorption isotherms or even quantum chemistry.

3.2 Results of the ab initio calculations

As an example the results of the structure optimizations and the thermodynamic data, calculated with ab-initio methods, for one of the species are shown below. The full thermodynamic data for each species considered with respect to the temperature can be found in the appendix.

AlCl2NH2 Thermodynamic data for Chemkin Fit Hf = -138.01 KCAL/MOLE								
T	H-H0 rot	H-H0trans	H-H0vib	H-H0	S	Cp	S kor.	H-H298
0	0	0	0	0,000	-	-	-	-2,443
298	0,889	0,889	8,445	2,443	79,407	20,877	78,029	0,000
300	0,894	0,894	8,525	2,465	79,536	20,921	78,158	0,021
400	1,192	1,192	12,977	3,671	85,833	22,811	84,455	1,228
500	1,49	1,49	17,626	4,925	91,067	24,062	89,689	2,482
600	1,788	1,788	22,382	6,204	95,537	24,963	94,159	3,761
700	2,087	2,087	27,201	7,499	99,440	25,665	98,062	5,055
800	2,385	2,385	32,061	8,803	102,906	26,25	101,528	6,359
900	2,683	2,683	36,949	10,114	106,028	26,761	104,650	7,670
1000	2,981	2,981	41,857	11,429	108,872	27,216	107,494	8,986
1100	3,279	3,279	46,780	12,748	111,485	27,626	110,107	10,305
1200	3,577	3,577	51,713	14,070	113,905	27,996	112,527	11,626
1300	3,875	3,875	56,655	15,393	116,159	28,33	114,781	12,950
1500	4,471	4,471	66,556	18,045	120,255	28,899	118,877	15,601
1700	5,067	5,067	76,476	20,700	123,901	29,358	122,523	18,257
1900	5,663	5,663	86,408	23,359	127,187	29,727	125,809	20,915
2100	6,26	6,26	96,348	26,020	130,177	30,025	128,799	23,577
2300	6,856	6,856	106,295	28,682	132,920	30,268	131,542	26,239
2500	7,452	7,452	116,246	31,346	135,452	30,467	134,074	28,902
2700	8,048	8,048	126,202	34,010	137,804	30,631	136,426	31,567
2900	8,644	8,644	136,160	36,675	139,997	30,768	138,619	34,232
3100	9,24	9,24	146,121	39,341	142,053	30,883	140,675	36,897
3300	9,837	9,837	156,084	42,007	143,987	30,98	142,609	39,564
3500	10,433	10,433	166,048	44,674	145,813	31,063	144,435	42,230
3700	11,029	11,029	176,014	47,340	147,541	31,134	146,163	44,897
3900	11,625	11,625	185,981	50,007	149,181	31,196	147,803	47,564
4100	12,221	12,221	195,949	52,675	150,743	31,25	149,365	50,231
4300	12,817	12,817	205,918	55,342	152,232	31,296	150,854	52,899
4500	13,414	13,414	215,888	58,010	153,656	31,337	152,278	55,567
4700	14,01	14,01	225,858	60,678	155,020	31,374	153,642	58,235
4900	14,606	14,606	235,829	63,346	156,328	31,406	154,950	60,903
5000	14,904	14,904	240,814	64,680	156,962	31,421	155,584	62,237

Table 3 Thermodynamic data of $AlCl_2NH_2$ calculated using ab-initio methods ©

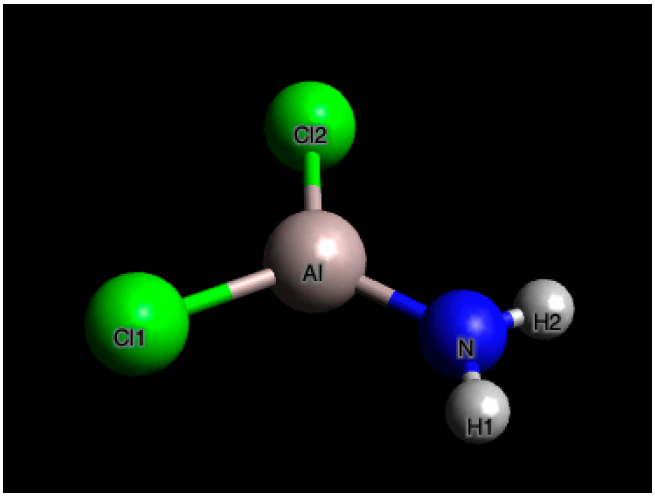

Figure 17 B3LYP optimized structure of $AlCl_2NH_2$ ©

Stated down below are the results of the nasa-7 polynomial fitting together with some of the transport data obtained by ab-initio calculations.

Fitted parameters for Chemkin-thermodynamics using data calculated by ab initio methods							
	AlCl	AlCl3	Al2Cl6	AlCl2NH2	TiCl4	TiCl3	TiCl4(NH3)2
a1	4,35E+00	9,31E+00	2,06E+01	1,03E+01	1,92E+01	9,52E+00	1,92E+01
a2	1,91E-04	8,54E-04	1,70E-03	4,95E-03	1,63E-02	5,98E-04	1,63E-02
a3	-9,09E-08	-4,03E-07	-8,07E-07	-1,83E-06	-6,31E-06	-2,85E-07	-6,31E-06
a4	1,87E-11	8,28E-11	1,66E-10	3,18E-10	1,13E-09	5,87E-11	1,13E-09
a5	-1,40E-15	-6,17E-15	-1,24E-14	-2,11E-14	-7,62E-14	-4,39E-15	-7,62E-14
a6	-7,98E+03	-7,39E+04	-1,64E+05	-7,28E+04	-1,26E+05	-6,78E+04	7,92E+04
a7	2,58E+00	-1,57E+01	-6,13E+01	-2,10E+01	-5,72E+01	-1,32E+01	-5,72E+01
a8	3,47E+00	5,79E+00	1,31E+01	5,14E+00	1,33E+01	6,78E+00	1,33E+01
a9	3,86E-03	1,52E-02	3,32E-02	2,71E-02	3,88E-02	1,21E-02	3,88E-02
a10	-5,81E-06	-2,22E-05	-4,98E-05	-3,75E-05	-3,82E-05	-1,82E-05	-3,82E-05
a11	3,98E-09	1,48E-08	3,40E-08	2,57E-08	2,11E-08	1,25E-08	2,11E-08
a12	-1,03E-12	-3,75E-12	-8,75E-12	-6,77E-12	-4,75E-12	-3,23E-12	-4,75E-12
a13	-7,81E+03	-7,32E+04	-1,63E+05	-7,19E+04	-1,25E+05	-6,73E+04	8,04E+04
a14	6,79E+00	1,24E+00	-2,50E+01	3,37E+00	-2,83E+01	-6,11E-02	-2,83E+01
Calculated parameters for Chemkin-transport using ab initio methods							
μ [Debye]	1,864	0,000	0,000	2,869	0,000	0,000	7,842
α [a.u.]	45,470	47,408	96,719	44,652	77,808	62,099	102,573

Table 4 Fitted Nasa 7 polynomial coefficients and transport data obtained by ab-initio methods. ©

3.3 Simulations results from Chemkin

All input files for the different calculations can be found the appendix.

3.3.1 Growth rates of aluminum nitride in the PSR

The results of the parameter studies that are shown below. The studies were conducted using a fixed surface temperature of 800K and a gas composition 2:1 for NH3:AlCl3. Shown in figures 18-20 is the growth rate with respect to the temperature at different pressures. Going through the figures it may be observed how both the deposition rate and also the temperature dependency of the growth rate vary for different pressures. The parameter study with respect to the pressure (fig. 21) shows a clear linear trend for the deposition rate with increasing pressure. We are not aware of any study in the literature reporting growth rates for exactly the same parameters investigated here. However when looking at ref. (47), which also provided the reaction mechanism used in this work, the authors have reported experimental values for the growth rate between 5 and 35µm per hour (0,0833-0,5833µm/min) (using different deposition parameters). Therefore, our results are in a reasonable range. When it comes to the reaction path diagrams one can clearly see how the deposition is favored at high temperatures. An interesting finding is that at all temperature levels the main reaction path to deposition is always happening with the intermediary compound $AlCl_2NH_2$, which is due to the high rate of conversion and the accelerated rate of the surface reactions.

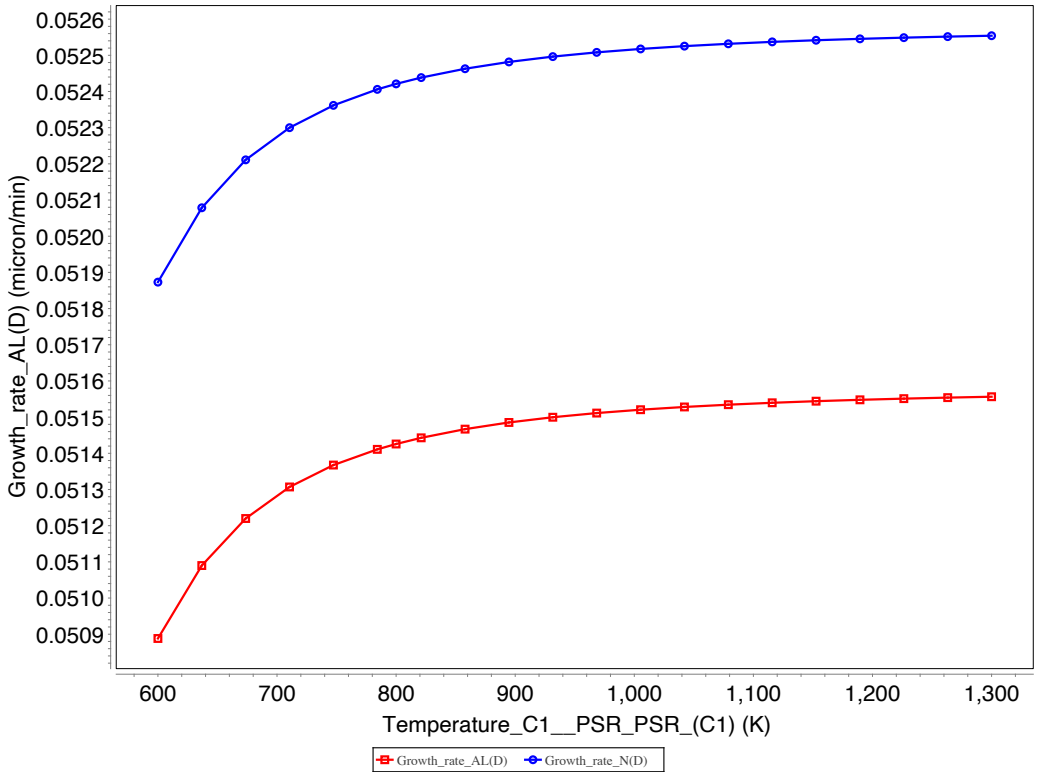

Figure 18 Graph of the growth rate vs gas temperature of TiN CVD system at a pressure of 1 Torr ©

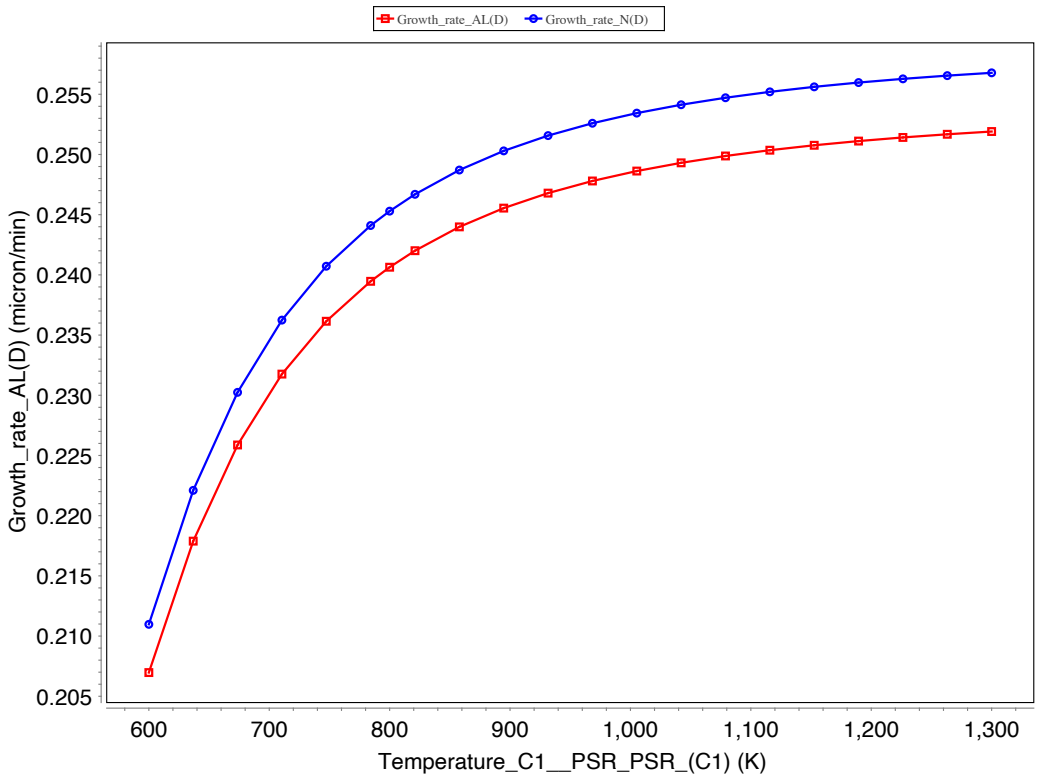

Figure 19 Graph of the growth rate vs gas temperature of TiN CVD system at a pressure of 5 Torr ©

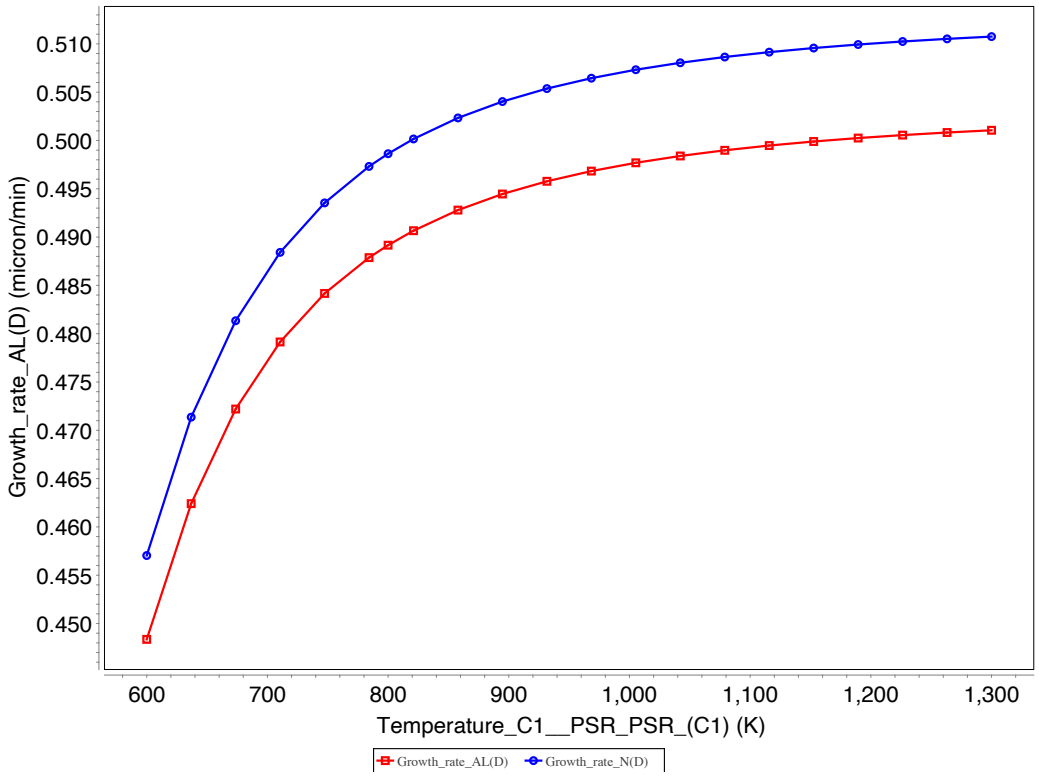

Figure 20 Graph of the growth rate vs gas temperature of TiN CVD system at a pressure of 10 Torr ©

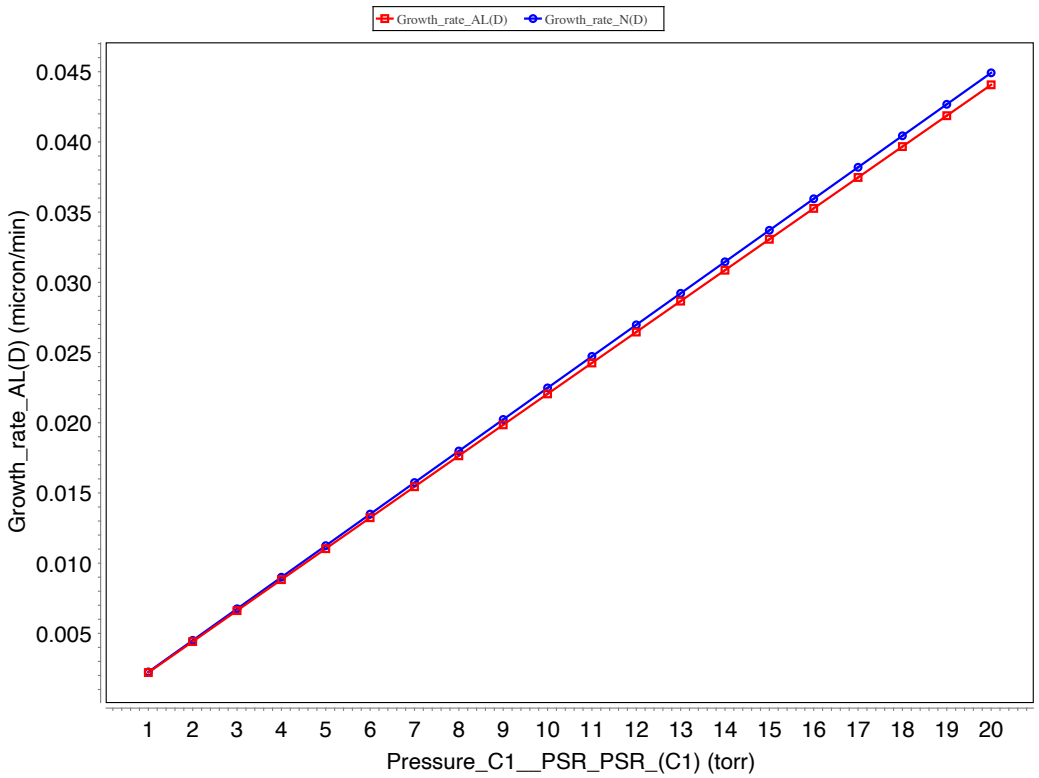

Figure 21 Graph of the growth rate vs pressure of TiN CVD system at a gas temperature of 800K ©

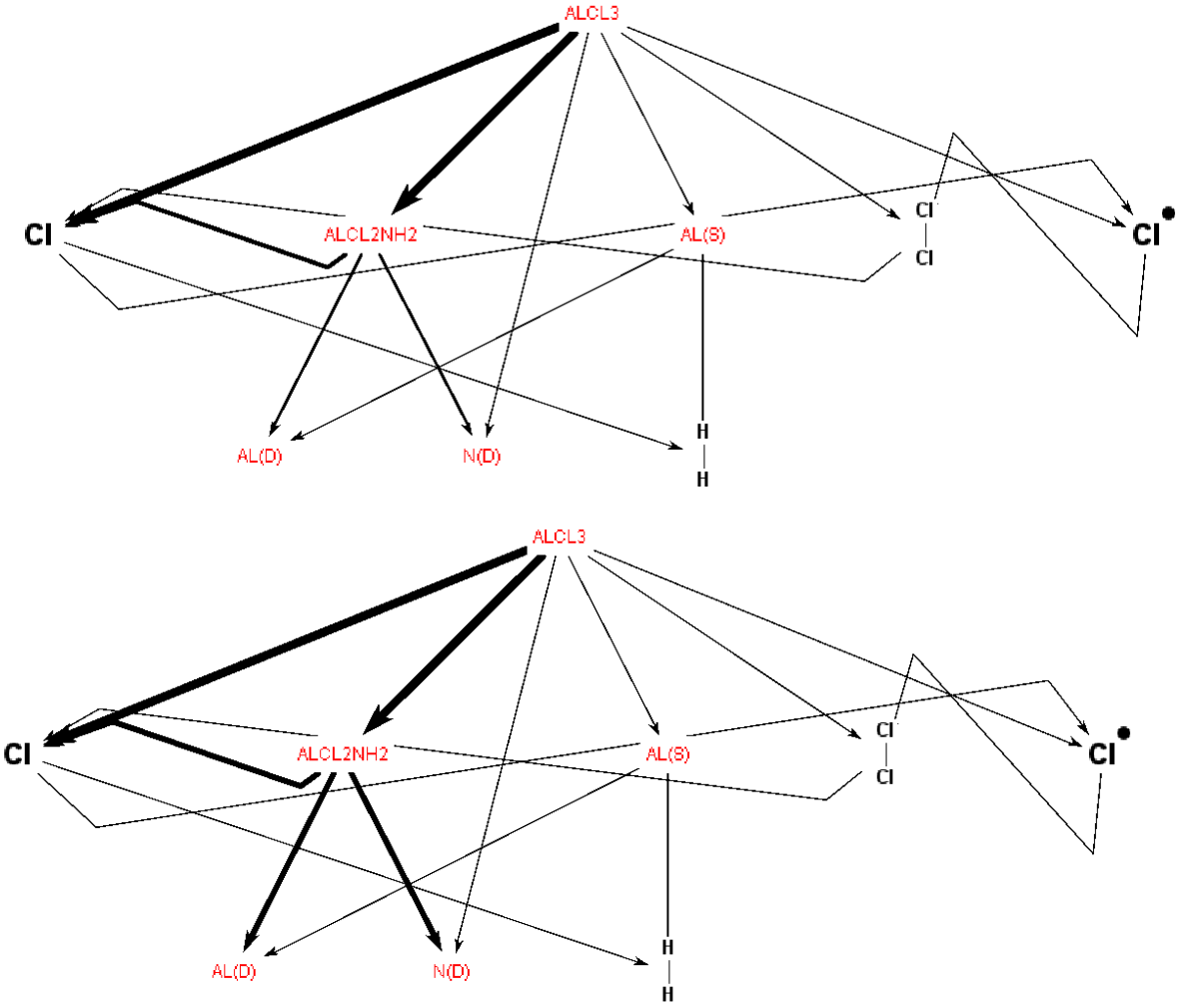

Figure 22a Reaction paths of AlN deposition at 500K Reaction paths at 1000K ©

3.3.2 Growth rates of titanium nitride in the PSR

The plots for growth rate vs gas temperature at different pressures of the TiN CVD system can be found below. In figures 23 and 24 we can observe that the deposition rate is dropping in the region of 600-1100K before rising steeply and capping out again once 1400K is reached. In figure 25 we can observe a steep increase in the growth rate with respect to pressure. This might be due to the high formation of complexes in this temperature region. The PSR studies were set up at a gas composition NH_3:$TiCl_4$ of 6:5 and the dependence of the growth rate on gas temperature was studied at 5 and 10 Torr. The dependence on pressure was simulated at a gas temperature of 800K. For all the simulations, we kept a constant substrate temperature of 800K. Experimental data for comparison from ref (53) show that at temperatures between 600 and 1400°C and pressures of 1kPa (7,5 Torr) the deposition rate is between 1 and 3,8 µm/h (0,01667-0,0633 µm/min). In this study, the gas phase composition was varied between 1,5 and 4,5 NH_3/$TiCL_4$. These parameters do not quite match with the once studied by us, however it gives a rough estimate and the order of magnitude. The results of the PSR simulation show a good agreement with the experimental data. The reaction path diagram in figure 26 indicates a high amount of unwanted complex formation especially at low temperatures.

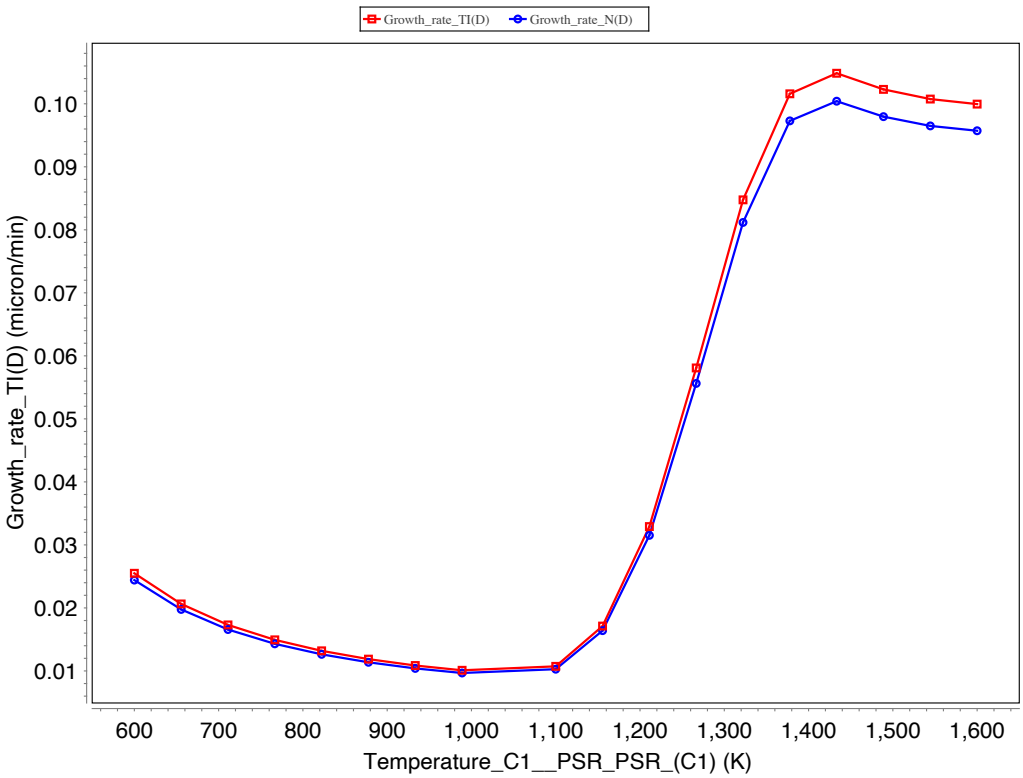

Figure 23 Graph of the growth rate vs gas temperature of TiN CVD system at a pressure of 5 Torr ©

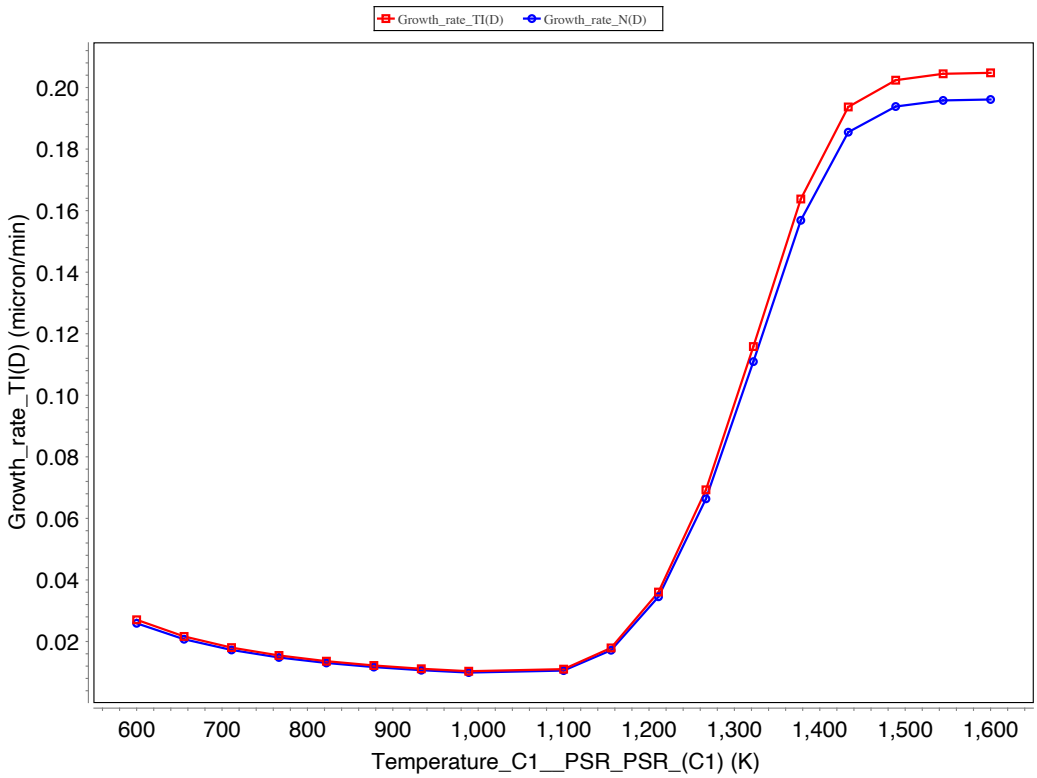

Figure 24 Graph of the growth rate vs gas temperature of TiN CVD system at a pressure of 10 Torr ©

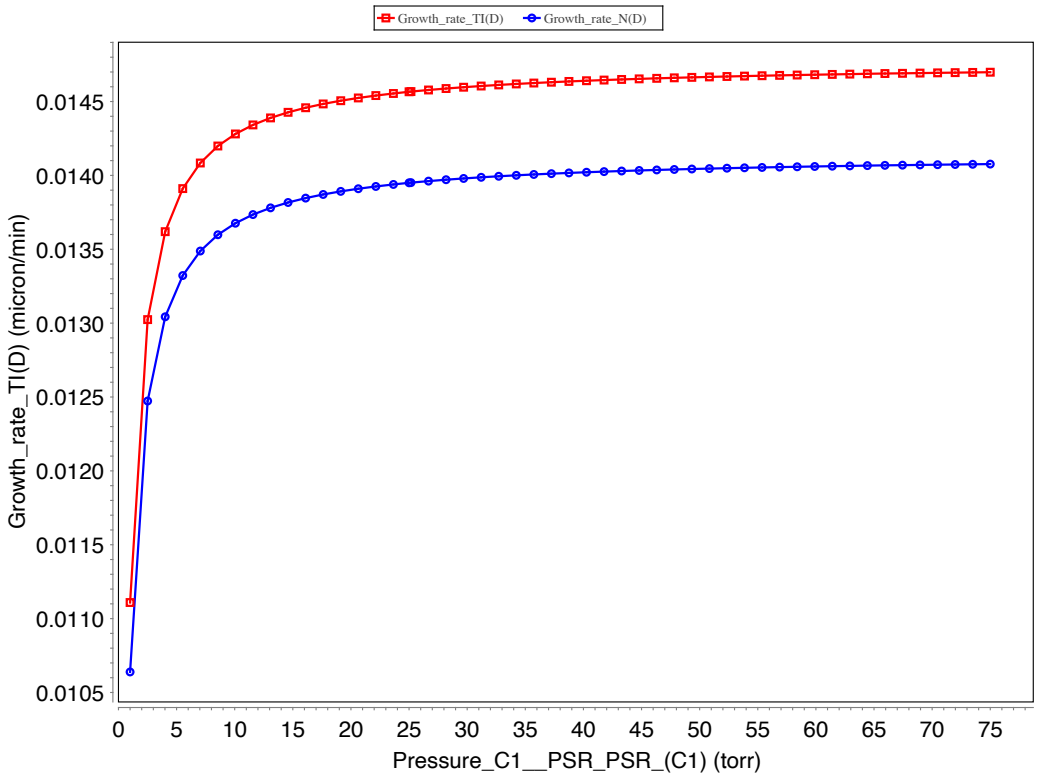

Figure 25 Graph of the growth rate vs pressure of TiN CVD system at a gas temperature of 800K ©

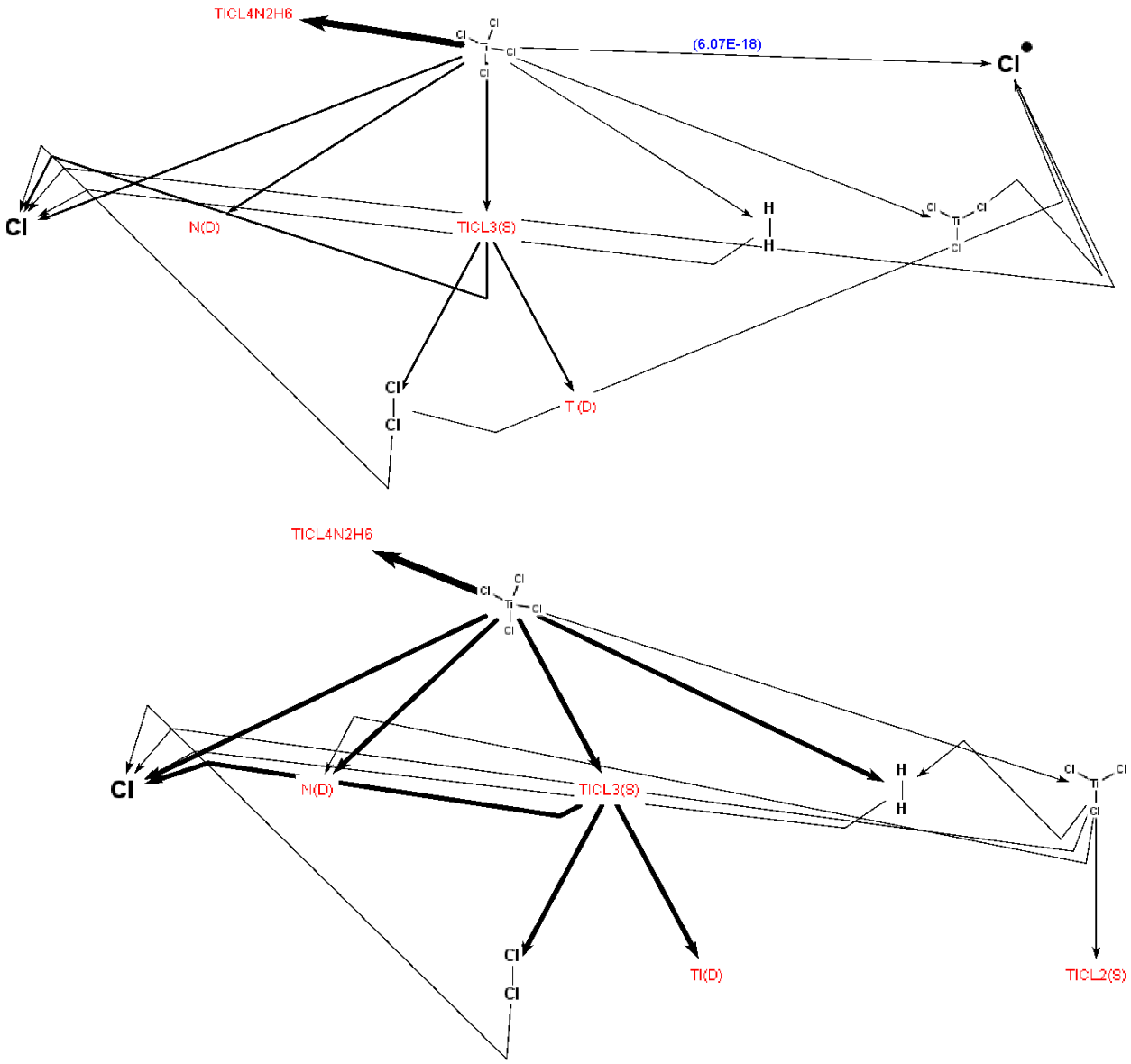

Figure 26 Reaction paths of TiN deposition at 500K Reaction paths at 1300K ©

3.3.3 Growth rate of titanium aluminum nitride in the PSR

The results of the TiAlN PSR analysis can be found below. When comparing the different plots on can recognize a strong influence of the gas composition on the deposition rates as well as on gas temperature. These trends can be observed by analyzing figures 27-33 and figures 36-41 which show the results of the simulations using different gas compositions and pressures. It can see in figures 33-35 that at a fixed gas temperature and pressure the variation of surface/substrate temperature exhibits the same effect on growth behavior irrespective of gas composition. In ref (67) experimental growth of TiAlN using the same precursor gas (however with unknown gas composition) at temperatures between 650 and 750 degrees Celsius and pressures between 5 and 25 mbar (3,75-18,75 Torr) has been reported. The team determined deposition rates between 0,023 and 0,217 µm per minute. This result is in the same order of magnitude as the performed simulation in the given range of temperature and pressure. The obtained growth rates however are higher than the ones in the experimental case which is expected ever since the mass transport was set to be "infinitely" fast in the simulations. Also reaction path analyses can be found below, one starting from $TiCl_4$ and one from $AlCl_3$. When it comes to the reaction path diagrams (42 and 43) we can see that during these simulations no titanium complex was formed. Complex formation might be suppressed by the high reaction rates of aluminum complex formation as both of these complexes need ammonia to be created.

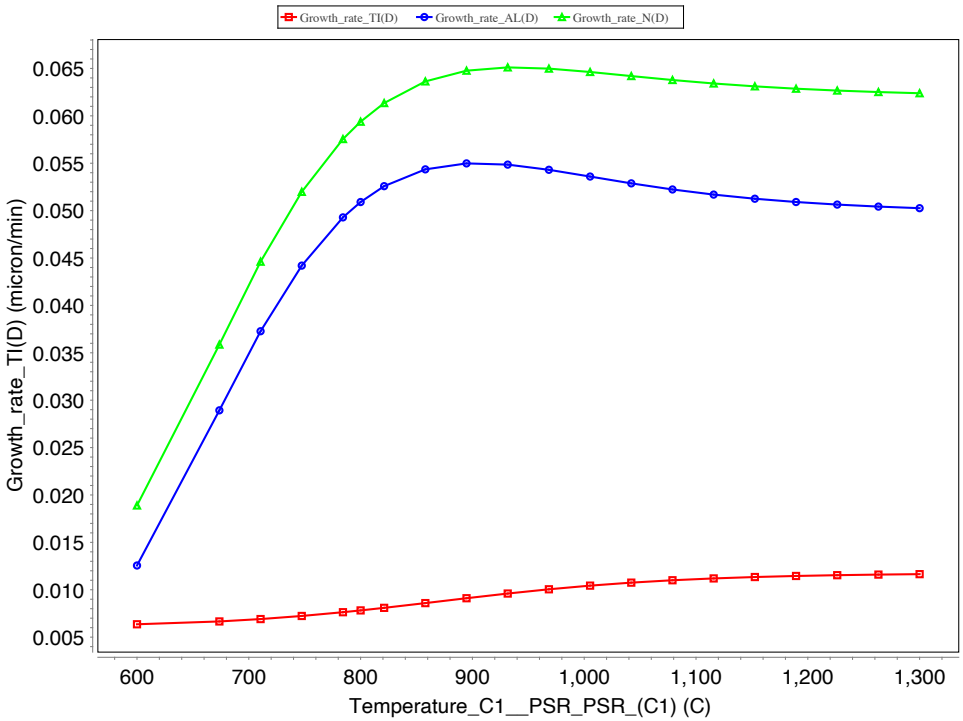

Figure 27 Resulting graph of the growth rate vs gas temperature at a surface temperature of 800°C, 2:0,5:1,5 NH3:TiCl4:AlCl3 and a pressure of 5 Torr ©

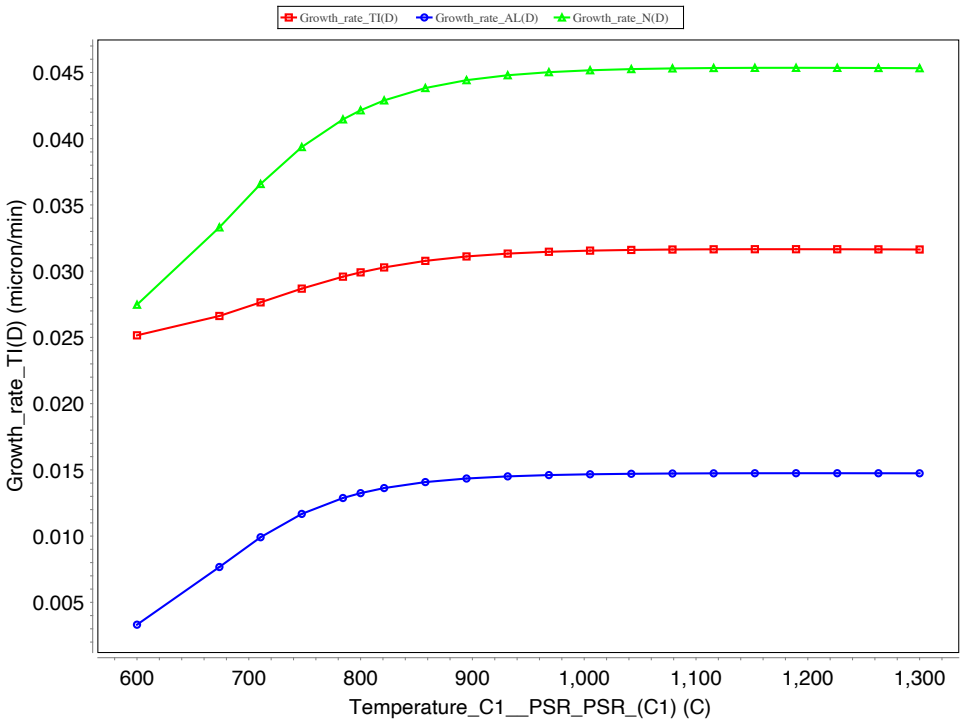

Figure 28 Resulting graph of the growth rate vs gas temperature at a surface temperature of 800°C, 2:1,5:0,5 NH3:TiCl4:AlCl3 and a pressure of 5 Torr ©

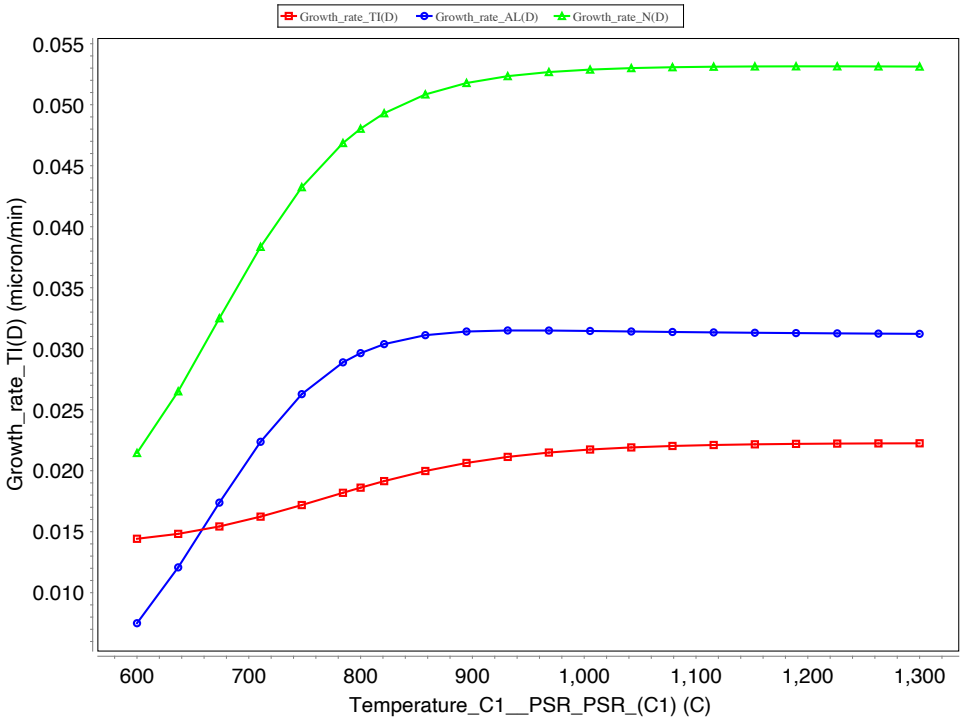

Figure 29 Resulting graph of the growth rate vs gas temperature at a surface temperature of 800°C, 2:1:1 NH3:TiCl4:AlCl3 and a pressure of 5 Torr ©

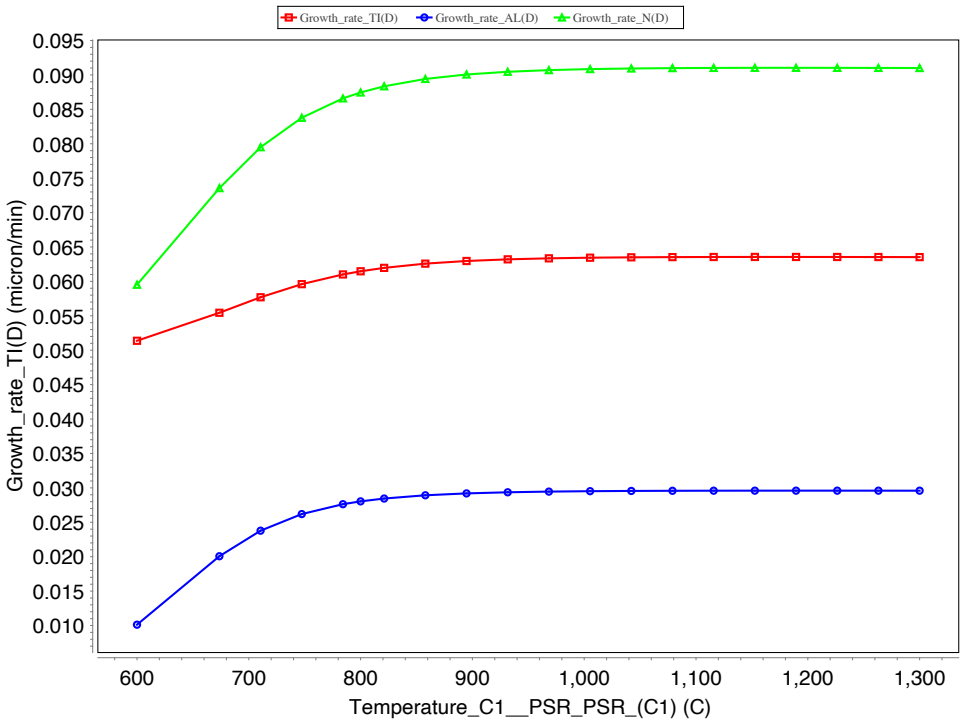

Figure 30 Resulting graph of the growth rate vs gas temperature at a surface temperature of 800°C, 2:1,5:0,5 NH3:TiCl4:AlCl3 and a pressure of 10 Torr ©

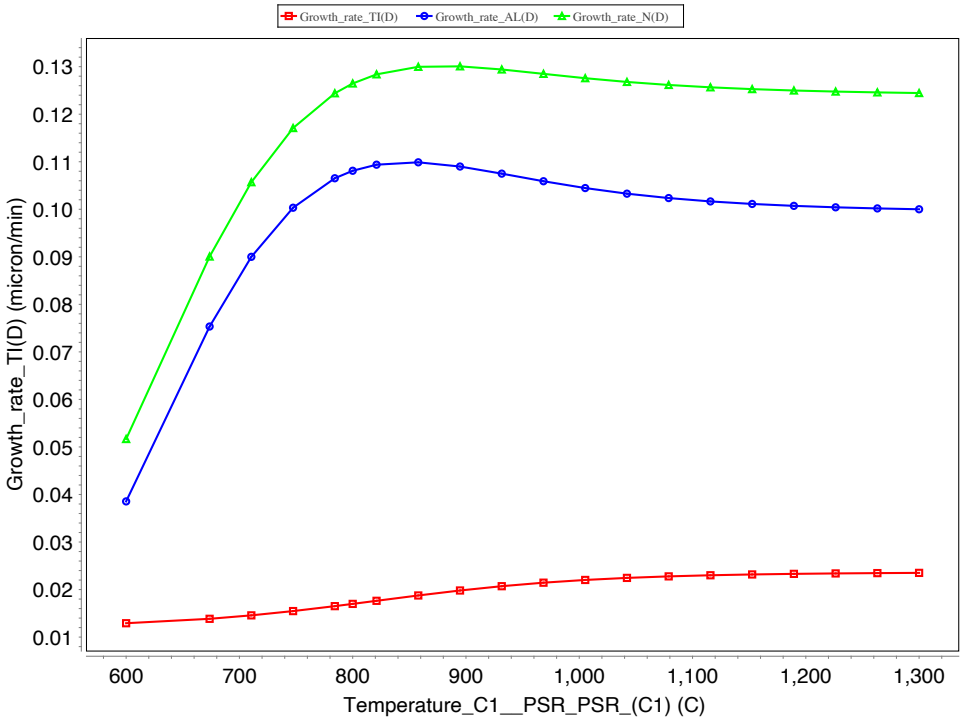

Figure 31 Resulting graph of the growth rate vs gas temperature at a surface temperature of 800°C, 2:0,5:1,5 NH3:TiCl4:AlCl3 and a pressure of 10 Torr ©

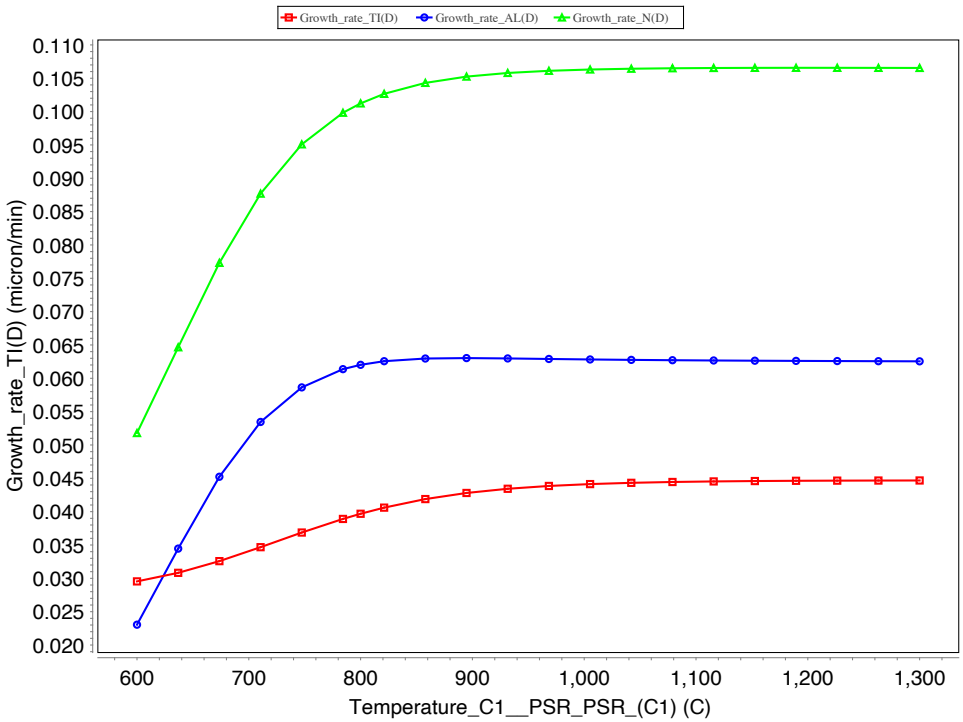

Figure 32 Resulting graph of the growth rate vs gas temperature at a surface temperature of 800°C, 2:1:1 NH3:TiCl4:AlCl3 and a pressure of 10 Torr ©

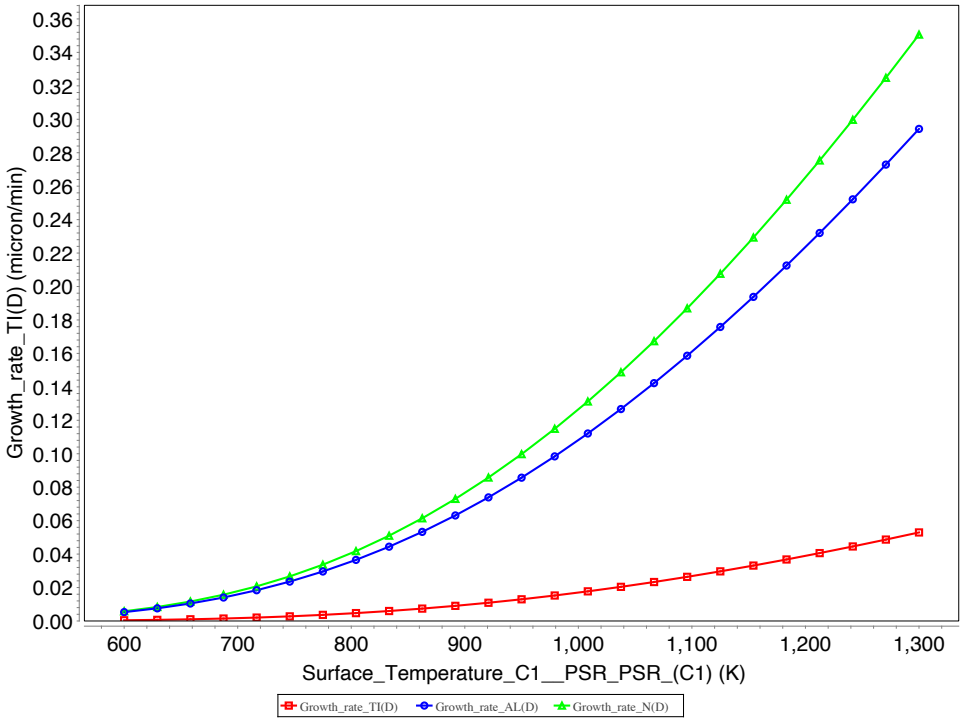

Figure 33 Resulting graph of the growth rate vs substrate temperature at a gas temperature of 800°C, 2:0,5:1,5 NH3:TiCl4:AlCl3 and a pressure of 10 Torr ©

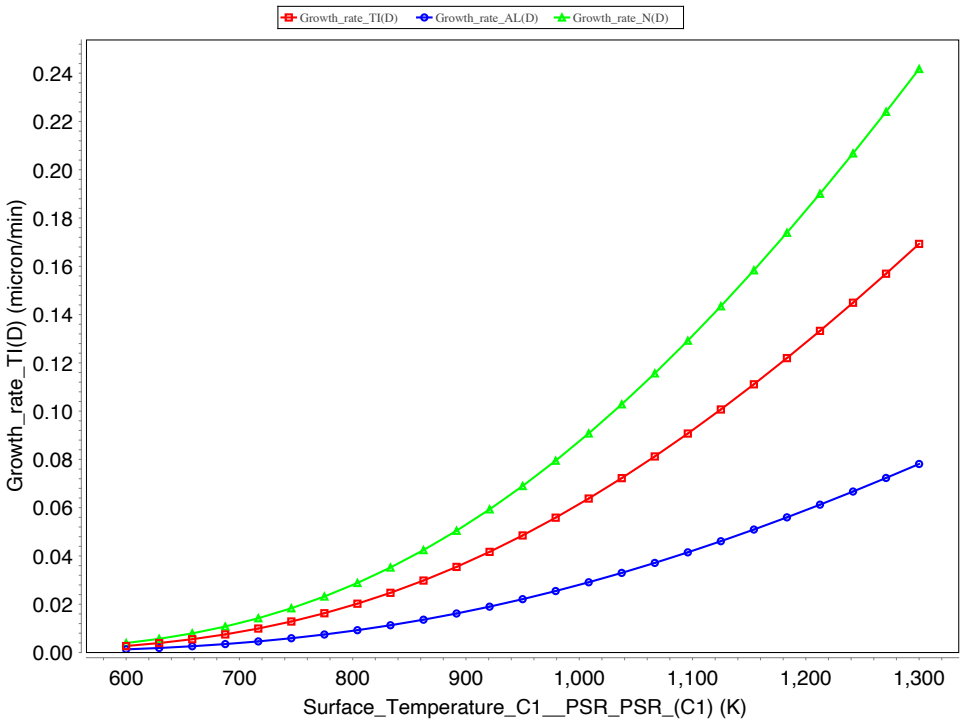

Figure 34 Resulting graph of the growth rate vs substrate temperature at a gas temperature of 800°C, 2:1,5:0,5 NH3:TiCl4:AlCl3 and a pressure of 10 Torr ©

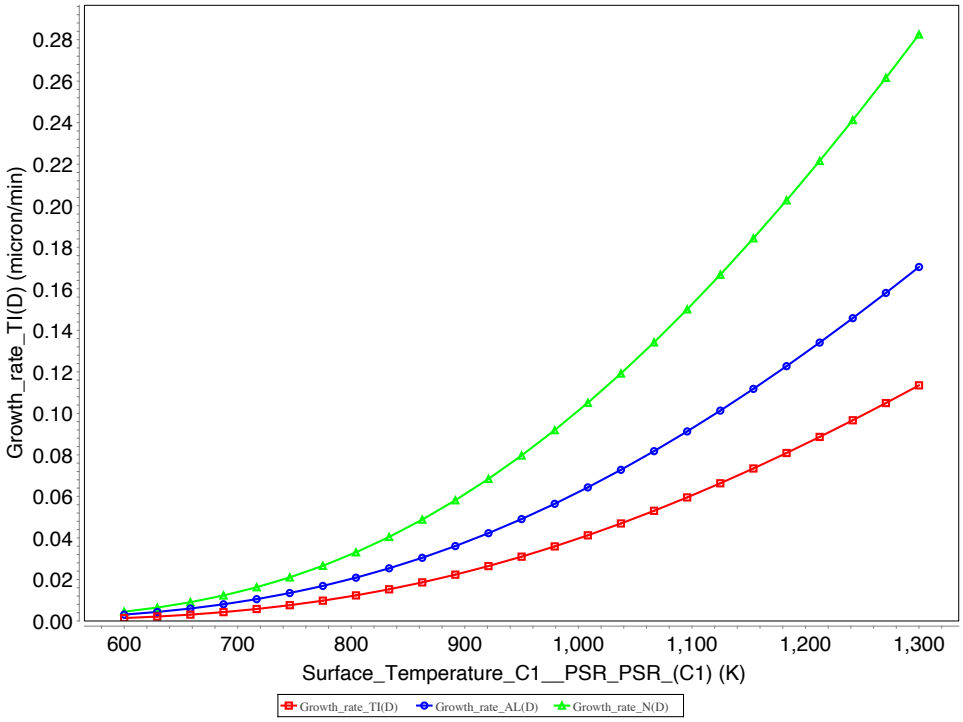

Figure 35 Resulting graph of the growth rate vs substrate temperature at a gas temperature of 800°C, 2:1:1 NH3:TiCl4:AlCl3 and a pressure of 10 Torr ©

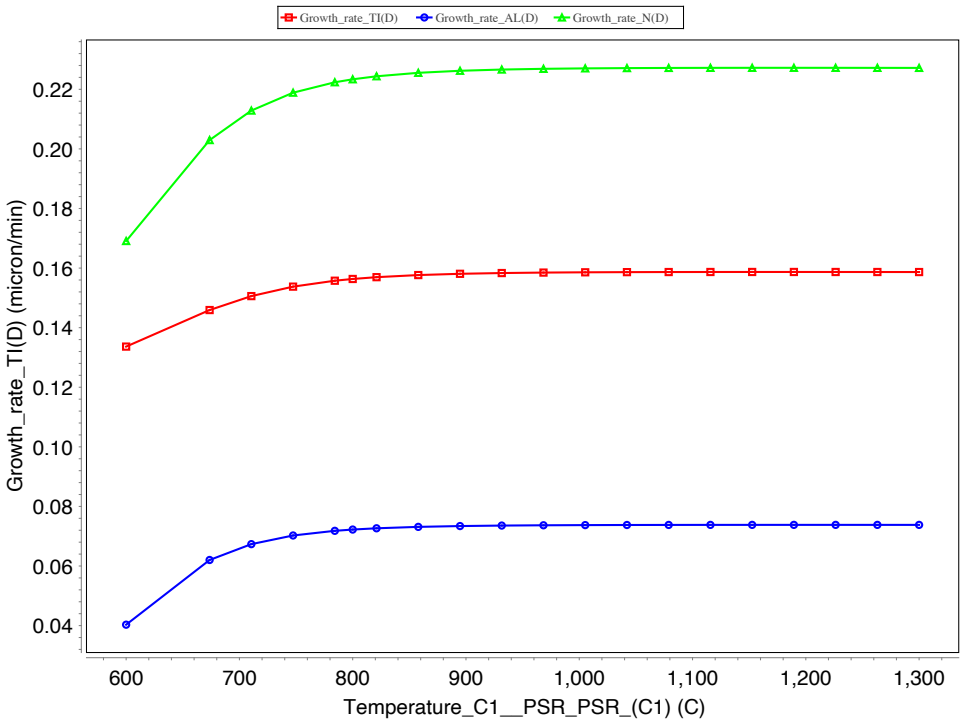

Figure 36 Resulting graph of the growth rate vs gas temperature at a surface temperature of 800°C, 2:1,5:0,5 NH3:TiCl4:AlCl3 and a pressure of 25 Torr ©

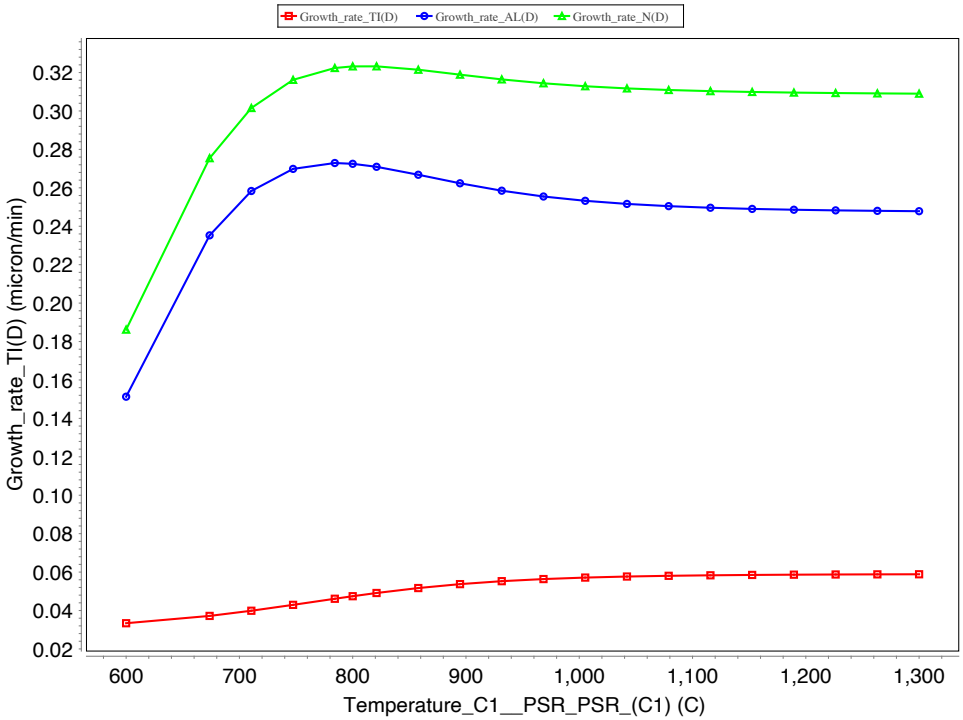

Figure 37 Resulting graph of the growth rate vs gas temperature at a surface temperature of 800°C, 2:0,5:1,5 NH3:TiCl4:AlCl3 and a pressure of 25 Torr ©

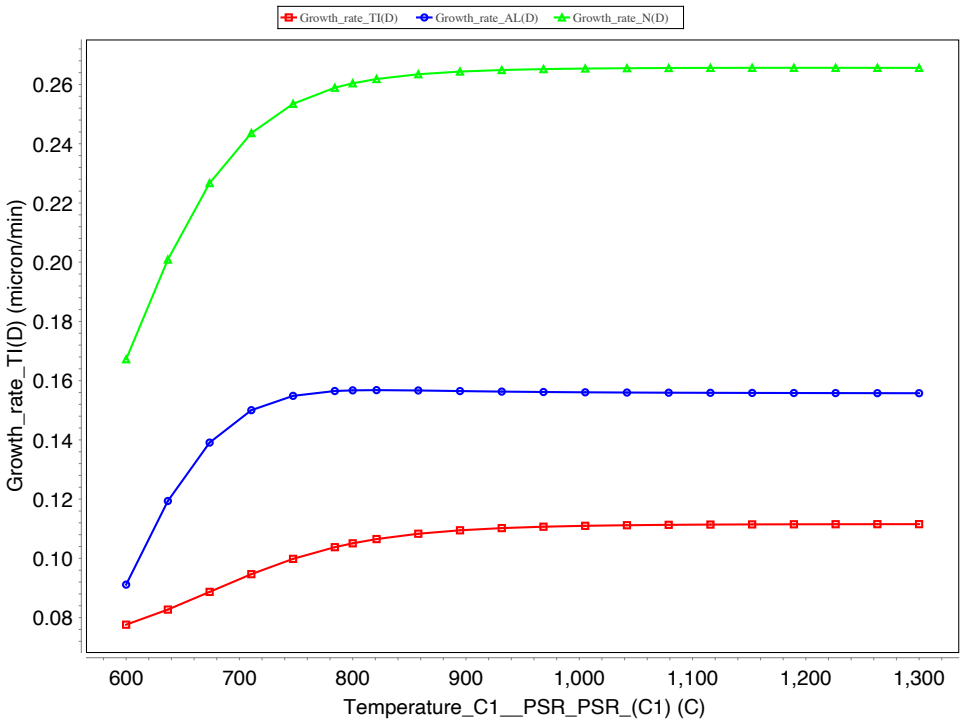

Figure 38 Resulting graph of the growth rate vs gas temperature at a surface temperature of 800°C, 2:1:1 NH3:TiCl4:AlCl3 and a pressure of 25 Torr ©

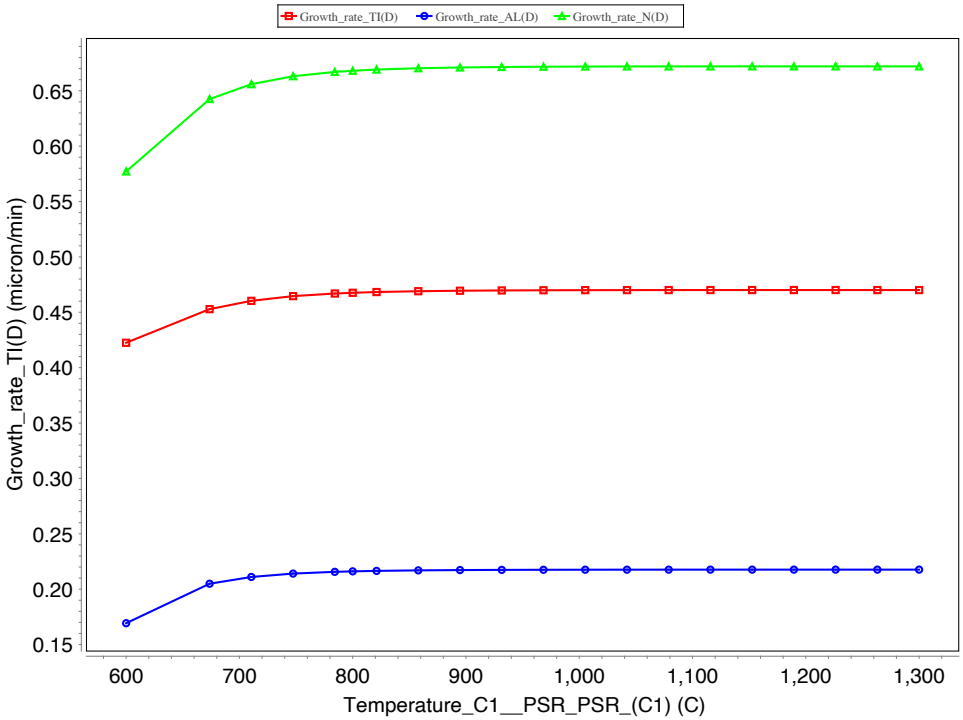

Figure 39 Resulting graph of the growth rate vs gas temperature at a surface temperature of 800°C, 2:1,5:0,5 NH3:TiCl4:AlCl3 and a pressure of 75 Torr ©

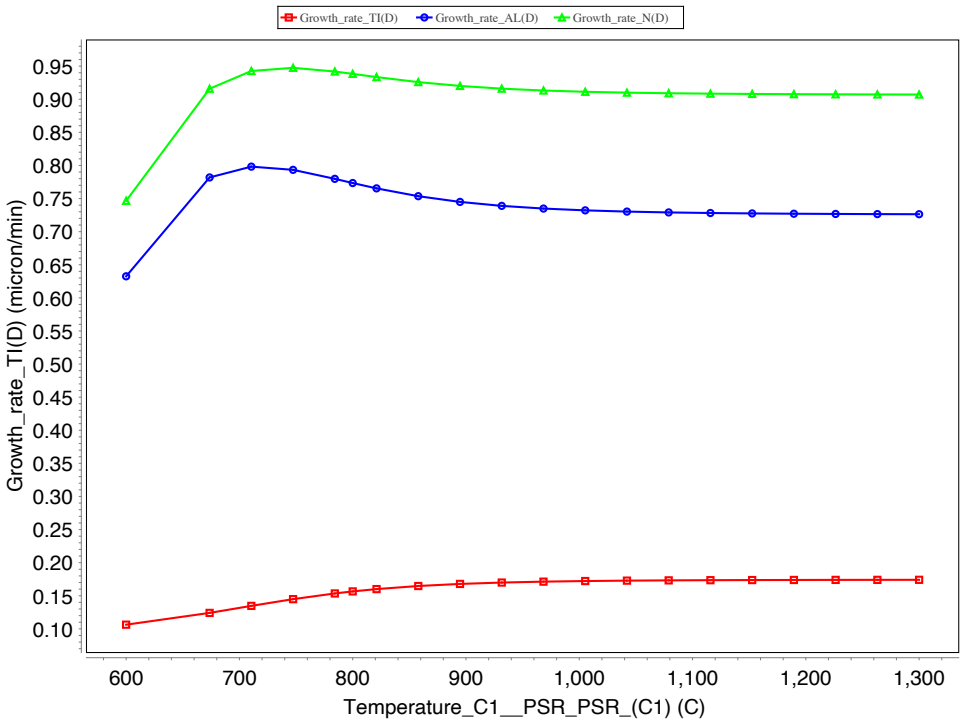

Figure 40 Resulting graph of the growth rate vs gas temperature at a surface temperature of 800°C, 2:0,5:1,5 NH3:TiCl4:AlCl3 and a pressure of 75 Torr ©

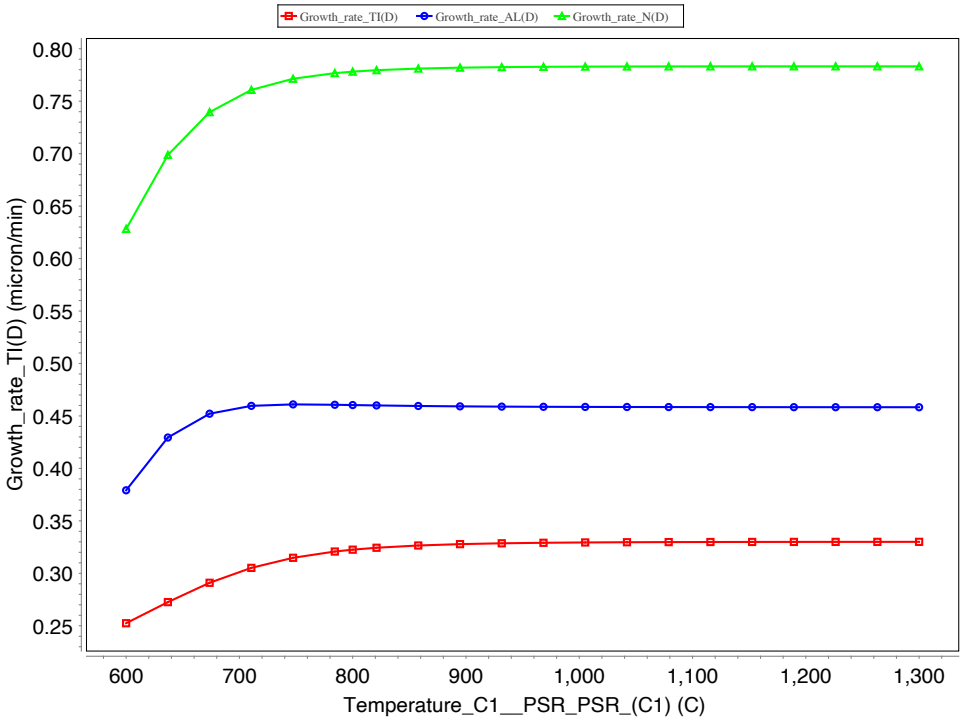

Figure 41 Resulting graph of the growth rate vs gas temperature at a surface temperature of 800°C, 2:1:1 NH3:TiCl4:AlCl3 and a pressure of 75 Torr ©

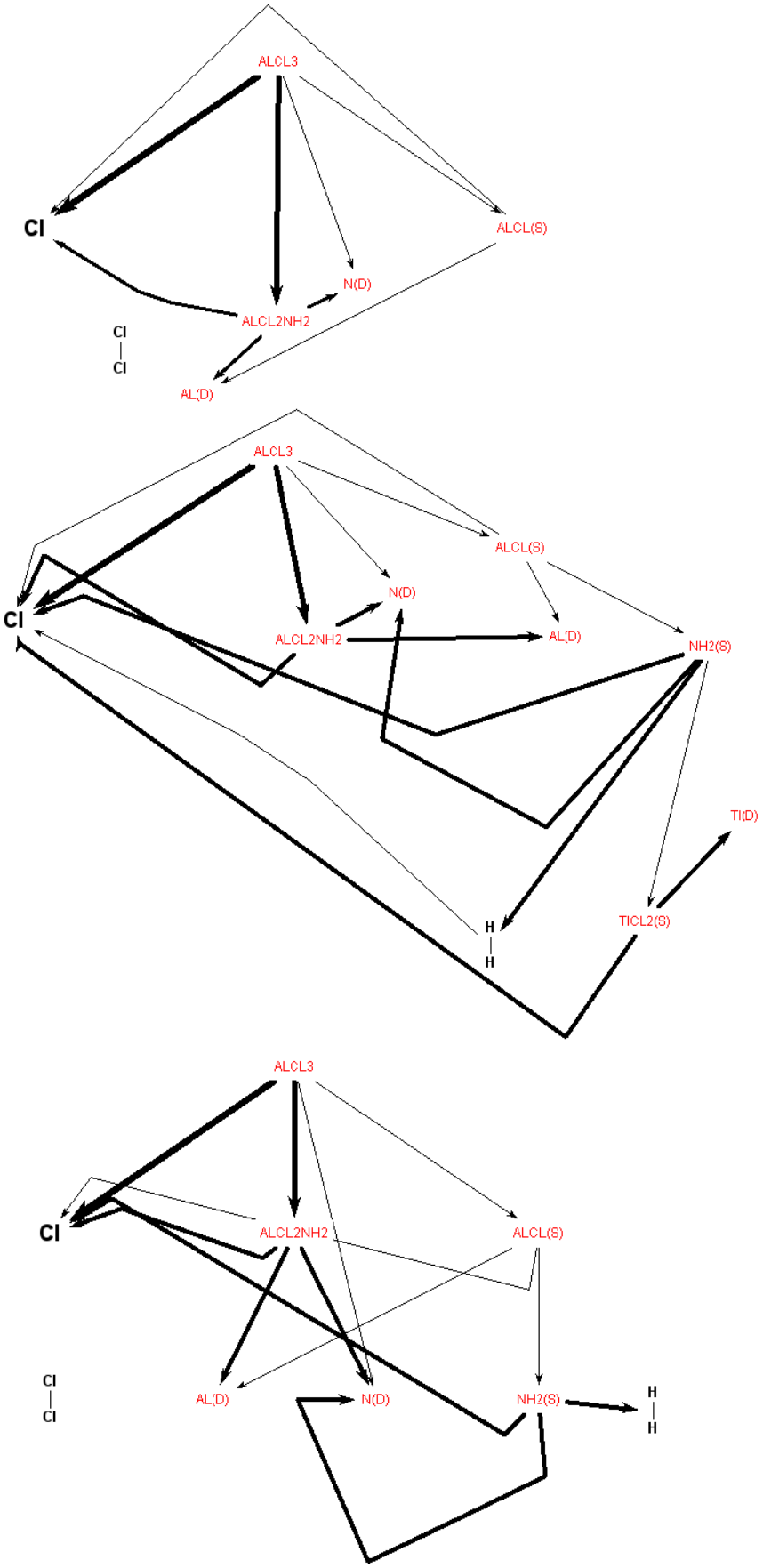

Figure 42 a.) Reaction path starting from AlCl3 at 600°C gas temperature, Reaction path starting from AlCl3 at 800°C gas temperature, Reaction path starting from AlCl3 at 1100°C gas temperature ©

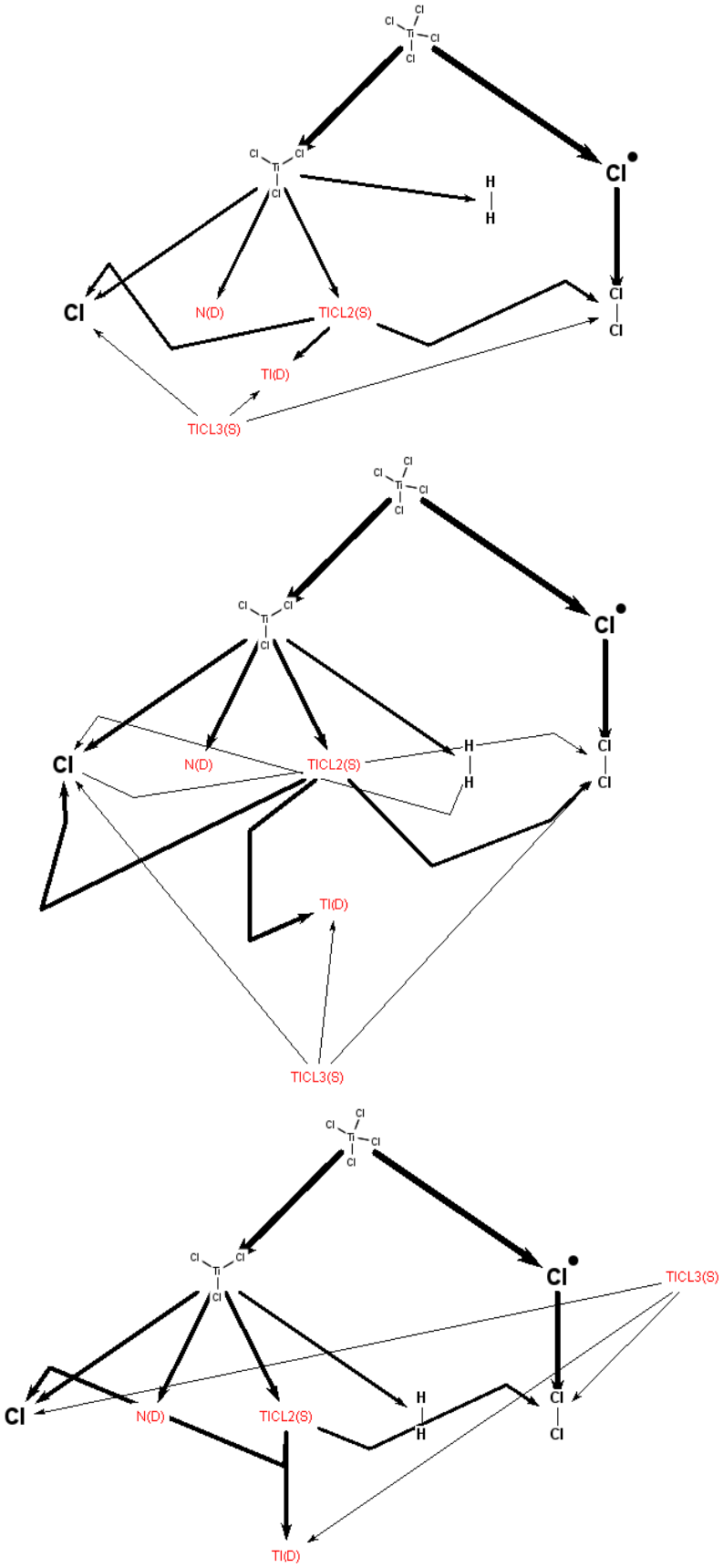

Figure 43 Reaction path starting from TiCl4 at 600°C gas temperature, Reaction path starting from TiCl4 at 800°C gas temperature, Reaction path starting from TiCl4 at 1100°C gas temperature ©

4 Conclusion

To sum up the thesis, first a theoretical analysis of the crystalline surfaces used for the deposition was performed. We conducted ab initio studies of the chemical species which are supposed to form during the CVD processes. Both of this aforementioned calculations were done in order to set up the reacting flow problems. Chemical kinetics of the different CVD systems were analyzed using CFD/reacting flow simulations. Finally, co-deposition of titanium aluminum nitride was simulated utilizing the reaction mechanisms from the titanium nitride and aluminum nitride CVD systems.

An interesting discovery of this thesis is that the growth rates produced by the simulation of titanium aluminum nitride matched very well with the experimental data available. This indicates that the reaction mechanism using the co-deposition approach describes the real system with a decent accuracy. Another interesting finding is that the simulation predicts that with our deposition parameters there is no complex formation of the titanium complex $TiCl_4(NH_3)_2$. This is despite the fact that it predicts a lot of complex formation in the pure titanium nitride CVD system. However, the aluminum complex $AlCl_2NH_2$ is predicted to be created in high amounts. This could also be the reason why the titanium complex is not able to form.

Looking at the results the reaction mechanism used in this thesis might be a good starting point for even more detailed mechanisms and analyses. Due to the high influence of the gas composition there could be local phenomena (maybe created by different gas transport behavior) in the gas phase which in the right circumstances might be able explain the periodic gradient in the titanium aluminum nitride system. With that said, it might be worth it to take a deeper look into the gas-phase-based systems. This includes more detailed simulation-based methods, i.e. 3D reacting flow models including mass transport which could be further combined with methods like kinetic Monte Carlo and molecular dynamics. It could also be worth it to conduct experiments such as chemical analysis of the inflowing and outflowing gas flow using, e.g. ER-Spectroscopy.

5 References

1. *Chemical Vapor Deposition of Electronic Materials.* Tietjen, James. 1, RCA Laboratories, Princeton, New Jersey : s.n., 1973, Annual Review of Materials Science, Vol. 3, pp. 317-326.
2. Park, Jong-Hee. *Surface engineering series.* Argonne National Laboratory : ASM International, 2001.
3. Xu, Yongdong and Xiu-Tian, Yan. *Chemical Vapour Deposition.* Xian China : Springer-Verlag London Limited, 2008. pp. 146-162.
4. Jiadai, An. Kinetic Monte Carlo Simulation of the Growth of AlN Films by Metal Organic Chemical Vapor Deposition. *Physica status solidi (RRL) – Rapid Research Letters.* July 2019, Vol. 256, 12, pp. 1900114 (1-8).
5. Jansen, A. *An Introduction to Kinetic Monte Carlo Simulations of Surface.* s.l. : Springer-Verlag Berlin Heidelberg, 2012. pp. 135-167.
6. ANSYS-Inc. *Ansys Chemkin-Pro Theory Manual.* 2600 Ansys Drive Canonsburg, PA 15317 : s.n., 2022.
7. Oura, K. et. al. *Surface Science.* Department of Electronic Engineering, Faculty of Engineering, Osaka University, Osaka, Japan : Springer Berlin, Heidelberg, 2003.
8. [Online] https://www.iue.tuwien.ac.at/phd/singulani/dissse20..
9. [Online] https://www.iue.tuwien.ac.at/phd/singulani/dissse20.html.
10. Tura´nyi, Tama´s. *Analysis of Kinetic Reaction Mechanisms.* Budapest : Springer-Verlag Berlin Heidelberg, 2014.
11. BYJU'S. [Online] 2022. https://byjus.com/jee/activation-energy/.
12. Technology, National Institute of Standards and. Computational Chemistry Comparison and Benchmark DataBase. [Online] May 22, 2022. https://cccbdb.nist.gov/thermox.asp.
13. Truhlar, D. Current Status of Transition-State Theory. *Journal of Physical Chemistry.* 1996, Vol. 100, 31, pp. 12771–12800.
14. Group, Simutech. [Online] Oktober 1st, 2022. https://simutechgroup.com/ansys-software/fluids/chemkin-pro/.
15. ANSYS, Inc. *Ansys Chemkin-Pro Input Manual.* 2600 Ansys Drive Canonsburg, PA 15317 : s.n., 2022.
16. *Näherungsmethode zur Lösung des quantenmechanischen Mehrkörperproblems.* Fock, V. s.l. : Springer, 1930, Zeitschrift für Physik, Vol. 61, pp. 126-148.
17. *Self-consistent field, with exchange, for beryllium.* Hartree, D. and Hartree, W. 869, s.l. : The royal society Pub., 1935, Proceeding of the royal society a, Vol. 150, pp. 9-33.
18. Szabo, A. and Ostlund, N. *Modern Quantum Chemistry: Introduction to Advanced Electronic Structure Theory.* New York : Dover Pub., 1996.
19. *The Self Consistent Field and the Structure of Atoms.* Slater, J. 3, s.l. : APS, 1928, PHYSICAL REVIEW JOURNALS ARCHIVE, Vol. 32, pp. 339-348.
20. *Self-Consistent Equations Including Exchange and Correlation Effects.* Kohn, W. and Sham, L. 4A, s.l. : APS, 1965, PHYSICAL REVIEW JOURNALS ARCHIVE, Vol. 140, pp. A1133-A1138.
21. Sholl, D. and Steckel , J. *DENSITY FUNCTIONAL THEORY A Practical Introduction.* s.l. : John Wiley and Sons, 2009.
22. *Inhomogeneous Electron Gas.* Kohn, W. and Hohenberg, P. 3B, s.l. : APS, 1964, PHYSICAL REVIEW JOURNALS ARCHIVE, Vol. 136, pp. B864-B871.
23. Perdew, J. Some Fundamental Issues in Ground-State Density Functional Theory: A Guide for the Perplexed. *Journal of Chemical Theory and Computation.* 2009, Vol. 5, 4, pp. 902-908.

24. *Self-Consistent Molecular-Orbital Methods. IX. An Extended Gaussian-Type Basis for Molecular-Orbital Studies of Organic Molecules.* Pople, J., Ditchfield, R. and Hehre, W. 2, s.l. : AIP Pub., 1971, The Journal of Chemical Physics, Vol. 54, pp. 724-728.
25. *Self-consistent molecular orbital methods 25. Supplementary functions for Gaussian basis sets.* Pople, J. and Frisch, M. 7, s.l. : AIP Pub., 1984, The Journal of Chemical Physics, Vol. 80, pp. 3265-3269.
26. *Gaussian basis sets for use in correlated molecular calculations. I. The atoms boron trough neon and hydrogen.* Dunning Jr., T. 2, s.l. : AIP Pub., 1989, The Journal of Chemical Physics, Vol. 90, pp. 1007-1023.
27. *Gaussian basis sets for use in correlated molecular calculations. VII. Valence, core-valence, and scalar relativistic basis sets for Li, Be, Na, and Mg.* Prascher, B., Woon, D. and Peterson, K. 1, s.l. : Springer, 2011, Theoretical Chemistry Accounts, Vol. 128, pp. 69-82.
28. *Gaussian basis sets for use in correlated molecular calculations. IX. The atoms gallium through krypton.* Wilson, A., et al. 16, s.l. : AIP Pub., 1999, The Journal of Chemical Physics, Vol. 110, pp. 7667-7676.
29. *Electron affinities of the first-row atoms revisited. Systematic basis sets and wave functions.* Kendall, R. and Dunning Jr., T. 9, s.l. : AIP Pub., 1992, The Journal of Chemical Physics, Vol. 96, pp. 6796-6806.
30. *Gaussian basis sets for use in correlated molecular calculations. III. The atoms aluminium through argon.* Woon, D. and Dunning Jr., T. 2, s.l. : The Journal of Chemical Physics, 1993, Vol. 98, pp. 1358-1371.
31. *Parallel Douglas-Kroll energy and gradients in NWChem; Estimating scalar relativistic effects using Douglad-Kroll contracted basis sets.* De Jong, W., Harrison, R. and Dixon, D. 1, s.l. : AIP Pub., 2001, The Journal of Chemical Physics, Vol. 114, pp. 48-53.
32. *Systematically convergent basis sets with relativistic pseudopotentials. I. Correlation consistent basis sets for the post-d group 13-15 elements.* Peterson, K. 21, s.l. : AIP Pub., 2003, The Journal of Chemical Physics, Vol. 119, pp. 11099-11112.
33. *Systematically convergent basis sets for transition metals. I. All-electron correlation consistent basis sets for the 3d elements Sc-Zn.* Balabanov, N. and Peterson, K. 6, s.l. : AIP Pub., 2005, The Journal of Chemical Physics, Vol. 123, pp. 064107-1 - 064107-15.
34. *Perspective on ``Density functional thermochemistry. III. The role of exact exchange''.* Becke, A. D. s.l. : AIP Publishing, 1993, The Journal of Chemical Physics , Vol. 98, pp. 361-363.
35. *Development of the Colle-Salvetti correlation-energy formula into a functional of the electron density.* Lee, Chengteh, Yang, Weitao and Parr, Robert G. s.l. : APS, 1988, PHYSICAL REVIEW B, Vol. 37, pp. 785-789.
36. *Accurate spin-dependent electron liquid correlation energies for local spin density calculations: a critical analysis.* Vosko, S. H. , Wilk, L. and Nusair, M. . s.l. : Canadian Science Publishing, 1980, Canadian Journal of Physics, Vol. 58, pp. 1200-1211.
37. *Variational configuration interaction methods and comparison with perturbation theory.* Pople, J. 11, s.l. : Wiley, January 1977, International Journal of Quantum Chemistry, Vol. 12, pp. 149-163.
38. *A biography of the coupled cluster method.* Kümmel, H. 1, s.l. : World Scientific Pub., 2002, Recent Progress in Many-Body Theories, Vol. 1, pp. 334-348.
39. Cramer, C. *Essentials of Computational Chemistry* . s.l. : John Wiley & Sons, 2002. pp. 191-232. Vol. 2.
40. Shavitt, I. *Many-Body Methods in Chemistry and Physics: MBPT and Coupled-Cluster Theory.* s.l. : Cambridge University Press, 2009.
41. Stewart, J. MOPAC . [Online] 2007. http://openmopac.net/manual/Hessian_Matrix.html.

42. Wilson, E. *Molecular vibrations the theory of infrared and Raman vibrational spectra.* s.l. : McGraw-Hill, 1955. Vol. 1.
43. NIST. CCCBDB. [Online] May 22, 2022. https://cccbdb.nist.gov/enthcalcx.asp.
44. *Gaussian-3 theory using reduced Moller-Plesset order.* Curtiss, L. 10, s.l. : AIP Pub., 1999, The Journal of Chemical Physics, Vol. 110, pp. 4703-4709.
45. *Gaussian-3 (G3) theory for molecules containing first and second-row atoms.* Curtiss, L. 18, s.l. : AIP Pub., 1998, The Journal of Chemical Physics, Vol. 109, pp. 7764-7776.
46. Lee, Woo Y., Lackey, W. J. and Agrawal, P. K. Kinetic and Thermodynamic Analyses of Chemical Vapor Deposition of Aluminum Nitride. *Journal of the american ceramics society.* 8, 1991, Vol. 74, pp. 1821-1827.
47. *Epitaxial and polycrystalline growth of AlN by high temperature CVD: Experimental results and simulation.* Boichot, R. s.l. : Elsevier, 2010, Vol. 205, pp. 1294-1301.
48. Dollet, A. Chemical vapour deposition of polycrystalline AlN films from AlCl3–NH3 mixtures.: Analysis and modelling of transport phenomena. *Thin Solid Films.* 2002, Vol. 406, 1-2, pp. 1-16.
49. GRUJICIC, M. and LAI, S. G. Multi-length scale modeling of chemical vapor deposition of titanium nitride coatings. *JOURNAL OF MATERIALS SCIENCE.* 2001, 36, pp. 2937-2953.
50. Su, Juan et. al. Chemical vapor deposition of titanium nitride thin films: kinetics and experiments. *CrystEngComm.* 2019, Vol. 21, pp. 3974–3981.
51. Kuo, Dong-Hau and Huang, Kwon-Wen. Kinetics and microstructure of TiN coatings by CVD. *Surface and Coatings Technology.* 2000, 135, pp. 150-157.
52. *A reaction mechanism for titanium nitride CVD from TiCl4 and NH3.* Allendor, Mark and Richard, Larson. 96, 1996, Proceedings of the 13th International Symposium on Chemical Vapor Deposition, pp. 41-46.
53. *Chemical vapor deposition of titanium nitride thin films: kinetics and experiments.* Su, J. and Boichot, R. s.l. : The Royal Society of Chemistry, 2019, CrystEngComm, Vol. 21, pp. 3974-3981 .
54. *Kinetic analysis of face-centered-cubic Ti1-xAlxN film deposition by chemical vapor deposition.* Momoko, D. s.l. : Elsevier, 2021, Materials Science & Enigneering B, Vol. 264, pp. 114992-1 - 114992-6.
55. *CVD TiAlN - development and challenges for use in mass production.* Czettl, C. Reutte : ResearchGate, 2017. 19th Plansee Seminar. HM 45/1-HM 45/13.
56. *Deposition and Analysis of Al-Rich c-AlxTi1-xN Coating with Preferred Orientation.* Paseuth, Anongsack. 1, s.l. : The American Ceramic Society, 2017, Journal of The American Ceramic Society, Vol. 100, pp. 1-9.
57. *Self-organized periodic soft-hard nanolamellae in polycrystalline TiAlN.* Keckes, J., Daniel, R. and Mitterer, C. s.l. : Elsevier, 2013, Thin Solid Films, Vol. 545, pp. 29-32.
58. *Al-rich cubic Al0.8Ti0.2N coating with self-organized nano-lamellar microstructure: Thermal and mechanical properties.* Todt, J., Zalesak, J. and Daniel, R. s.l. : Elsevier, 2016, Surface & Coatings Technology, Vol. 291, pp. 89-93.
59. *Influence of the deposition parameters on the nanolamella periodicity of chemical vapor deposited Ti1-xAlxN.* Saringer, C. and Tkadletz, M. s.l. : Elsevier, 2021, Materials Letters, Vol. 305, pp. 130819-1 - 130819-4.
60. [Online] https://www.sciencedirect.com/science/article/abs/pii/S0167577X21015160?via%3Dihub.
61. [Online] https://www.researchgate.net/profile/Christoph-Czettl/publication/318116102_CVD_TiAlN_-_Development_and_challenges_for_use_in_mass_production_History_and_development_of_CVD-TiAlN/links/595a9265a6fdcc36b4d7b891/CVD-TiAlN-Development-and-challenges-for-use-.

62. *Recent developments in the general atomic and molecular electronic structure system.* Bertoni, Colleen, et al. 152, s.l. : AIP Publishing, 2020, The Journal of Chemical Physics, pp. 154102-1 - 154102-26.
63. *Avogadro: an advanced semantic chemical editor, visualization, and analysis platform.* Hanwell, Markus, Curtis, Donald E and Lonie, David C. 17, s.l. : BMC, 2012, Journal of Cheminformatics, Vol. 4, pp. 1-32.
64. Conolly College of liberal arts and sciences, Chemistry Departement. GAMESS Input Documentation: FFCALC section. [Online] July 7, 2017. http://myweb.liu.edu/~nmatsuna/gamess/input/FFCALC.html.
65. Laboratories, Sandia National. [Online] 2000. https://www3.nd.edu/~powers/ame.60636/kee2000.pdf.
66. Nix, Roger (Queen Mary University of London). LibreTexts Chemistry. [Online] February 21, 2022. https://chem.libretexts.org/Bookshelves/Physical_and_Theoretical_Chemistry_Textbook_Maps/Book%3A_Surface_Science_(Nix).
67. Qiu, R. CVD TiAlN coatings with tunable nanolamella architectures. *Surface and Coatings Technology.* 2021, Vol. 413, pp. 127076[1]-127076[10].
68. *Moller-Plesset perturbation theory: from small molecule methods to methods for thousands of atoms.* Cremer, Dieter. 4, s.l. : John Wiley & Sons, August 2011, Advanced Review, Vol. 1, pp. 509-530.
69. *Note on an Approximation Treatment for Many-Electron Systems.* Moller, C. and Plesset, M. 7, s.l. : APS, October 1934, Physical Review Journals Archive, Vol. 46, pp. 618-622.
70. *Contribution of triple substitutions to the electron correlational energy in fourth order perturbation theory.* Krishnan, R., Frisch, M. and Pople, J. 7, s.l. : AIP, 1980, The Journal of Chemical Physics, Vol. 72, pp. 4244-4245.
71. *Gaussian-4 theory.* Curtiss, L. 8, s.l. : AIP Pub., 2007, The Journal of Chemical Physics, Vol. 126, pp. 084108-1 - 084108-12.
72. *Self-Consistent Orbitals for Radicals.* Pople, J. and Nesbet, R. 3, s.l. : AIP Pub., 1954, The Journal of Chemical Physics, Vol. 22, pp. 571-572.
73. *Self-Consistent Field Theory for Open Shells of Electronic Systems.* Roothaan, C. s.l. : APS, 1960, REVIEWS OF MODERN PHYSICS, Vol. 32, pp. 179-185.
74. *Ab initio and analytical intermolecular potential for Cl O-H2O.* Du, S. and Francisci, J. 11, s.l. : AIP Pub., 2007, The Journal of Chemical Physics, Vol. 126, pp. 114304-1 114304-10.

6 Appendix

Calculated thermodynamic data by ab initio methods

Until explicitly stated all units for temperature are given in K, all heat capacities and entropies are given in calories per (mole*K) and all entropies are given in kcal per mole. Hf refers to the formation enthalpies at 298K. Also screenshots of all the molecules can be found below with their respective species.

Al2Cl6 Thermodynamic data for Chemkin Fit Hf = -313.99 KCAL/MOLE								
T	H-H0 rot	H-H0trans	H-H0vib	H-H0	S	Cp	S kor.	H-H298
0	0	0	0	0,000	-	-	-	-7,949
298	0,889	0,889	6,171	7,949	116,787	38,443	114,030	0,000
300	0,894	0,894	6,228	8,016	117,025	38,494	114,268	0,068
400	1,192	1,192	9,445	11,829	128,403	40,485	125,646	3,880
500	1,49	1,49	12,793	15,773	137,563	41,548	134,806	7,824
600	1,788	1,788	16,213	19,789	145,198	42,17	142,441	11,841
700	2,087	2,087	19,677	23,851	151,730	42,562	148,973	15,902
800	2,385	2,385	23,168	27,938	157,431	42,823	154,674	19,990
900	2,683	2,683	26,679	32,045	162,486	43,006	159,729	24,096
1000	2,981	2,981	30,203	36,165	167,025	43,138	164,268	28,216
1100	3,279	3,279	33,737	40,295	171,141	43,237	168,384	32,346
1200	3,577	3,577	37,278	44,432	174,907	43,312	172,150	36,483
1300	3,875	3,875	40,825	48,575	178,376	43,372	175,619	40,627
1500	4,471	4,471	47,932	56,874	184,589	43,457	181,832	48,926
1700	5,067	5,067	55,052	65,186	190,032	43,514	187,275	57,237
1900	5,663	5,663	62,179	73,505	194,874	43,555	192,117	65,557
2100	6,26	6,26	69,313	81,833	199,235	43,584	196,478	73,884
2300	6,856	6,856	76,451	90,163	203,201	43,606	200,444	82,214
2500	7,452	7,452	83,592	98,496	206,837	43,624	204,080	90,547
2700	8,048	8,048	90,736	106,832	210,195	43,637	207,438	98,883
2900	8,644	8,644	97,882	115,170	213,314	43,648	210,557	107,221
3100	9,24	9,24	105,030	123,510	216,225	43,657	213,468	115,561
3300	9,837	9,837	112,179	131,853	218,955	43,664	216,198	123,904
3500	10,433	10,433	119,329	140,195	221,524	43,67	218,767	132,246
3700	11,029	11,029	126,480	148,538	223,951	43,675	221,194	140,589
3900	11,625	11,625	133,632	156,882	226,250	43,679	223,493	148,933
4100	12,221	12,221	140,785	165,227	228,435	43,683	225,678	157,278
4300	12,817	12,817	147,938	173,572	230,515	43,686	227,758	165,623
4500	13,414	13,414	155,092	181,920	232,502	43,689	229,745	173,971
4700	14,01	14,01	162,246	190,266	234,401	43,691	231,644	182,317
4900	14,606	14,606	169,400	198,612	236,222	43,693	233,465	190,664
5000	14,904	14,904	172,978	202,786	237,105	43,694	234,348	194,837

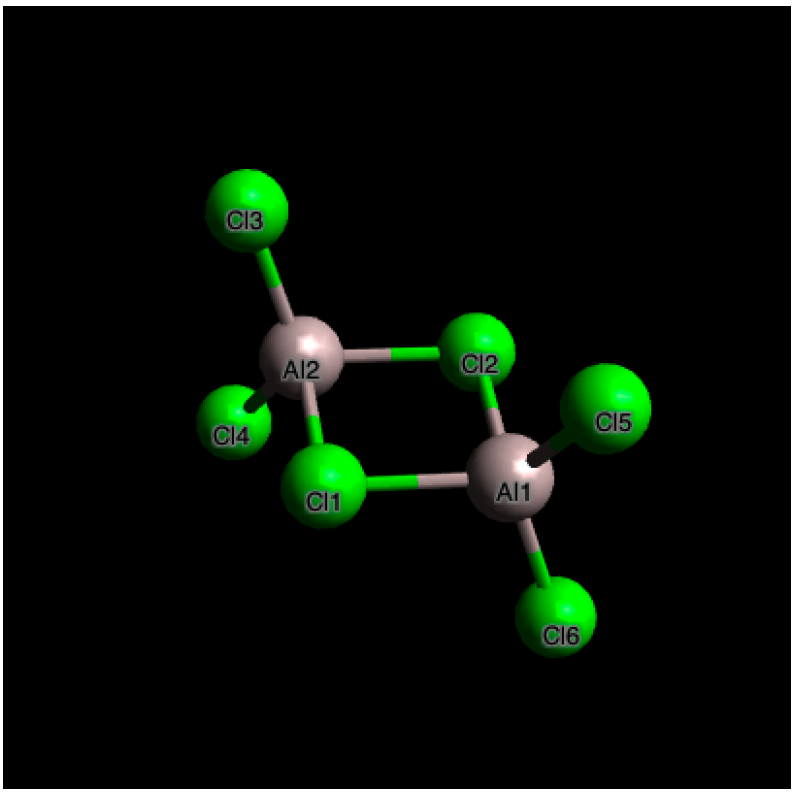

AlCl Thermodynamic data for Chemkin Fit Hf = -13.22 KCAL/MOLE								
T	H-H0 rot	H-H0trans	H-H0vib	H-H0	S	Cp	S kor.	H-H298
0	0	0	0,000	0,000	-	-	-	-1,947
298	0,889	0,889	0,169	1,947			0	0,000
300	0,894	0,894	0,172	1,960	54,639	8,345	54,639	0,013
400	1,192	1,192	0,323	2,707	57,075	8,575	57,075	0,760
500	1,49	1,49	0,491	3,471	59,003	8,697	59,003	1,524
600	1,788	1,788	0,669	4,245	60,596	8,768	60,596	2,298
700	2,087	2,087	0,852	5,026	61,951	8,813	61,951	3,079
800	2,385	2,385	1,040	5,810	63,130	8,842	63,13	3,863
900	2,683	2,683	1,229	6,595	64,172	8,863	64,172	4,648
1000	2,981	2,981	1,421	7,383	65,107	8,877	65,107	5,436
1100	3,279	3,279	1,614	8,172	65,953	8,889	65,953	6,225
1200	3,577	3,577	1,808	8,962	66,727	8,897	66,727	7,015
1300	3,875	3,875	2,002	9,752	67,440	8,904	67,44	7,805
1500	4,471	4,471	2,393	11,335	68,714	8,913	68,714	9,388
1700	5,067	5,067	2,785	12,919	69,831	8,92	69,831	10,972
1900	5,663	5,663	3,179	14,505	70,823	8,924	70,823	12,558
2100	6,26	6,26	3,573	16,093	71,716	8,927	71,716	14,146
2300	6,856	6,856	3,968	17,680	72,528	8,93	72,528	15,733
2500	7,452	7,452	4,364	19,268	73,273	8,932	73,273	17,321
2700	8,048	8,048	4,759	20,855	73,961	8,933	73,961	18,908
2900	8,644	8,644	5,155	22,443	74,599	8,935	74,599	20,496
3100	9,24	9,24	5,552	24,032	75,195	8,935	75,195	22,085
3300	9,837	9,837	5,948	25,622	75,754	8,936	75,754	23,675
3500	10,433	10,433	6,345	27,211	76,279	8,937	76,279	25,264
3700	11,029	11,029	6,741	28,799	76,776	8,938	76,776	26,852
3900	11,625	11,625	7,138	30,388	77,247	8,938	77,247	28,441
4100	12,221	12,221	7,535	31,977	77,694	8,938	77,694	30,030
4300	12,817	12,817	7,932	33,566	78,119	8,939	78,119	31,619
4500	13,414	13,414	8,329	35,157	78,526	8,939	78,526	33,210
4700	14,01	14,01	8,726	36,746	78,914	8,939	78,914	34,799
4900	14,606	14,606	9,123	38,335	79,287	8,94	79,287	36,388
5000	14,904	14,904	9,322	39,130	79,468	8,94	79,468	37,183

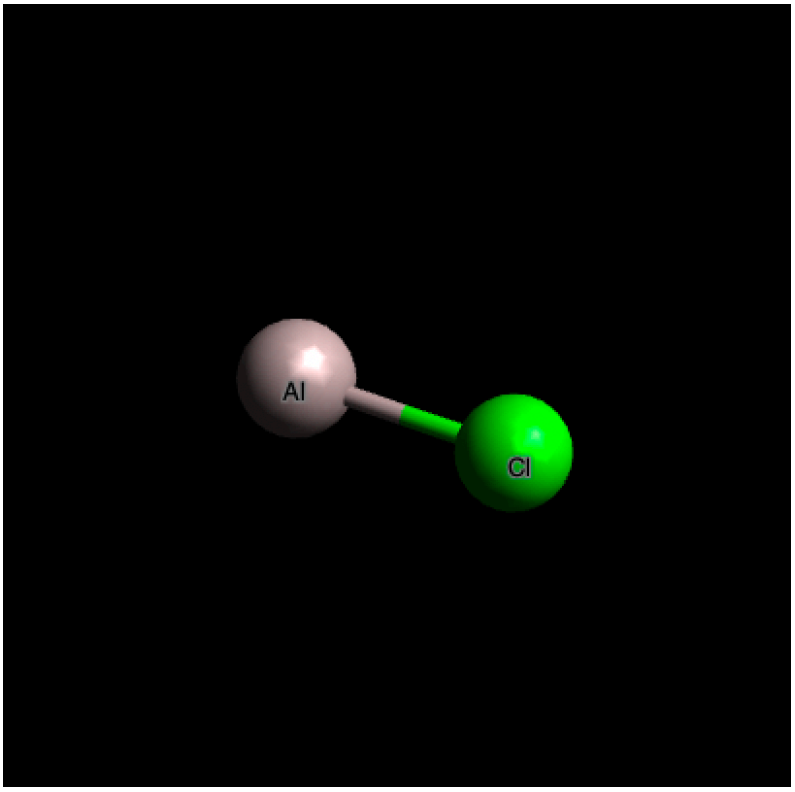

AlCl2NH2 Thermodynamic data for Chemkin Fit Hf = -138.01 KCAL/MOLE								
T	H-H0 rot	H-H0trans	H-H0vib	H-H0	S	Cp	S kor.	H-H298
0	0	0	0	0,000	-	-	-	-2,443
298	0,889	0,889	8,445	2,443	79,407	20,877	78,029	0,000
300	0,894	0,894	8,525	2,465	79,536	20,921	78,158	0,021
400	1,192	1,192	12,977	3,671	85,833	22,811	84,455	1,228
500	1,49	1,49	17,626	4,925	91,067	24,062	89,689	2,482
600	1,788	1,788	22,382	6,204	95,537	24,963	94,159	3,761
700	2,087	2,087	27,201	7,499	99,440	25,665	98,062	5,055
800	2,385	2,385	32,061	8,803	102,906	26,25	101,528	6,359
900	2,683	2,683	36,949	10,114	106,028	26,761	104,650	7,670
1000	2,981	2,981	41,857	11,429	108,872	27,216	107,494	8,986
1100	3,279	3,279	46,780	12,748	111,485	27,626	110,107	10,305
1200	3,577	3,577	51,713	14,070	113,905	27,996	112,527	11,626
1300	3,875	3,875	56,655	15,393	116,159	28,33	114,781	12,950
1500	4,471	4,471	66,556	18,045	120,255	28,899	118,877	15,601
1700	5,067	5,067	76,476	20,700	123,901	29,358	122,523	18,257
1900	5,663	5,663	86,408	23,359	127,187	29,727	125,809	20,915
2100	6,26	6,26	96,348	26,020	130,177	30,025	128,799	23,577
2300	6,856	6,856	106,295	28,682	132,920	30,268	131,542	26,239
2500	7,452	7,452	116,246	31,346	135,452	30,467	134,074	28,902
2700	8,048	8,048	126,202	34,010	137,804	30,631	136,426	31,567
2900	8,644	8,644	136,160	36,675	139,997	30,768	138,619	34,232
3100	9,24	9,24	146,121	39,341	142,053	30,883	140,675	36,897
3300	9,837	9,837	156,084	42,007	143,987	30,98	142,609	39,564
3500	10,433	10,433	166,048	44,674	145,813	31,063	144,435	42,230
3700	11,029	11,029	176,014	47,340	147,541	31,134	146,163	44,897
3900	11,625	11,625	185,981	50,007	149,181	31,196	147,803	47,564
4100	12,221	12,221	195,949	52,675	150,743	31,25	149,365	50,231
4300	12,817	12,817	205,918	55,342	152,232	31,296	150,854	52,899
4500	13,414	13,414	215,888	58,010	153,656	31,337	152,278	55,567
4700	14,01	14,01	225,858	60,678	155,020	31,374	153,642	58,235
4900	14,606	14,606	235,829	63,346	156,328	31,406	154,950	60,903
5000	14,904	14,904	240,814	64,680	156,962	31,421	155,584	62,237

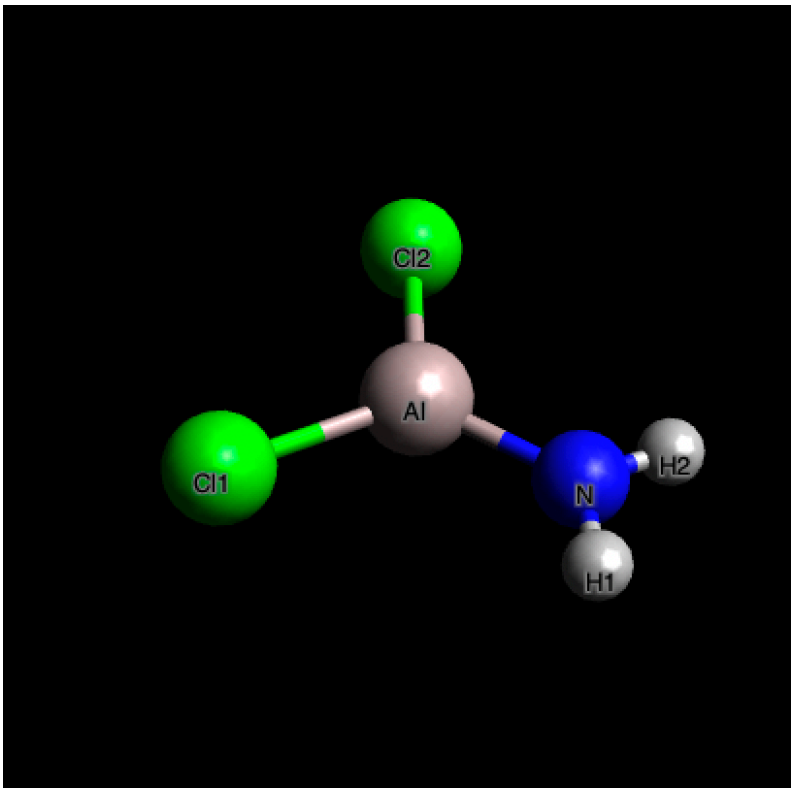

AlCl3 Thermodynamic data for Chemkin Fit Hf = -141.05 KCAL/MOLE								
T	H-H0 rot	H-H0trans	H-H0vib	H-H0	S	Cp	S kor.	H-H298
0	0,000	0,000	0,000	0,000	-	-	-	-3,481
298	0,889	0,889	1,703	3,481	78,404	17,089	74,844	0,000
300	0,894	0,894	1,721	3,509	78,967	17,303	75,407	0,028
400	1,192	1,192	2,732	5,116	84,088	18,243	80,528	1,635
500	1,490	1,490	3,808	6,788	88,220	18,765	84,660	3,307
600	1,788	1,788	4,919	8,495	91,671	19,077	88,111	5,014
700	2,087	2,087	6,052	10,226	94,627	19,275	91,067	6,745
800	2,385	2,385	7,200	11,970	97,211	19,409	93,651	8,489
900	2,683	2,683	8,357	13,723	99,502	19,503	95,942	10,242
1000	2,981	2,981	9,522	15,484	101,561	19,571	98,001	12,003
1100	3,279	3,279	10,691	17,249	103,429	19,622	99,869	13,768
1200	3,577	3,577	11,865	19,019	105,138	19,661	101,578	15,537
1300	3,875	3,875	13,041	20,791	106,713	19,692	103,153	17,310
1500	4,471	4,471	15,400	24,342	109,534	19,736	105,974	20,861
1700	5,067	5,067	17,766	27,900	112,006	19,766	108,446	24,419
1900	5,663	5,663	20,136	31,462	114,206	19,787	110,646	27,981
2100	6,260	6,260	22,509	35,029	116,187	19,802	112,627	31,548
2300	6,856	6,856	24,884	38,596	117,989	19,814	114,429	35,115
2500	7,452	7,452	27,261	42,165	119,641	19,822	116,081	38,684
2700	8,048	8,048	29,640	45,736	121,167	19,830	117,607	42,255
2900	8,644	8,644	32,019	49,307	122,584	19,835	119,024	45,826
3100	9,240	9,240	34,400	52,880	123,907	19,840	120,347	49,399
3300	9,837	9,837	36,781	56,455	125,148	19,843	121,588	52,974
3500	10,433	10,433	39,163	60,029	126,315	19,847	122,755	56,547
3700	11,029	11,029	41,545	63,603	127,418	19,849	123,858	60,122
3900	11,625	11,625	43,927	67,177	128,463	19,852	124,903	63,696
4100	12,221	12,221	46,310	70,752	129,456	19,853	125,896	67,271
4300	12,817	12,817	48,694	74,328	130,402	19,855	126,842	70,847
4500	13,414	13,414	51,077	77,905	131,305	19,857	127,745	74,424
4700	14,010	14,010	53,461	81,481	132,168	19,858	128,608	78,000
4900	14,606	14,606	55,845	85,057	132,996	19,859	129,436	81,576
5000	14,904	14,904	57,037	86,845	133,397	19,860	129,837	83,364

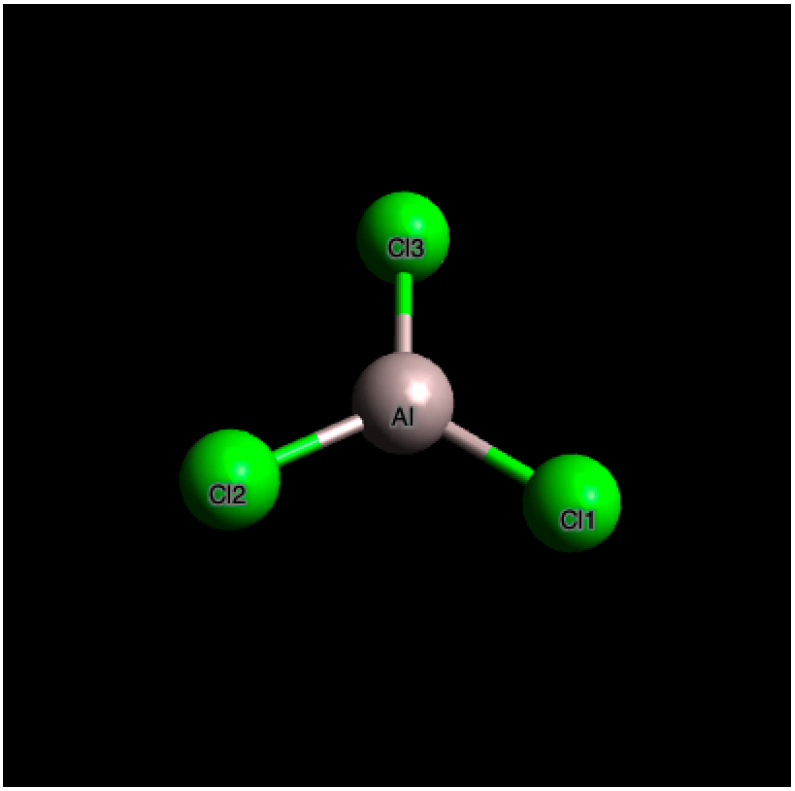

TiCl3 Thermodynamic data for Chemkin Fit Hf = -519.52 kJ/mol								
T	H-H0 rot	H-H0trans	H-H0vib	H-H0	S	Cp	S kor	H-H298
0	0	0	0	0,000	-	-	-	-10,223
298	0,889	0,889	8,445	10,223	84,548	17,995	82,363	0,000
300	0,894	0,894	8,525	10,313	84,659	18,014	82,474	0,090
400	1,192	1,192	12,977	15,361	89,951	18,731	87,766	5,138
500	1,49	1,49	17,626	20,606	94,176	19,11	91,991	10,383
600	1,788	1,788	22,382	25,958	97,681	19,33	95,496	15,734
700	2,087	2,087	27,201	31,375	100,672	19,468	98,487	21,152
800	2,385	2,385	32,061	36,831	103,278	19,56	101,093	26,608
900	2,683	2,683	36,949	42,315	105,586	19,624	103,401	32,092
1000	2,981	2,981	41,857	47,819	107,656	19,67	105,471	37,596
1100	3,279	3,279	46,780	53,338	109,532	19,704	107,347	43,114
1200	3,577	3,577	51,713	58,867	111,248	19,731	109,063	48,644
1300	3,875	3,875	56,655	64,405	112,828	19,751	110,643	54,181
1500	4,471	4,471	66,556	75,498	115,657	19,781	113,472	65,275
1700	5,067	5,067	76,476	86,610	118,134	19,801	115,949	76,387
1900	5,663	5,663	86,408	97,734	120,337	19,815	118,152	87,510
2100	6,26	6,26	96,348	108,868	122,321	19,825	120,136	98,645
2300	6,856	6,856	106,295	120,007	124,125	19,833	121,940	109,783
2500	7,452	7,452	116,246	131,150	125,779	19,839	123,594	120,927
2700	8,048	8,048	126,202	142,298	127,306	19,844	125,121	132,074
2900	8,644	8,644	136,160	153,448	128,724	19,847	126,539	143,225
3100	9,24	9,24	146,121	164,601	130,048	19,851	127,863	154,378
3300	9,837	9,837	156,084	175,758	131,289	19,853	129,104	165,534
3500	10,433	10,433	166,048	186,914	132,457	19,855	130,272	176,691
3700	11,029	11,029	176,014	198,072	133,560	19,857	131,375	187,849
3900	11,625	11,625	185,981	209,231	134,606	19,858	132,421	199,008
4100	12,221	12,221	195,949	220,391	135,599	19,86	133,414	210,168
4300	12,817	12,817	205,918	231,552	136,545	19,861	134,360	221,329
4500	13,414	13,414	215,888	242,716	137,448	19,862	135,263	232,492
4700	14,01	14,01	225,858	253,878	138,312	19,863	136,127	243,654
4900	14,606	14,606	235,829	265,041	139,139	19,863	136,954	254,817
5000	14,904	14,904	240,814	270,622	139,541	19,864	137,356	260,399

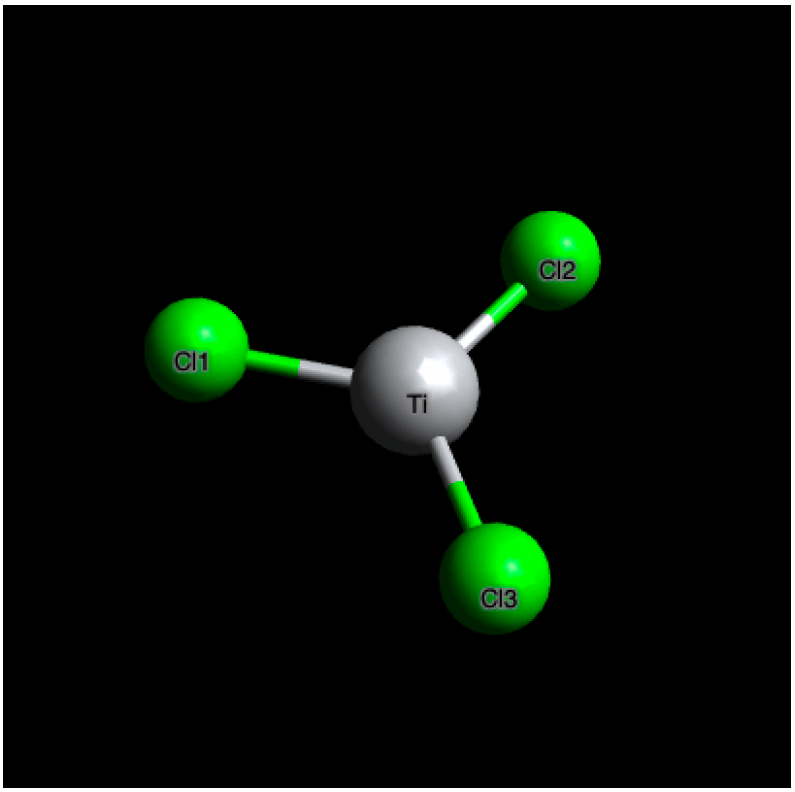

TiCl4 Thermodynamic data for Chemkin Fit Hf = -810.20 kJ/mol								
T	H-H0 rot	H-H0trans	H-H0vib	H-H0	S	Cp	S kor.	H-H298
0	0	0	0	0,000	-	-	-	-4,729
298	0,889	0,889	2,951	4,729	89,765	23,012	84,823	0,000
300	0,894	0,894	2,979	4,767	89,843	23,039	84,902	0,039
400	1,192	1,192	4,576	6,960	96,636	24,119	91,695	2,232
500	1,49	1,49	6,244	9,224	102,086	24,689	97,145	4,495
600	1,788	1,788	7,950	11,526	106,619	25,019	101,678	6,797
700	2,087	2,087	9,678	13,852	110,492	25,227	105,551	9,124
800	2,385	2,385	11,422	16,192	113,870	25,364	108,929	11,464
900	2,683	2,683	13,176	18,542	116,863	25,46	111,922	13,813
1000	2,981	2,981	14,936	20,898	119,550	25,53	114,609	16,170
1100	3,279	3,279	16,702	23,260	121,986	25,582	117,045	18,532
1200	3,577	3,577	18,472	25,626	124,213	25,621	119,272	20,898
1300	3,875	3,875	20,245	27,995	126,265	25,652	121,324	23,266
1500	4,471	4,471	23,797	32,739	129,940	25,697	124,999	28,011
1700	5,067	5,067	27,356	37,490	133,158	25,727	128,217	32,762
1900	5,663	5,663	30,919	42,245	136,021	25,748	131,080	37,517
2100	6,26	6,26	34,486	47,006	138,598	25,764	133,657	42,277
2300	6,856	6,856	38,054	51,766	140,943	25,775	136,002	47,037
2500	7,452	7,452	41,624	56,528	143,092	25,784	138,151	51,800
2700	8,048	8,048	45,196	61,292	145,077	25,791	140,136	56,563
2900	8,644	8,644	48,769	66,057	146,920	25,797	141,979	61,328
3100	9,24	9,24	52,342	70,822	148,641	25,801	143,700	66,094
3300	9,837	9,837	55,917	75,591	150,254	25,805	145,313	70,862
3500	10,433	10,433	59,491	80,357	151,772	25,808	146,831	75,629
3700	11,029	11,029	63,067	85,125	153,207	25,811	148,266	80,396
3900	11,625	11,625	66,643	89,893	154,565	25,813	149,624	85,164
4100	12,221	12,221	70,219	94,661	155,856	25,815	150,915	89,932
4300	12,817	12,817	73,795	99,429	157,086	25,817	152,145	94,701
4500	13,414	13,414	77,372	104,200	158,260	25,818	153,319	99,472
4700	14,01	14,01	80,949	108,969	159,382	25,819	154,441	104,241
4900	14,606	14,606	84,526	113,738	160,458	25,821	155,517	109,010
5000	14,904	14,904	86,315	116,123	160,980	25,821	156,039	111,394

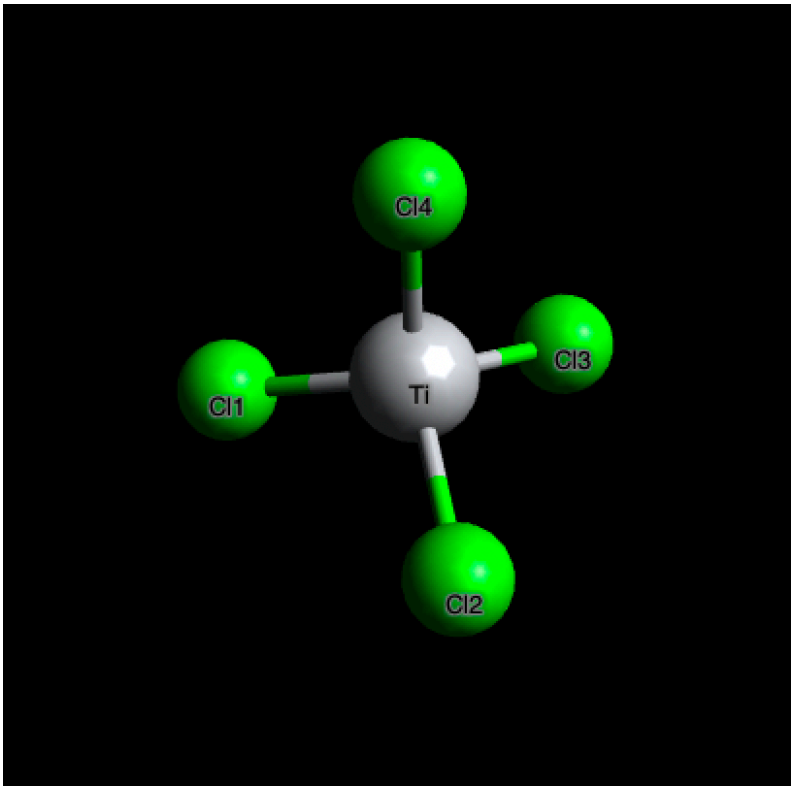

TiCl4(NH3)2 Thermodynamic data for Chemkin Fit Hf = -991,23 kJ/mol								
T	H-H0 rot	H-H0trans	H-H0vib	H-H0	S	Cp	S kor.	H-H298
0	0	0	0	0,000	-	-	-	-8,290
298	0,889	0,889	6,512	8,290	114,351	43,683	114,351	0,000
300	0,894	0,894	6,578	8,366	114,622	43,769	114,622	0,076
400	1,192	1,192	10,369	12,753	127,779	47,688	127,779	4,463
500	1,49	1,49	14,502	17,482	138,757	50,703	138,757	9,192
600	1,788	1,788	18,907	22,483	148,226	53,169	148,226	14,194
700	2,087	2,087	23,540	27,714	156,584	55,275	156,584	19,425
800	2,385	2,385	28,371	33,141	164,088	57,127	164,088	24,851
900	2,683	2,683	33,376	38,742	170,914	58,777	170,914	30,453
1000	2,981	2,981	38,538	44,500	177,184	60,251	177,184	36,210
1100	3,279	3,279	43,839	50,397	182,990	61,565	182,990	42,107
1200	3,577	3,577	49,264	56,418	188,397	62,734	188,397	48,128
1300	3,875	3,875	54,799	62,549	193,461	63,77	193,461	54,260
1500	4,471	4,471	66,152	75,094	202,712	65,499	202,712	66,804
1700	5,067	5,067	77,811	87,945	210,996	66,853	210,996	79,655
1900	5,663	5,663	89,711	101,037	218,493	67,919	218,493	92,747
2100	6,26	6,26	101,801	114,321	225,333	68,764	225,333	106,031
2300	6,856	6,856	114,043	127,755	231,620	69,442	231,620	119,466
2500	7,452	7,452	126,408	141,312	237,434	69,992	237,434	133,022
2700	8,048	8,048	138,871	154,967	242,838	70,441	242,838	146,678
2900	8,644	8,644	151,417	168,705	247,886	70,813	247,886	160,416
3100	9,24	9,24	164,031	182,511	252,619	71,124	252,619	174,221
3300	9,837	9,837	176,702	196,376	257,074	71,385	257,074	188,086
3500	10,433	10,433	189,421	210,287	261,281	71,607	261,281	201,997
3700	11,029	11,029	202,181	224,239	265,265	71,796	265,265	215,950
3900	11,625	11,625	214,977	238,227	269,049	71,96	269,049	229,937
4100	12,221	12,221	227,803	252,245	272,652	72,102	272,652	243,955
4300	12,817	12,817	240,655	266,289	276,089	72,225	276,089	257,999
4500	13,414	13,414	253,531	280,359	279,375	72,334	279,375	272,069
4700	14,01	14,01	266,427	294,447	282,522	72,429	282,522	286,157
4900	14,606	14,606	279,341	308,553	285,542	72,514	285,542	300,263
5000	14,904	14,904	285,804	315,612	287,008	72,553	287,008	307,322

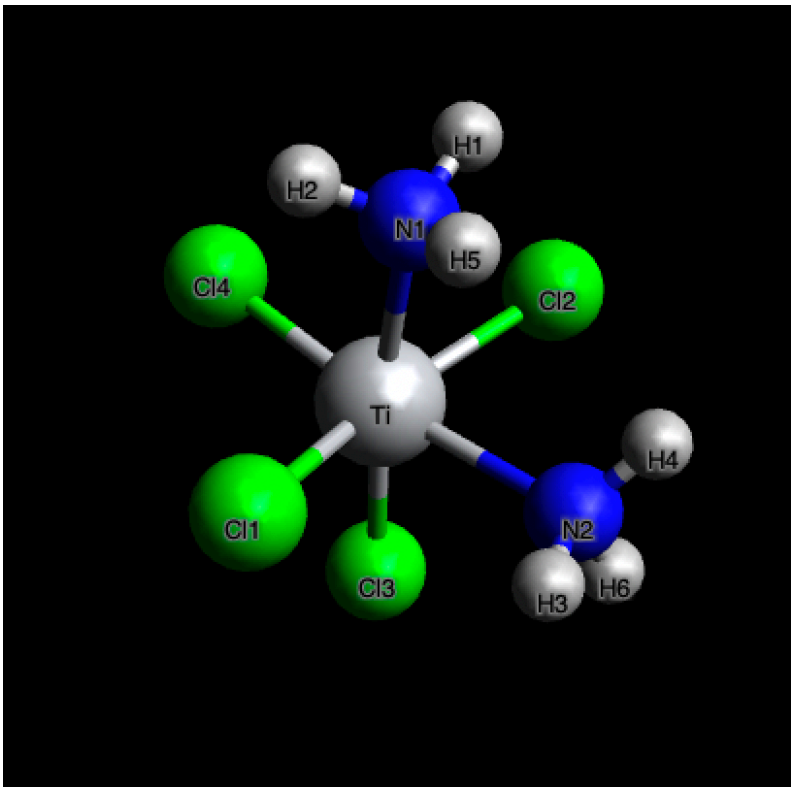

Chemkin input files

All Gas and Surface kinetic input files from Chemkin can be found below.

AlN:

```
ELEMENTS
H N AL CL
END
SPECIES
H2 H CL CL2 HCL NH3 ALCL3 ALCL2NH2
END

THERMO
ALCL3                   AL  1CL  3          G   300.000  5000.000 1000.00      1
 9.31278495E+00 8.53520149E-04-4.03437389E-07 8.27902269E-11-6.16923111E-15    2
-7.39040741E+04-1.56886400E+01 5.79299180E+00 1.51575843E-02-2.21968710E-05    3
 1.48366376E-08-3.75085396E-12-7.32113601E+04 1.23610451E+00                   4
ALCL2NH2                AL  1CL  2N   1H   2G   300.000  5000.000 1000.00      1
 1.02729534E+01 4.95031284E-03-1.83347057E-06 3.18203379E-10-2.10616426E-14    2
-7.28485157E+04-2.10006004E+01 5.13758846E+00 2.71070973E-02-3.74916344E-05    3
 2.57056373E-08-6.77175132E-12-7.19022090E+04 3.37073566E+00
END
REACTIONS JOULES/MOLE
H              + CL              + M => M       + HCL    7.20E+21  -2.0 0.0
2CL              + M => M       + CL2    2.00E+14  0.0 -7491
H              + HCL => H2       + CL    1.69E+13  0.0 17310
ALCL3             + NH3 => ALCL2NH2      + HCL    4.21E+11  0.0 34902
CL2              + H => HCL       + CL    8.60E+13  0.0 4905
2H              + H2 => 2H2    9.70E+16  -0.6 0
H2              + M => 2H       + M    2.20E+14  0.5 401566
HCL         + M => H       + CL       + M   7.90E+25 -3 445646
2H + M => H2 + M 6.53E+17 -1 0
END
```

```
SITE/AlN/    SDEN/1.556E-9/
   N(S)/1/ AL(S)/1/
END
BULK AL(D)/2.698/
BULK N(D) /1.374/END
THERMO
AL(S)              62987AL  1               G   300.000  5000.000  600.00      1
 2.55958900e+00-1.06322400e-04 7.20282800e-08-2.12110500e-11 2.28942900e-15    2
 3.89021400e+04 5.23452200e+00 2.73682500e+00-5.91237400e-04-4.03393800e-07    3
 2.32234300e-09-1.70559900e-12 3.88679500e+04 4.36388000e+00                   4
AL(D)              62987AL  1               G   300.000  5000.000  600.00      1
 2.55958900e+00-1.06322400e-04 7.20282800e-08-2.12110500e-11 2.28942900e-15    2
 3.89021400e+04 5.23452200e+00 2.73682500e+00-5.91237400e-04-4.03393800e-07    3
 2.32234300e-09-1.70559900e-12 3.88679500e+04 4.36388000e+00                   4
N(S)              120186N   1               G   300.000  5000.000 1000.00      1
 2.45026800e+00 1.06614600e-04-7.46533700e-08 1.87965200e-11-1.02598400e-15    2
 5.61160400e+04 4.44875800e+00 2.50307100e+00-2.18001800e-05 5.42052900e-08    3
-5.64756000e-11 2.09990400e-14 5.60989000e+04 4.16756600e+00                   4
N(D)              120186N   1               G   300.000  5000.000 1000.00      1
 2.45026800e+00 1.06614600e-04-7.46533700e-08 1.87965200e-11-1.02598400e-15    2
 5.61160400e+04 4.44875800e+00 2.50307100e+00-2.18001800e-05 5.42052900e-08    3
-5.64756000e-11 2.09990400e-14 5.60989000e+04 4.16756600e+00                   4
END


REACTIONS JOULES/MOLE
NH3             + AL(S) => AL(D)        + N(S)        + H2        +    H 4.453E+10  0.5 71949
ALCL3             + N(S) => N(D)        + AL(S)        + CL        + CL2    1.590E+10  0.5 64018
ALCL2NH2             + AL(S) =>  AL(D)        + N(D)        + AL(S)        + 2HCL    1.720E+10  0.5 42401
ALCL2NH2             + N(S) =>  N(D)        +AL(D)        + N(S)        + 2HCL    1.720E+10  0.5 42401
END
```

TiAlN:

```
ELEMENTS
H N TI CL AL
END
SPECIES
NH3 N2 TICL4 HCL TICL3 H2 CL2 ALCL3 H CL ALCL2NH2 TICL4N2H6
END
THERMO
ALCL3                   AL  1CL  3          G   300.000  5000.000 1000.00      1
 9.31278495E+00 8.53520149E-04-4.03437389E-07 8.27902269E-11-6.16923111E-15    2
-7.39040741E+04-1.56886400E+01 5.79299180E+00 1.51575843E-02-2.21968710E-05    3
 1.48366376E-08-3.75085396E-12-7.32113601E+04 1.23610451E+00                   4
TICL4N2H6               TI  1CL  4N   2H   6G   300.000  5000.000 1000.00      1
 1.92372093E+01 1.63167938E-02-6.30634833E-06 1.12721006E-09-7.61606145E-14    2
-1.25860697E+05-5.72306101E+01 1.32984738E+01 3.88107887E-02-3.81559203E-05    3
 2.10993111E-08-4.75394915E-12-1.24609903E+05-2.82644077E+01                   4
ALCL2NH2                AL  1CL  2N   1H   2G   300.000  5000.000 1000.00      1
 1.02729534E+01 4.95031284E-03-1.83347057E-06 3.18203379E-10-2.10616426E-14    2
-7.28485157E+04-2.10006004E+01 5.13758846E+00 2.71070973E-02-3.74916344E-05    3
 2.57056373E-08-6.77175132E-12-7.19022090E+04 3.37073566E+00                   4
END

REACTIONS CAL/MOLE
H              + CL              + M => M        + HCL    7.20E+21  -2.0 0.0
2CL              + M => M        + CL2    2.00E+14  0.0 -7491
H              + HCL => H2        + CL    1.69E+13  0.0 17310
CL2              + H => HCL        + CL    8.60E+13  0.0 4905
2H             + H2 => 2H2    9.70E+16  -0.6 0
H2             + M => 2H        + M    1.720E+08  0.5 401566
ALCL3             + NH3 => ALCL2NH2       + HCL    4.21E+13  0.0 34902
TICL4             + 2NH3 => TICL4N2H6    3.5E+18  0.0 38245
TICL4 => TICL3        + CL    2.32E+21 -1.17 387.9
END
```

```
SITE/TIALN/    SDEN/1.318E-8/
   N(S)/1/ TI(S)/1/ TICL3(S)/1/ TICL2(S)/1/ NH2(S)/1// ALCL(S)/1/
END
BULK TI(D)/4.500/
BULK AL(D)/2.698/
BULK N(D) /1.374/
END
THERMO
TI(S)               62987TI  1               G   300.000  5000.000  600.00      1
 2.55958900e+00-1.06322400e-04 7.20282800e-08-2.12110500e-11 2.28942900e-15    2
 3.89021400e+04 5.23452200e+00 2.73682500e+00-5.91237400e-04-4.03393800e-07    3
 2.32234300e-09-1.70559900e-12 3.88679500e+04 4.36388000e+00                   4
N(S)                62987N   1               G   300.000  5000.000  600.00      1
 2.55958900e+00-1.06322400e-04 7.20282800e-08-2.12110500e-11 2.28942900e-15    2
 3.89021400e+04 5.23452200e+00 2.73682500e+00-5.91237400e-04-4.03393800e-07    3
 2.32234300e-09-1.70559900e-12 3.88679500e+04 4.36388000e+00                   4
TICL2(S)          J14    TI  1CL  2          G   200.000  6000.000  800.00      1
 9.22517250e+00 8.98917361e-04-3.85692482e-07 7.03161823e-11-4.59177658e-15    2
-7.31586882e+04-1.52557384e+01 4.65587536e+00 2.18510800e-02-3.61191419e-05    3
 2.68883110e-08-7.46025276e-12-7.23669824e+04 6.14773433e+00                   4
TICL3(S)          J14    TI  1CL  3          G   200.000  6000.000  800.00      1
 9.22517250e+00 8.98917361e-04-3.85692482e-07 7.03161823e-11-4.59177658e-15    2
-7.31586882e+04-1.52557384e+01 4.65587536e+00 2.18510800e-02-3.61191419e-05    3
 2.68883110e-08-7.46025276e-12-7.23669824e+04 6.14773433e+00                   4
NH2(S)            J14    N   1H   2          G   200.000  6000.000  800.00      1
 9.22517250e+00 8.98917361e-04-3.85692482e-07 7.03161823e-11-4.59177658e-15    2
-7.31586882e+04-1.52557384e+01 4.65587536e+00 2.18510800e-02-3.61191419e-05    3
 2.68883110e-08-7.46025276e-12-7.23669824e+04 6.14773433e+00                   4
TI(D)               62987TI  1               G   300.000  5000.000  600.00      1
 2.55958900e+00-1.06322400e-04 7.20282800e-08-2.12110500e-11 2.28942900e-15    2
 3.89021400e+04 5.23452200e+00 2.73682500e+00-5.91237400e-04-4.03393800e-07    3
 2.32234300e-09-1.70559900e-12 3.88679500e+04 4.36388000e+00                   4
N(D)                62987N   1               G   300.000  5000.000  600.00      1
 2.55958900e+00-1.06322400e-04 7.20282800e-08-2.12110500e-11 2.28942900e-15    2
 3.89021400e+04 5.23452200e+00 2.73682500e+00-5.91237400e-04-4.03393800e-07    3
 2.32234300e-09-1.70559900e-12 3.88679500e+04 4.36388000e+00                   4
ALCL(S)            62987AL  1CL  1          G   300.000  5000.000  600.00      1
 2.55958900e+00-1.06322400e-04 7.20282800e-08-2.12110500e-11 2.28942900e-15    2
 3.89021400e+04 5.23452200e+00 2.73682500e+00-5.91237400e-04-4.03393800e-07    3
 2.32234300e-09-1.70559900e-12 3.88679500e+04 4.36388000e+00                   4
AL(D)              62987AL  1               G   300.000  5000.000  600.00      1
 2.55958900e+00-1.06322400e-04 7.20282800e-08-2.12110500e-11 2.28942900e-15    2
 3.89021400e+04 5.23452200e+00 2.73682500e+00-5.91237400e-04-4.03393800e-07    3
 2.32234300e-09-1.70559900e-12 3.88679500e+04 4.36388000e+00                   4
END
REACTIONS JOULE/MOLE
TICL3 + NH2(S) => N(D) + TICL2(S) + HCL + 0.5H2 1E+08 0.5 40800
TICL4 + NH2(S) => N(D) + TICL3(S) + HCL + 0.5H2 1E+08 0.5 40800
NH3 + TICL2(S) => TI(D) + NH2(S) + HCL + 0.5CL2 1.8E+08 0.5 40800
NH3 + TICL3(S) => TI(D) + NH2(S) + HCL + CL2 1.8E+08 0.5 40800
NH3             + ALCL(S) => AL(D)       + NH2(S)      +    HCL 4.453E+08  0.5 80000
ALCL3             + NH2(S) => N(D)       + ALCL(S)       + 2HCL   1.590E+08  0.5 64000
ALCL2NH2            + ALCL(S) =>  AL(D)       + N(D)       + ALCL(S)       + 2HCL    1.720E+08  0.5 42000
ALCL2NH2            + NH2(S) =>  N(D)       +AL(D)       + NH2(S)       + 2HCL    1.720E+08  0.5 42000
END
```

TiN:

```
ELEMENTS
H N TI CL
END
SPECIES
NH3 N2 TICL4 HCL TICL4N2H6 TICL3 H2 CL2 H CL TICL TICL2 TI
END
THERMO
TICL4N2H6               TI  1CL  4N   2H   6G   300.000  5000.000 1000.00      1
 1.92372093E+01 1.63167938E-02-6.30634833E-06 1.12721006E-09-7.61606145E-14    2
-1.25860697E+05-5.72306101E+01 1.32984738E+01 3.88107887E-02-3.81559203E-05    3
 2.10993111E-08-4.75394915E-12-1.24609903E+05-2.82644077E+01                   4
END
REACTIONS KJOULE/MOLE
TICL4             + 2NH3 => TICL4N2H6    1.75E+18  0.0 38.2
TICL4 => TICL3       + CL    2.32E+20 -1.17 387.9
TICL3 => TICL2       + CL    1.02E+18 -0.742 422.6
TICL2 => TICL       + CL    3.65E+20 -1.06 509.6
TICL4             + H => TICL3             + HCL    5.11E+06 2.5 12.6
TICL3             + H => TICL2             + HCL    1.11E+06 2.5 33.5
TICL2             + H => TICL             + HCL    3.05E+06 2.5 145.2
TICL            + H => TI             + HCL    4.09E+05 2.5 24.7
H             + CL              + M => M       + HCL    7.20E+21  -2.0 0.0
2CL             + M => M       + CL2    2.00E+14  0.0 -7.5
H             + HCL => H2       + CL    1.69E+13  0.0 17.2
CL2             + H => HCL       + CL    8.60E+13  0.0 4.905
2H            + H2 => 2H2    9.70E+16  -0.6 0
H2            + M => 2H       + M    2.20E+14  0.0 402.1
HCL             + M => H             + CL             + M    7.90E+25 -3 445.6
CL            + H2 => H             + HCL    2.95E+13 0.0 21.3
2H            + M => H2             + M    6.53E+17 -1 0
END
```

```
SITE/TIN/    SDEN/1.318E-8/
   N(S)/1/ TI(S)/1/ TICL3(S)/1/ TICL2(S)/1/ NH2(S)/1/
END
BULK TI(D)/4.500/
BULK N(D) /1.374/END
THERMO
TI(S)               62987TI  1               G   300.000  5000.000  600.00      1
 2.55958900e+00-1.06322400e-04 7.20282800e-08-2.12110500e-11 2.28942900e-15    2
 3.89021400e+04 5.23452200e+00 2.73682500e+00-5.91237400e-04-4.03393800e-07    3
 2.32234300e-09-1.70559900e-12 3.88679500e+04 4.36388000e+00                   4
N(S)                62987N   1               G   300.000  5000.000  600.00      1
 2.55958900e+00-1.06322400e-04 7.20282800e-08-2.12110500e-11 2.28942900e-15    2
 3.89021400e+04 5.23452200e+00 2.73682500e+00-5.91237400e-04-4.03393800e-07    3
 2.32234300e-09-1.70559900e-12 3.88679500e+04 4.36388000e+00                   4
TICL2(S)          J14    TI  1CL  2          G   200.000  6000.000  800.00      1
 9.22517250e+00 8.98917361e-04-3.85692482e-07 7.03161823e-11-4.59177658e-15    2
-7.31586882e+04-1.52557384e+01 4.65587536e+00 2.18510800e-02-3.61191419e-05    3
 2.68883110e-08-7.46025276e-12-7.23669824e+04 6.14773433e+00                   4
TICL3(S)          J14    TI  1CL  3          G   200.000  6000.000  800.00      1
 9.22517250e+00 8.98917361e-04-3.85692482e-07 7.03161823e-11-4.59177658e-15    2
-7.31586882e+04-1.52557384e+01 4.65587536e+00 2.18510800e-02-3.61191419e-05    3
 2.68883110e-08-7.46025276e-12-7.23669824e+04 6.14773433e+00                   4
NH2(S)            J14    N   1H   2          G   200.000  6000.000  800.00      1
 9.22517250e+00 8.98917361e-04-3.85692482e-07 7.03161823e-11-4.59177658e-15    2
-7.31586882e+04-1.52557384e+01 4.65587536e+00 2.18510800e-02-3.61191419e-05    3
 2.68883110e-08-7.46025276e-12-7.23669824e+04 6.14773433e+00                   4
TI(D)               62987TI  1               G   300.000  5000.000  600.00      1
 2.55958900e+00-1.06322400e-04 7.20282800e-08-2.12110500e-11 2.28942900e-15    2
 3.89021400e+04 5.23452200e+00 2.73682500e+00-5.91237400e-04-4.03393800e-07    3
 2.32234300e-09-1.70559900e-12 3.88679500e+04 4.36388000e+00                   4
N(D)                62987N   1               G   300.000  5000.000  600.00      1
 2.55958900e+00-1.06322400e-04 7.20282800e-08-2.12110500e-11 2.28942900e-15    2
 3.89021400e+04 5.23452200e+00 2.73682500e+00-5.91237400e-04-4.03393800e-07    3
 2.32234300e-09-1.70559900e-12 3.88679500e+04 4.36388000e+00                   4
END
REACTIONS JOULE/MOLE
TICL3 + NH2(S) => N(D) + TICL2(S) + HCL + 0.5H2 1E+14 0.5 40740
TICL4 + NH2(S) => N(D) + TICL3(S) + HCL + 0.5H2 1E+14 0.5 40740
NH3 + TICL2(S) => TI(D) + NH2(S) + HCL + 0.5CL2 1.8E+08 0.5 40740
NH3 + TICL3(S) => TI(D) + NH2(S) + HCL + CL2 1.8E+08 0.5 40740
END
```